Universidad Pública de Navarra

ESCUELA TECNICA SUPERIOR DE INGENIEROS AGRONOMOS

Nafarroako Unibertsitate Publikoa

NEKAZARITZAKO INGENIARIEN GOI MAILAKO ESKOLA TEKNIKOA

Extraction and determination of lipid and protein oxidation marker compounds in horse meat, employing MIR spectroscopy

Extracción y determinación de compuestos marcadores de la oxidación lipídica y proteica en carne de potro mediante medidas espectrales en el infrarrojo medio

Presented by / presentado por

Fernando Zulategui Beñarán *(e)k*

aurkeztua

MSc IN AGRICULTURAL ENGINEERING / MÁSTER UNIVERSITARIO EN INGENIERÍA AGRONÓMICA

June, 2018 / Junio, 2018

Acknowledgement

I would like to express my deep gratitude to Prof. María José Beriáin and Dr. Kizkitza Insausti, my research supervisors and directors, for their patient guidance, enthusiastic encouragement and useful critiques of this research work. I would also like to thank Dr. Miguel Beruete, for his help offered during my training in MIR technique, and for the chance to develop it in Navarra Biomed's laboratory facilities.

I would also like to extend my thanks to every professor, colleague, student and staff from Universidad Pública de Navarra who has helped me along my whole university stay at the Escuela Superior de Ingenieros Agronómos of UPNA, for the guidance, support and knowledge provided during these almost 6 years of education.

Thank you all.

Abstract

This project is the result of a wider research thesis in which authors try to find better profitability on the meat equine sector. This work deepens in the study of lipid and protein oxidation marker compounds in horse meat, employing the innovative technology of Fourier-Transform Mid-Infrared Spectroscopy (FT-MIR).

Once the extraction of these marker compounds is performed, from 23 foals of two study groups differenced by the finishing diets and animals' slaughtering age, a study of their absorbance spectra will be carried out in order to stablish prediction models (calibration and validation) between them and the classical quantification of the compounds. What is intended is to decide if this technology is useful to estimate the values of this kind of marker compounds employing MIR measurements of raw meat samples directly, or if it is preferable to perform a previous extraction of these compounds before executing their MIR analysis.

Marker compounds results show more consistent predictive models than the ones stablished in the quantitative analysis of the spectra obtained from raw meat in previous studies. Lipid oxidation compounds predictive model obtained in this work offered an R^2_{cv} of 63.18% versus the R^2_{cv} of 2.43% obtained in previous works employing raw meat. Regarding protein oxidation, R^2_{cv} obtained in this project showed a value of 54.24% while in previous works employing raw meat, it was obtained an R^2_{cv} of 24.6%.

Key words: FT-MIR spectroscopy, lipid oxidation, protein oxidation, marker compounds, horse meat, innovation, equine sector.

Resumen

Este trabajo es resultado de un proyecto de investigación más amplio en el cual se trata de mejorar la rentabilidad del sector cárnico equino. Éste consiste en profundizar en el estudio de los compuestos marcadores de la oxidación lipídica y proteica de la carne de potro a través del empleo de una tecnología novedosa como es la espectroscopía en el Infrarrojo Medio (MIR).

Partiendo de los compuestos marcadores extraídos de un total de 23 potros de dos grupos diferenciados por la edad al sacrificio y el tipo de alimentación, se procederá al estudio de sus espectros de absorbancia para intentar establecer modelos de predicción (calibración y validación) entre estos y la cuantificación clásica de los propios extractos. Lo que se tratará es de decidir si esta técnica es útil para estimar el valor de los compuestos marcadores de oxidación a través del análisis MIR de muestras de carne fresca directamente, o si es preferible una previa extracción de estos compuestos y su posterior analítica en el infrarrojo medio.

Los resultados obtenidos en este proyecto muestran unos modelos predictivos más consistentes que los obtenidos en los análisis cuantitativos de los espectros de absorbancia de la carne fresca en estudios anteriores. El modelo predictivo de los compuestos de oxidación lipídica mostró un valor de R^2_{cv} de 63,18%, frente al 2,43% obtenido en estudios anteriores empleando carne cruda. En cuanto a los compuestos de oxidación proteica, destacar que se obtuvo un valor de R^2_{cv} de 54,24% frente al 24,6% de estudios anteriores con las muestras en crudo.

Palabras clave: Espectroscopía FT-MIR, oxidación lipídica, oxidación proteica, compuestos marcadores, carne de potro, innovación, sector equino.

General Index

Figures Index

Tables Index

Abbreviations

AAS	α -amino adipic semialdehyde
ATR	Attenuated Total Reflectance
A-C	Adult Conventional
DMb	deoxymyoglobin
DNPH	2,4-dinitro-phenylhydrazine
FA	Fatty acids
FIR	Far infrared
FT	Fourier transform
FTIR	Fourier transform infrared
GC	Gas chromatography
GGS	γ-glutamic semialdehyde
HNE	4-hydroxy-2-nonenal
HPLC	High perfomance liquid chromatography
IR	Infrared
LO	Lipid oxidation
MCO	Metal-catalyzed oxidation
MDA	Malondialdehyde
MIR	Mid infrared
MMb	Metmyoglobin
MS	Mass spectrometry
MSC	Multiplicative scattering correction
n	Number of samples used in calibration/validation
NIR	Near infrared
OMb	Oxymyoglobin
p	Number of terms included in the equation
PLS	Partial Least Square
PO	Protein oxidation
PUFA	Poly Unsaturated Fatty Acids
R	Rank (Number of PLS factors)
RMSEE	Root mean square error of calibration
RMSECV	Root mean square error of cross-validation
RPD	Residual Prediction Deviation
ROS	Reactive Oxygen Species
R^2	Coefficient of determination for calibration
R^2_{cv}	Coefficient of determination for cross validation
SFA	Saturated Fatty acids
SNV	Standard normal variate
TBA	Thiobarbituric acid
TCA	Trichloroacetic acid
TBARS	Thiobarbituric acid reactive substances
UV-Vis	Ultraviolet-visible
Y-L	Young Linseed

Chapter I. Introduction

1. Horse meat.

In this first paragraph the material studied during this project is presented: horse meat. Its worldwide and national importance will be presented, its consumption and production along time and currently, bearing in mind the principal properties and characteristics of this particular kind of meat.

1.1 Horse meat production and consumption

Despite the evidences of its consumption during Paleolithic (10.000 B.C) (Belaunzaran et al., 2015), along Spanish history horse meat has never enjoyed great popularity, because of several reasons.

First of all, horses have been traditionally considered as war or labor animals. This way, these animals' meat was only consumed during famines and penury periods, associated to war times and marginal social classes. Because of this, nowadays persists the popular belief that horse meat is synonym of an old, useless or discarded animal (Fdez. de Labastida, 2011).

Added to previously said, nowadays horses are popularly appreciated as a leisure animal, generating positive affectionate and nearness feelings, one of the most important reasons that has notably conditioned its consumption in a great number of nations worldwide (Belaunzaran et al., 2015). That is why the unpopularity of this kind of meat can even be justified by the average citizen, bearing in mind the tradition of consumption that horse meat has had, and the current "pet" feeling towards these animals.

Besides, currently horse meat has been and is a focus of controversy, due to adulterations and frauds done in meat products with the aim of cheapening the final price of other animals' species meat sales (Lorenzo et al., 2017). Although these modifications of meat products do not present any risk at all towards consumers health or regarding food safety issues, these situations have created a great confidence gap between consumers and equine meat (Premanandh, 2013), generating a decrease in the sales of processed meat products and spreading a general reject feeling towards horse meat in particular.

Taking all of that into consideration, it is not a great surprise to notice that the productions of this kind of meat is minor globally, in comparison with other meats consumption as it can be perceived in the Figure 1.

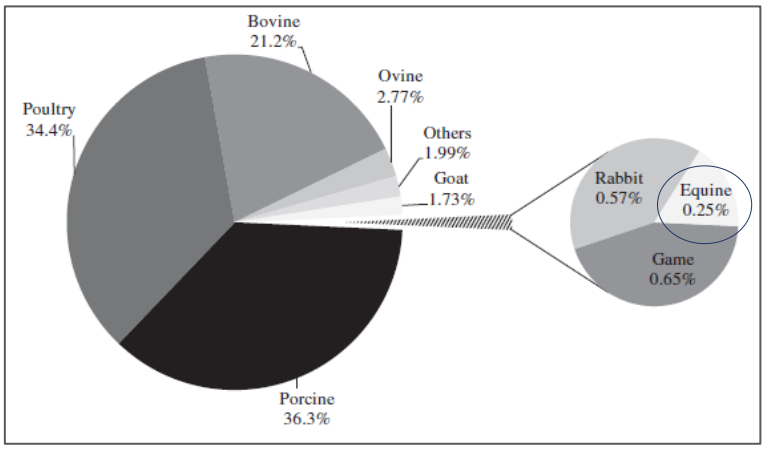

Figure 1: World's meat production (%) by species in 2013 (Source: Belaunzaran et al. 2015, taken from FAO 2015)

Nevertheless, these statements are just due to the existing ignorance about current production and production methods employed globally in equine meat. While historically horse breeds used for consumption came from old animals previously employed for field labor, nowadays these animals come from selected breeds with meat production purposes (Martuzzi, Catalano & Sussi, 2001).

On the other hand, rejection feeling towards horse meat due to recent food frauds is totally unjustified too, since changes in composition would not suppose any risk regarding food safety, nutrition or health. The problem just resides in loosing honesty when labelling these products and faking traceability, which produces confusion among average consumers.

During 2014, almost 5 million horses were sacrificed worldwide for its consumption, where up to 643.827 were performed in Europe (FAO, 2015). This way, it can be intuited how horse meat consumption in European countries is much lower than the one in other nations across the globe. Figure 2 presents a world map that reflects with different colors the world zones and its respective ranges of equine production, expressed in tons for the year 2014.

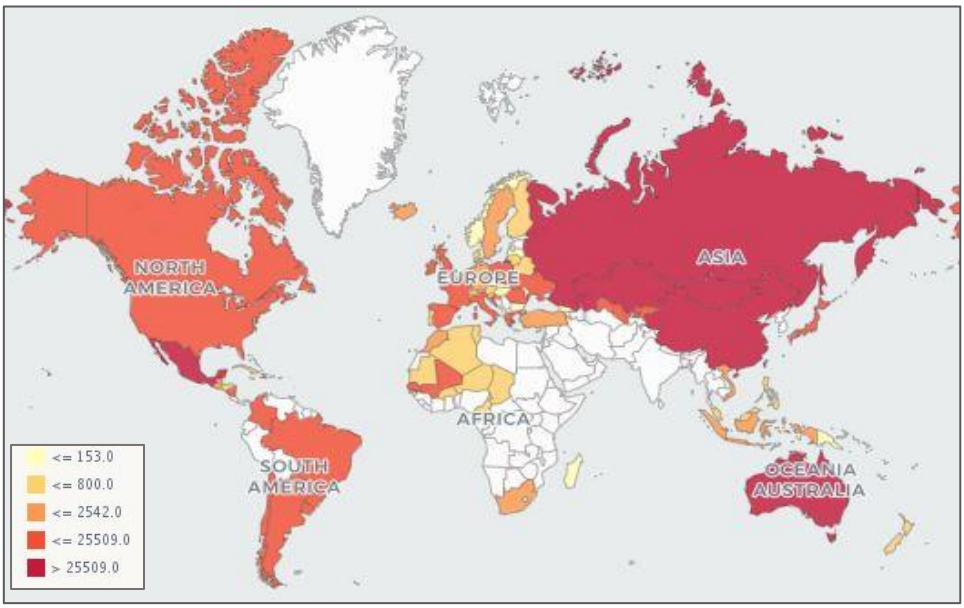

Figure 2: World map with horse meat production by countries, in tons for 2014 (Source: FAO 2015)

As it is shown in last Figure 2, horse meat most productive worldwide regions are the aggregate of Asiatic countries and the Americas. Figure 3 shows a circular graph with percentage worldwide productions for 2014, in order to visualize this data easier.

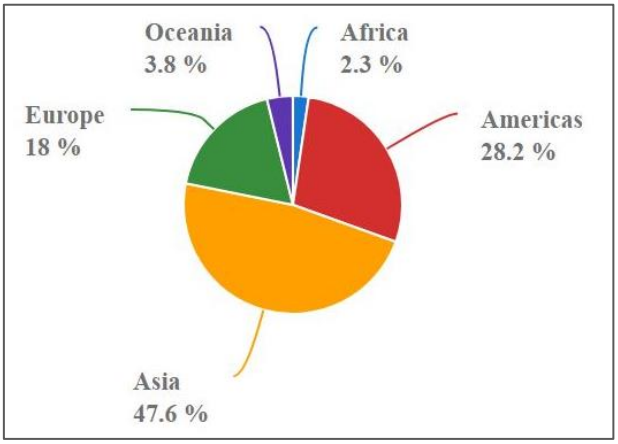

Figure 3: Graph of the percentage worldwide productions of horse meat for 2014 (Source: FAO 2015)

As above mentioned, Europe's foal meat production (18% of worldwide production) is significantly lower than the one in America's and Asia's areas, which suppose a 28% and almost a 48% of this production, respectively.

However, despite what it could seem at first sight, this percentage of European production is relatively important, bearing in mind the significant smaller population with regard to America and Asia and taking into account the poor popularity that this kind of meat has had along most of the European countries along history.

Around 700.000 horses graze in Spanish lands (Caballero, 2017) and about 50,000 livestock heads are slaughtered annually, specifically 48,100 during year 2014 (FAO, 2015). Table 1 presents data of the number of heads sacrificed, production in tons and carcass yield in kg/animal for year 2014 of the mean and aggregate of Europe and Spain.

Table 1: Horse meat production data in Europe and Spain for the year 2014 (Source: FAO 2015)

LOCATION	ELEMENT	UNIT	VALUE
EUROPE (35)	Production	Heads	**643,827**
	Production	tons	**133,436**
	Yield	kg/animal	**207,3**
EUROPE (MEAN)	Production	Heads	**18,395**
	Production	tons	**3,812**
	Yield	kg/animal	**207.3**
SPAIN	Production	Heads	**48,100**
	Production	tons	**11,530**
	Yield	kg/animal	**239.7**

As it shown in Table 1, Spain is highly above the European mean regarding number of heads slaughtered annually (2.5 times the value of aggregate's mean) which suppose a 7.5% of the aggregate of European 35 countries. This way, it can be asserted that Spain within Europe is a remarkably important horse meat producer. Nonetheless, as it is now presented in Figure 4, consumption of this kind of meat in Spain is quite smaller than the one registered in other countries along Europe.

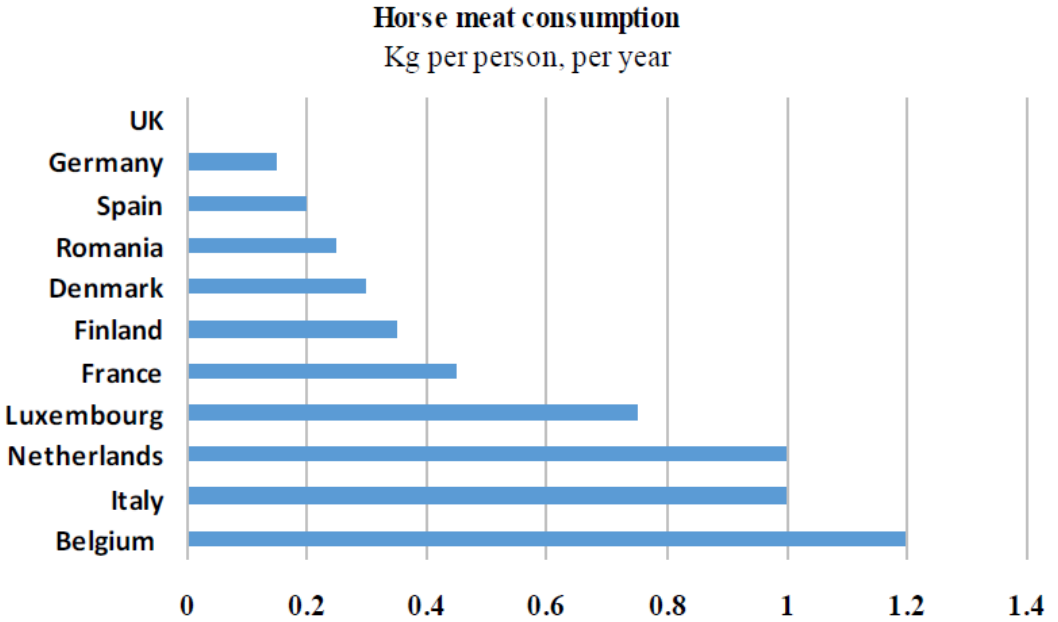

Figure 4: Horse meat consumption (kg/person and year) in main European countries for the year 2014 (Source: Stanciu, 2014)

These data make out that Spain is positioned as an important foal meat exporter, as it is one of the biggest European producers, despite not carrying out an important consumption of this kind of meat. Specifically, Spain is found among the top 10 horse meat exporter countries in the world, preceded by Belgium, Poland, France, Holland and Romania at European level. (Stanciu, 2014).

Regarding meat purpose horse breeding in Spain, it should be noted that it has always been linked to the north zone of the country: Mountain Aragon, Cantabria, Asturias, north of Castilla and León, Basque Country, Navarre, La Rioja and Catalonia. In these areas, crosses of regional mares with foreign stallions gave rise to the main equine populations that are nowadays employed for meat purpose horse production. These breeds are: the *Hispano-bretón* (french-spanish cross); the *Asturian mountain horse*; the *Monchino cántabro*; the *Burguete* (a cross of *jaca navarra* with foreign breeds *Postier bretón, Percherón, Ardanés* or *Contois*); the *Basque country mountain horse* and the *Pirenaico catalán* as well as, to a lesser extent, the *Basque potokka* and the *Asturcón* (Caballero, 2017).

In the case of Navarre, breeds raised for meat purpose are mainly *Burguete* and *Jaca Navarra*. Foals raised for commercialization are animals between 7-9 months of slaughtering age (*lechales* foals) or between 15-16 months of slaughtering age (*quincenos* foals) (Sarriés, 2005), so this indeed demystifies the extended belief that horse meat always comes from an old and rejected animal employed for other purposes.

1.2 Horse meat characteristics and composition

Foal meat presents some distinctive characteristics and several differences in terms of composition towards other types of meat as beef or pork meat. In the first place, as a remarkable peculiarity, horse meat has a slightly higher content of protein and a minor content of fats than other meats which are popularly more appreciated (Lorenzo et al., 2017). Table 2 shows the approximate mean composition of horse meat in terms of main biomolecules (water, proteins, lipids and carbohydrates).

Table 2: Approximate mean composition of horse meat (Source: Rossier, 1998)

Composition (g/100g of meat)	Approximate mean value
Energy (kcal)	95-100
Water	75
Proteins	23
Lipids	2
Carbohydrates	1

Among the set known as “red meats”, nowadays it is stated that horse meat is considered as “dietetic” mainly due to its low-fat content and to its fatty acids (FA) profile (Lorenzo et al, 2014). According to food composition tables from Moreiras et al. 2013, (MAPAMA b 2017), lean beef meat presents on average 131 kcal in 100g of meat, so it can be declared that generally this kind of meat is a 34% calories-higher in comparison with foal meat, considering energy per 100g shown above in Table 2.

This is partially due to the difference regarding **lipids** that exists between both kinds of meat. Horse meat present a 2% of total lipids in its composition (of which 32% are saturated FA) while lean beef meat rises values of 5.4 % of fats (of which 41% are saturated FA) (MAPAMA a, 2017). Although diversity of results regarding horse meat’s lipid composition exists, according to different authors and studies, monounsaturated fatty acids have rarely shown greater proportion than saturated fatty acids (SFA) or polyunsaturated fatty acids (PUFA) (Lorenzo et al, 2014). Besides, it has been observed in some studies that predominant FA in intramuscular fat of foal’s

different muscle tissues are PUFA, with ranges from 41.1 to 48.2% of total methyl esters (Lorenzo & Pateiro, 2013).

Horse meat contains between 0.5 and 3 times more **glycogen** than beef, providing it with a sweeter flavor. Due to its glycogen and ATP quantity, horse meat conserves plasticity and elasticity levels a longer time than other meats (Rossier, 1993). On the other hand, ageing of this kind of meat is reached in 4-5 days post-mortem and, therefore, pH decreases rapidly. This way, under a hygienic-health perspective and due to its high glycogen, lactic acid and non-protein nitrogen levels, self-life for commercial purposes of horse meat is shorter than for beef meat (Fàbregas, 2002).

Regarding **proteins**¸ horse meat is characterized by having a higher proportion of protein content than beef or pork, as it has been aforementioned. Besides presenting more protein, this content has a high-rise biological value, as it presents around 40% of essential amino acids. The amino acid composition of horse meat, both essential and non-essential, are presented in Table 3, set in order of abundance.

Table 3: Amino acid content in horse meat (mean ± st. dev.) (Source: Lorenzo & Pateiro, 2013)

Essential Amino acid	**Content (g/100g protein)**
Lysine	9.15 ± 0.22
Leucine	8,54 ± 0,18
Arginine	6,48 ± 0,75
Valine	5,32 ± 0,08
Isoleucine	5,23 ± 0,35
Treonine	5,09 ± 0,22
Histidine	4,60 ± 0,27
Fenilalanine	4,32 ± 0,09
Metionine	1,45 ± 0,26
Non- essential Amino acid	
Glutamic acid	15,32 ± 0,21
Aspartic acid	9,61 ± 0,21
Alanine	5,97 ± 0,12
Glycine	4,37 ± 0,20
Serine	4,06 ± 0,10
Proline	3,92 ± 0,18
Tirosine	3,46 ± 0,27

As it can be seen in previous Table 3, the most abundant essential amino acid is Lysine, followed by Leucine and Arginine. Between non-essential amino acids, the most abundant one is Glutamic acid followed by Aspartic acid.

2. Meat Oxidation

2.1. Background

Oxidation is one of the main causes, if not the principal, of the loss of meat quality during preservation as it affects lipids, proteins, carbohydrates and vitamins in meat, and consistently, texture, color and sensory properties in general. Apart from ante-mortem factors, there are two important post-mortem factors directly related to oxidative stability, and thus to the loss of meat quality: ageing and storage time. Oxidative processes begin when tissues and muscles are damaged after slaughter and will continue until meat reaches unacceptable levels to the average consumer.

Ageing enhances a series of changes in technological aptitude and sensory characteristics of the meat. It consists of an onward softening of the meat, a slight increase in water retention capacity and the development of flavors characteristic of non-fresh meat. All these changes are the result of degradation of proteins and lipids.

Depending on storage time, the high relationship between lipid and protein oxidation in fresh meat and its influence on the deterioration of meat quality is known (Lorenzo and Gómez, 2012). These processes are favored by long storage times in the presence of oxygen and produce, from the appearance of off-odors, to discoloration of the meat surface (Zakrys et al., 2008). Protein oxidation involves the oxidation of myoglobin, which is the color pigment in muscles and responsible for oxygen binding. Color changes in foal meat occur mainly due to the susceptibility of the myoglobin molecule, especially iron, to alterations in the chemical environment and to energy input (Brewer, 2004).

When meat is in contact with oxygen, oxymyoglobin (OMb) is the main pigment that gives meat a bright red color. In the absence of oxygen, the meat surface is dark red or purple (deoxymyoglobin, DMb), and a long time in the presence of air induces oxidation of myoglobin (metmyoglobin, MMb) which gives the meat a brown or reddish-brown color. Although this color change is not harmful and does not denote deterioration, it is considered undesirable by consumers (Voges et al., 2007).

On the other hand, tenderness is greatly affected by the oxidation of proteins. Changes in proteins are related to deterioration of the textural aspects of meat. Meat becomes harder and less juicy due to changes in protein cross-linking due to oxidation reactions (Zakrys-Waliwander et al., 2010).

During years, on the one hand **lipid oxidation** has been object of plenty of studies, what has let to get knowledge about principal mechanisms involved in fatty acids oxidation and parallel degradation.

On the other hand, **protein degradation** has not been so deeply studied in meat quality researches (Lund et al., 2011), despite having been proved that protein oxidation would importantly affect to functional properties of meat and in particular to horse meat (Estévez et al, 2011).

In these paragraphs, protein and lipid oxidation will be presented, as well as the most important compounds involved in their reactions, better known as protein or lipid **oxidation markers**.

2.2. Lipid Oxidation

As mentioned before, lipid oxidation in food systems has been interest of study during the years as it was proved that lipid compounds in presence of O_2, suffered from oxidative stress, consequence of an unbalance between reactive species and antioxidative defense mechanisms (Halliwell, 1995) mostly due to the presence of double bonds in Poly Unsaturated Fatty Acids (PUFA).

As mentioned by Armenteros et al. (2012), Reactive Oxygen Species (ROS) perform over membrane PUFAs leading to a fluency loss and cellular lysis as a consequence of lipid peroxidation.

Lipid peroxidation is initiated after the abstraction of an Hydrogen atom from the hydrocarbon chain of Poly Unsaturated Fatty Acids, forming a Carbonyl/Lipid Radical (R-) (known as *Initation*). In an aerobic ambience, an interaction is performed between the Carbonyl Radical with O_2, resulting in ROO- radical formation (Lipid Peroxy Radical, known as *Propagation*). After that, another H can be subtracted from another lipid (sequential reaction) leading to ROOH formation (Lipid Hydroperoxide), which would form the Alkoxy radical (RO-) through decomposition. Figure 5 shows the mechanism of this lipid peroxidation.

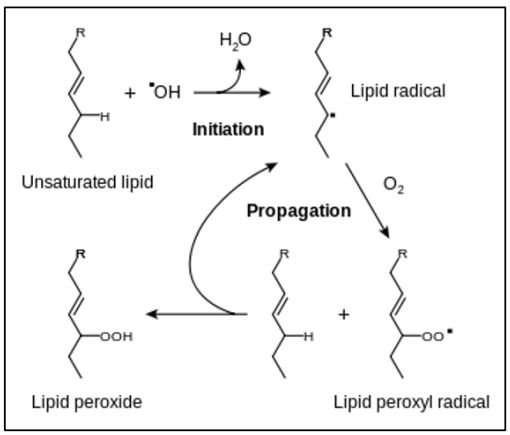

Figure 5: Mechanism of lipid peroxidation (Source: Armenteros et al., 2012)

To this first step, a series of propagation reaction is befell in order to finally produce more stable final products such as Malondialdehyde, commonly known as MDA (Rojano et al. 2008).

Associated changes to lipid oxidation constitute the principal cause of meat and meat products degradation, as they trigger bad odors and flavors formation, as well as color alteration, all of it having consequently a loss in organoleptic quality of the final product. Not only that but also, this lipid oxidation leads to a loss in meat's nutritional value and to formation of potentially harmful compounds related to different pathologies risks (Bou et al., 2009).

In this context, Lipid/Carbonyl Radicals, Hydroperoxides and **Malondialdehyde (MDA)** play a vital role in promoting *in vivo* oxidative reactions which have been proved to not only reduce meat's and food's quality but also to be harmful and damaging for health. That is why, through the years different techniques have been developed in order to detect and measure some of these compounds.

Lipid oxidation determination methods

As aforementioned, the process of lipid oxidation is complex and it is a function of the type of lipid substrate, the oxidation agents and general environmental factors (Barriuso et al. 2013). That is why finding proper measurement of lipid oxidation remains a challenging task.

Various methodologies have been developed and tried to be implemented so far, for determining primary both oxidation products and secondary oxidation products. Between a wide range of technologies, there are two most classical and employed procedures: the **Thiobarbituric Acid Reactive Substances method** (TBARS analysis) and **Chromatography,** both employed for secondary oxidation products, MDA specifically, as it constitutes the most abundantly generated aldehyde during secondary lipid oxidation and it is the most commonly used as **oxidation marker** (Barriuso et al. 2013).

2.2.1. Thiobarbituric Acid Reactive Substances method (TBARS)

The most classical and employed procedure to detect and quantify lipid oxidation of food is TBARS analysis, at least in order to measure secondary oxidative derivates in muscular systems' lipids (Armenteros, 2010).

This procedure consists of quantifying TBA index at the last stage of oxidation process. It is based in the detection of Malondialdehyde and other aldehydes generated at the oxidative decomposition of PUFA, aforementioned in the introduction of paragraph *2.2 Lipid Oxidation* and the *figure 5. Mechanism of lipid peroxidation.*

The basis of this method goes by attending that aldehydes (which include MDA principally) react with thiobarbituric acid in order to yield a chromogen/fluorescent product, which present an absorption peak at 532 nm (see Figure 6).

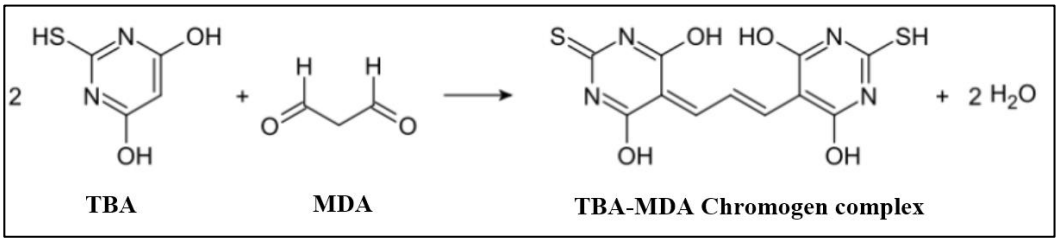

Figure 6: Reaction of TBA with MDA. (Source: López et al., 2014)

The most commonly used protocol is the acid extraction, as it is a simple and rapid procedure that involves not so many laboratory devices or equipment (López et al. 2014).

Despite its ease and simplicity, traditional TBARS test has been criticized for various reasons. Firstly, TBA is not selective to MDA, since it also reacts with many other compounds, such as other aldehydes, carbohydrates, amino acids and nucleic acids (Salih et al. 1987), interfering in the TBA assay and resulting in considerable overestimation, as well as low reliability due to variability in the results. Therefore, it is known as TBA reactive substances method (TBARS), referring to all the compounds that react with TBA. There is not only that but also a risk of underestimating the response since malondialdehyde can form, under *in vivo* conditions, linear or cyclical Schiff bases, or even crosslinked bonds, with lysine and arginine from proteins (Barriuso et al, 2013).

2.2.2. Chromatography

Once it has been shown the classical and most spread way to measure lipid oxidation in food samples and in order to overcome some of these limitations, more advanced chromatographic determinations were developed.

These techniques provide more accuracy, sensitivity and specificity for MDA. Some of them (Stalikas et al. 2001 and Mendes et al 2009) involve the formation of MDA-TBA complex, purification by chromatography (Gas Chromatography or High-Performance liquid chromatography) and subsequent detection by MS, UV-Vis or fluorometric detector while some others use derivatization of MDA instead of reaction with TBA, in order to obtain a detectable compound.

Focusing on Chromatography, on the one hand, **Gas Chromatography** coupled to mass spectrometry (GC-MS) can be used for the analysis of lipid hydroperoxides, but due to their thermolability, previous reduction of the hydroperoxides is needed. This fact, along with the prior lipid extraction and subsequent derivatization step, makes it a complicated and time-consuming method (Lagarda et al., 2003).

On the other hand, High-performance **Liquid Chromatography** (HPLC) is also being used to determine hydroperoxides. This method is highly sensitive and pretty versatile considering both column and detector properties, allowing to analyze compounds with different characteristics of volatility, molecular weight or polarity. However, sample preparation is frequently tedious and usually requires lipid extraction.

Reaction with 2,4-dinitro-phenylhydrazine (DNPH) or pentafluorophenylhydrazine and conversion into pyrazole and hydrazone derivatives are the most commonly used procedures with HPLC separation and spectrophotometric/fluorometric detection (Ichinose et al. 1989).

That is why, in comparison to other procedures such as TBARS analysis, these Chromatography based techniques involve much harder and longer experimental work, and high level of complexity in data processing, that is why they are not so extended and used in food systems.

Attending to all previously mentioned, it is important to find and develop alternative, non-destructive, easier and overall more accurate procedures in order to evaluate and measure the oxidation of lipids in meat and other food samples.

2.3. Protein Oxidation

As it has been aforementioned, Protein Oxidation (PO) was not interest of study until lipid oxidation was deeply studied due to the fact that it was early proved that degradation of fatty compounds had a direct impact over meat and food quality. At this time, there was a lack of knowledge about the oxidation reactions of proteins and the consequences of them in food quality, as the fact that food proteins may be sources and targets for reactive oxygen species (ROS) was mostly ignored (Estévez et al. 2012). It was not until mid-90's when it was noticed that proteins could be also susceptible of these oxidation reactions.

Protein Oxidation is responsible for the apparition of anomalous textures in fresh meat and by-products. Oxidized proteins present depleted functional properties, which involve technical and quality loss in food products, in particular in meat industry. Not only that, but also, PO triggers an irreversible essential amino acids loss and an alteration of the digestibility of oxidized proteins which leads to a nutritional value loss in meat and meat products (Estévez et al., 2012).

PO is a complex process as the pathways and the nature of the products depend on the targets and how the oxidative reactions start. Numerous ROS are able to initiate the oxidative damage to proteins and transition metals as well as oxidizing lipids are known to be influential (Stadtman & Levine, 2003). Some authors have proved Protein Oxidation in meat systems through various of its multiple chemical pathways including: sulfhydryl groups, loss of tryptophan fluorescence, gain of carbonyl derivatives and formation of intra- and intermolecular cross-links (Estévez et a., 2012).

From all these previous pathways, **formation** of **carbonyl compounds** (aldehydes and ketones) has been remarkably highlighted as one of the most important routes of PO. Carbonylation is a non-enzymatic and irreversible alteration of proteins which involves the formation of carbonyl moieties triggered by oxidative stress and other mechanisms. Carbonyls can appear in proteins through four different paths:

1) Direct oxidation of the side chains form lysine, threonine, arginine and proline.
2) Non-enzymatic glycation in presence of reducing sugars.
3) Oxidative cleavage of the peptide backbone via α-amidation pathway.
4) Covalent binding to non-protein carbonyl compounds such as HNE or MDA.

Among previous pathways, **direct oxidation** of **amino acid side chains** has been stablished as the main route for Carbonylation and the most important source of oxidative damage to proteins

in biological systems (Stadtman & Levine, 2000). The formation of carbonyl derivatives from lysine, threonine, arginine and proline side chains is usually attributed to metal-catalyzed oxidation (MCO) systems. Because of MCO, threonine is converted into α-amino-3- keto butyric acid, lysine into α-amino adipic semialdehyde (AAS), and arginine and proline into γ-glutamic semialdehyde (GGS). The two latter (**AAS** and **GGS**) were originally proposed as biomarkers of oxidative damage to proteins by Daneshvar, Frandsen, Autrup, and Dragsted (1997).

According to the formation pathway of these compounds, thoroughly described first by Stadtman and Oliver (1991) and afterwards by Akagawa et al. (2006), the side chains of the susceptible amino acids are oxidatively deaminated in the presence of transition metals such as iron and copper. The reactive species would attack the amino group from the amino acid side chain by abstracting a hydrogen atom from the neighboring carbon, leading to the formation of a carbon-centered protein radical. In a further step, oxidized forms of the metal ions would accept the lone electron of the carbon radical to form an imino group which is spontaneously hydrolyzed to yield the corresponding aldehyde moiety. In organic chemistry, a moiety is a part of a molecule. Moieties that constitute branches extending from the backbone of a hydrocarbon molecule, which can often be broken off and substituted with others, are called substituents or side chains. Large moieties are often functional groups. This reaction is shown in Figure 7.

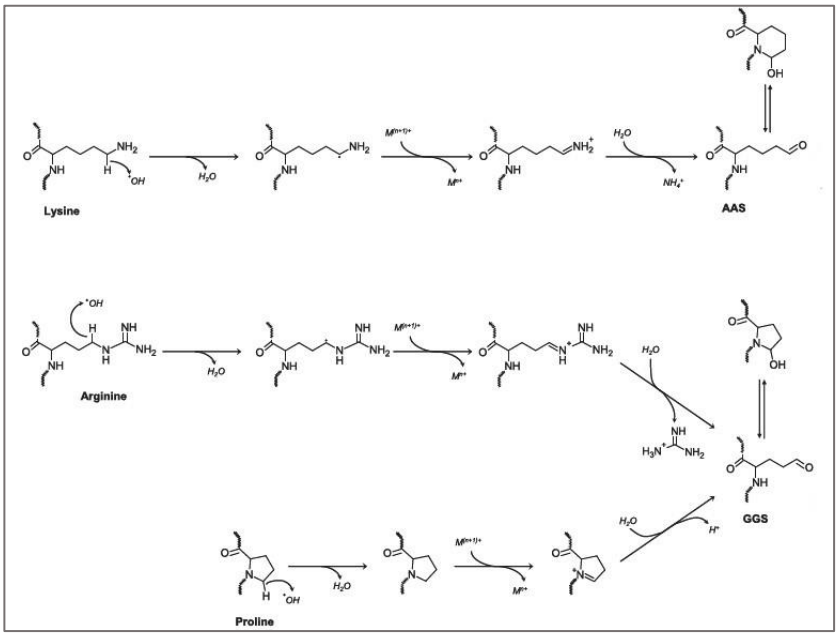

Figure 7: Formation pathway of specific protein carbonyls, α-aminoadipic and γ-glutamic semialdehydes, AAS and GGS, respectively (Source: M. Estévez, 2011)

Protein oxidation determination methods

According to PO, two main groups of quantification methods are currently employed: **Total carbonyl content** and **Specific Protein Carbonyls**. On the one hand the first one contemplates the quantification of the total amount of carbonyls from a protein sample and it is widely used as a general index of PO in meat and meat products (Estévez et al., 2008). On the other hand, specific protein carbonyls method is referred to the study of α-**aminoadipic** and **γ-glutamic semialdehydes** as PO biomarkers.

2.3.1 Total Carbonyl content (DNPH method)

In this way, the quantification of the total content of protein carbonyls by using the **dinitrophenylhydrazine** (**DNPH**) technique is probably the most frequent method for assessing Protein Oxidation in meat and biological systems (Estévez, Morcuende, & Ventanas, 2007).

The method is based on the reaction between the DNPH with protein carbonyl compounds to form a 2,4-dinitrophenyl (DNP) hydrazone product which displays a maximum absorbance peak at around 370 nm. Formation of this DNPhydrazone product is presented in Figure 8.

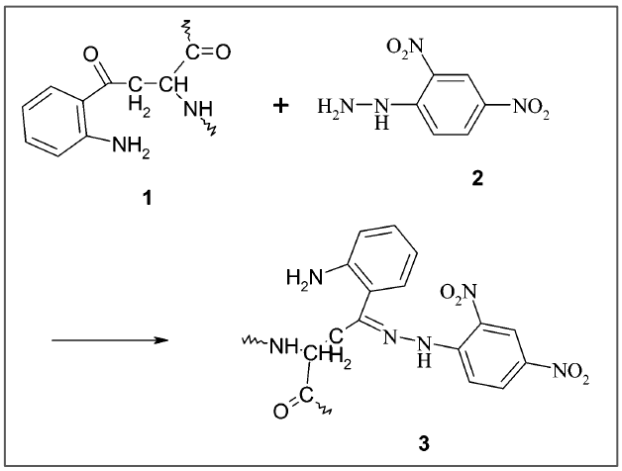

Figure 8: Formation of dinitrophenylhydrazone (3) from dinitrophenylhydrazine (DNPH) (2) and the oxidized form of tryptophan, N-formylkynurenine (1). (Source: Vuorela et al., 2005)

The procedure involves a simultaneous determination of carbonyl derivatives and protein content of the sample (Oliver et al., 1987). The original method from Oliver et al. (1987) was developed for analyzing oxidative stress in biological samples and has been afterwards employed with slight modifications by food scientists in recent years. Simplicity and convenience of DNPH analysis has helped to make it a widespread and inexpensive method for PO assessing, what implies that this method is considered one of the most relevant expressions of oxidative damage to proteins in biological systems (Shacter, 2000).

In spite of its popularity, the drawbacks of this procedure include the lack of specificity and a possible overestimation of carbonyl due to other artifacts. In natural science and signal processing, an artifact is any error in the perception of representation of any information, introduced by the involved equipment or technique. Carbonyl moieties can be present in proteins because of mechanisms that do not involve the oxidation of amino acid residues (Requena et al., 2003). This way, DNPH method would underestimate the overall oxidative damage to proteins and would overestimate the total amount of protein carbonyls by accounting absorbance from artifacts (Estévez, 2011).

2.3.2 Specific Protein Compounds

As previously mentioned, another way to assess Protein Oxidation is the study of **α-aminoadipic** and **γ-glutamic semialdehydes.**

Early after AAS and GGS were highlighted as reliable markers of oxidative damage to proteins in relation to age-related diseases, various methodologies were developed for the detection and quantification of both semialdehydes from different kind of samples (Estévez, 2011).

AAS and GGS are very sensible to acid hydrolysis and because of this, a derivatization procedure is required for stabilization of the compounds. In this context, several research groups developed different procedures to perform this. Firstly, Climent, Tsai and Levine (1989) proposed a derivatization procedure with fluoresceinamine prior to the analysis of the derivatized semialdehydes by HPLC-MS. Later on, Requena et al. (2001) developed a method based on gas chromatography (GC)-MS for the detection of α-aminoadipic and γ-glutamic semialdehydes in the form of their corresponding hydroxyl derivatives. Moreover, Akagawa et al. (2006) proposed the reductive amination of both semialdehydes in the presence of sodium cyanoborohydride

($NaCNBH_3$) and *p*-aminobenzoic acid, showing improved stability of the derivatized carbonyls against acid hydrolysis during long periods of cold storage.

In comparison with DNPH method, these procedures of AAS and GGS detection are quite more complicated and equipment demanding, as for example preprocesses of derivatization are needed and reagents employed are more expensive than DNPH method. This way, these methods are more often employed for high value biological systems.

According to bibliography, it is highly advisable to complement different methodologies in order to obtain more consistent results when studying Protein Oxidation processes (Soladoye et al. 2015). That is why in several research studies which approach the investigation of PO, different techniques are employed for the assessment of these processes within meat products. Table 5 shows some of these studies in which DNPH method appears to be the most commonly employed.

Table 4: Protein Oxidation assessment in several references (Source: Soladoye et al. 2015)

Processed meat product	Processing technique	Oxidation markers	Techniques for PO assessment	References
Beef heart surimi	Mincing and washing	Total carbonyl	2,4-Dinitrophenyl hydrazine (DNPH)	Srinivasan et al. (1996)
Beef meat	Maturation	Total carbonyl; reduced groups	DNPH; 2,2'dithiobis (5-nitropyridine), DTNP	Martinaud et al. (1997)
Broiler breast meat	Irradiation	Total carbonyl	DNPH method	Rababah et al. (2004)
Beef sausage	Irradiation	Total carbonyl	DNPH method	Badr and Mahmoud (2011)
Pork meat	Nitration	Reduced thiol group, total carbonyl	5,5'-Dithiobis (2-nitrobenzoic acid); DNPH method	Van Hecke et al. (2013); Vossen et al. (2012)
Chicken thigh meat	Irradiation	Total carbonyl	DNPH method	Xiao et al. (2013), Xiao et al. (2011)
Dry-cured ham	Dry curing	Total carbonyl	DNPH method	Armenteros et al. (2009); Ventanas et al. (2007)
Dry-cured loins	Dry curing	Total carbonyl; specific carbonyl (AAS and GGS)	DNPH method, fluorescence spectroscopy; LC-ESI-MS (liquid chromatography-electrospray ionization mass)	Armenteros et al. (2009); Ventanas et al. (2006)
Beef meat	Steam cooking, refrigeration storage	Free thiol; aromatic amino acid; total carbonyl; Schiff bases	DTNP method; UV spectroscopy; DNPH; fluorescent spectroscopy	Gatellier et al. (2010)
Pork meat	Cooking (boiling)	Total carbonyl; Schiff base, protein aggregate	DNPH method; fluorescent spectroscopy, Raleigh light scattering	Traore et al. (2012)
Beef meat	Cooking (boiling	Total carbonyl, free thiol group; protein aggregation	DNPH method; Ellaman's method; fluorescent spectroscopy,	Sant´e-Lhoutellier et al. (2008)
Pork muscle	Mincing, cooking, aging	Total carbonyl; protein aggregation	DNPH method; granulometry measurement	Bax et al. (2012)
Pork meat patties	Processing	Total Carbonyl	DNPH method	Vuorela et al. (2005)
Cooked pork burger patties	Processing, chilled storage	Total specific carbonyl (AAS, GGS)	DNPH method and LC-ESI-MS	Ganhao et al. (2010)
Cooked pork burger patties	Processing,	Total carbonyl	DNPH method	Salminen et al. (2006)
Dry cured ham	High hydrostatic pressure	Specific carbonyl	LC-ESI-MS	Fuentes et al. (2010)
Dry cured ham	High hydrostatic pressure	Total carbonyl	DNPH method	Cava et al. (2009)

To sum up with everything presented in these paragraphs, it has been shown the different pathways of Lipid and Protein oxidation in food systems, as well as the main procedures for their determination. It has been noticed that for both Lipid and Protein oxidation quantification a variety of methodologies exist.

However, most classical techniques show several weaknesses regarding sensitivity, susceptibility and/or overestimations (TBARS and DNPH), while more accurate ones present much more complex experimental procedures and tedious preparations and post-processing data (GC and LC).

According to agricultural industries' demand, it is vital to develop food analysis methods including speed, ease to use, with non-preparation or minimum sample preparation, with non-destruction of samples, and bearing in mind environmental sustainability. That is why, it seems necessary to find and develop alternative, non-destructive, simpler and more accurate procedures in order to evaluate and measure the oxidation of lipids and proteins in meat and other food samples.

According to this, through this project an alternative way to evaluate these oxidative processes hase been studied: **Infrared spectroscopy,** as all of the requirements aforementioned are fulfilled by IR technology. Next paragraph includes an introduction to this innovative technique applied to food quality, its fundamentals, instrumentation and varieties among this technology.

3. Infrarred Spectroscopy

As mentioned, first of all the fundamentals of this field will be discussed. Then, instrumentation employed in this technique will be presented, and finally the two main different methodologies employed in food quality assessment will be remarked, as well as a summary of all the references and bibliography found involving IR spectroscopy in meat systems.

3.1. Fundamentals

In the year 1.800 astronomer Friedrich Wilhelm Herschel analyzed the spectrum of sunlight. He created the spectrum by directing sunlight through a glass prism so that the light was divided into its different colors. Herschel measured the heating ability of each color using thermometers, and just beyond the red part of the spectrum he noticed some kind of "invisible" radiation. Herschel found that this area close to the red part had the highest heating ability of all, so he concluded that there must be a different kind of light beyond the red portion of the spectrum, which is not visible to the human eye. This light became known as "**infrared" light**.

Afterwards, Herschel placed a water-filled container between the prism, and the thermometer and could observe that temperature measured was lower than the one measured without the water. As a consequence, water must partially absorb the radiation. He also proved that depending on how the prism was rotated, the difference in the temperatures measured for each color varied. This was the beginning of **infrared spectroscopy** (Bruker, 2011b).

It is important to highlight that IR spectroscopy is an example of **absorption spectroscopy,** which is referred to a variety of techniques that employ the interaction of electromagnetic radiation with the matter. In absorption spectroscopy, intensity of a beam of light measured before and after the interaction with a sample is compared.

Visible light and infrarred light are two types of electromagnetic radiation, but with different wavelenghts or frequencies. In general, electromagnetic radiation is defined by the **wavelength λ** or by the **linear frequency ν.** The wavelenght is the distance between two maxima on a sinusoidal wave. The frequency is the number of wavelengths per unit time.

In infrared spectroscopy **wavenumber** is used to describe the electromagnetic radiation. Wavenumber is the number of wavelenghts per unit distance. For a wavelenght λ in microns (μm), the wavenumber, ν~, in cm^{-1}, is given by:

$$\nu\sim = 10{,}000 \cdot 1/\lambda \text{ , in } cm^{-1}$$

According to this, IR region of the electromagentic spectrum embraces the radiation with wavenumbers comprehended between 12,800 and 10 cm^{-1}, which corresponds to wavelenghts from 0.78 to 1,000 μm. Within this range, infrared is commonly subdivided into three different regions: the **Near-Infrared** (**NIR**) which is included between 12,800 and 4,000 cm^{-1}, the **Mid-Infrared (MIR)** from 4,000 cm^{-1} to 400 cm^{-1} and the **Far-Infrared (FIR)** between 400-100 cm^{-1}.

This is presented in Figure 9, which shows the representation of the electromagnetic sprectrum from gamma rays to radio waves.

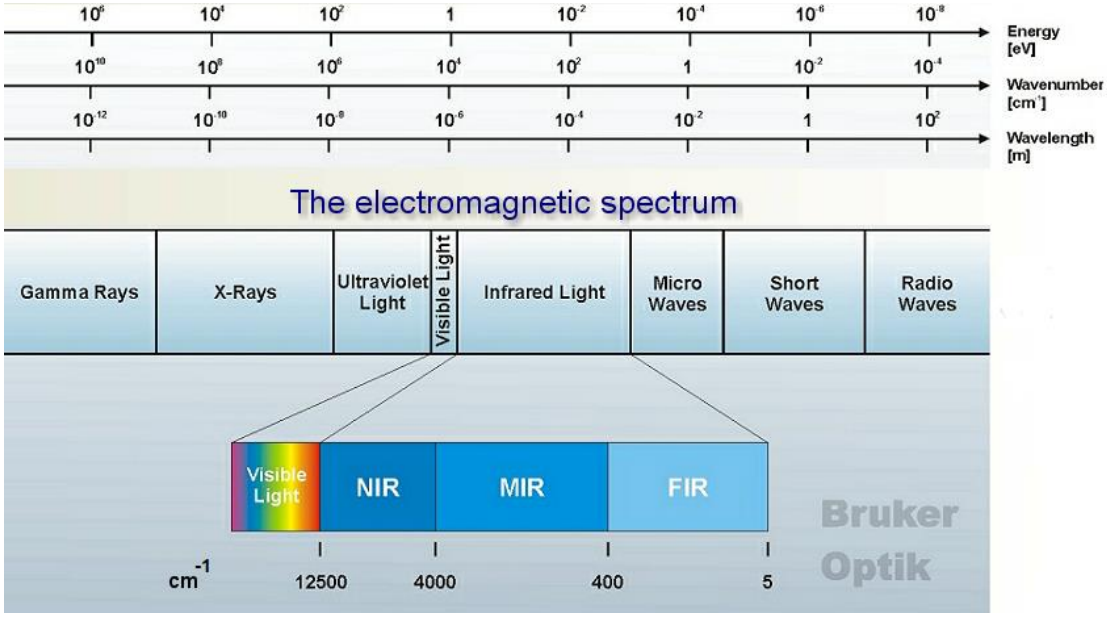

Figure 9: Electromagnetic spectrum representation (Source: Bruker, 2011b.)

Spectra from different molecular species in IR are the result of energetic changes produced in the transition of molecules from one vibrational and rotational energy state to another, existing slight energy differences between both states. These transitions produce a net change in dipole moment of the molecule and trigger changes in amplitude of some of its movements (Roming & Preindl, 2012).

IR radiation can only be absorbed by a molecule if the dipole moment of the related atomic group is changed during its vibration. The larger the change of the dipole moment is the more intensive the related IR absorption band becomes.

On the other hand, vibrations that are not accompanied by a change in the dipole moment cannot be excited and are called IR inactive. That is why, homonuclear species such as O_2, N_2 or Cl_2 that cannot suffer any net change during rotation or vibration, are not able to absorb in the IR range so they do not show a vibrational spectrum (Roming & Preindl, 2012).

Frequencies where these molecular oscillations occur are determined by the nature of the individual bonds within a molecule and by the different kind of functional groups that would associate directly with the oscillation. The two main vibrational categories that can be found are vibrations of **stretching** and **bending.**

- **Stretching vibrations:**

In this type of vibrations, the bond length is increased or decreased at regular intervals. There are two types of stretching vibrations: Symmetrical stretching and asymmetrical stretching. In the one, bond length increases or decreases symmetrically while in asymmetrically stretching length

of one bond increases and the other one decreases (Lancashire, 2004). Figure 10 shows a representation of these vibrational oscillations.

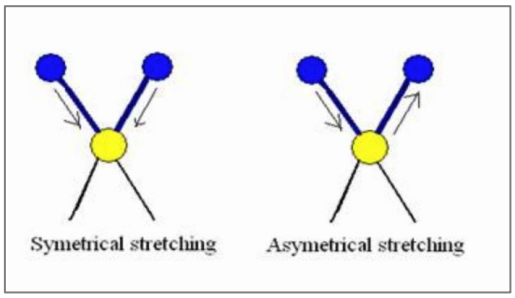

Figure 10: Stretching vibrations in Infrared rays. (Source: Lancashire, 2004)

- **Bending vibrations:**

In this type of vibrations, a change in bond angle occurs, between bonds with a common atom with respect to the remainder of the molecule. Four different vibrations appear: Scissoring and Rocking, which correspond to in-plane bending and Wagging and Twisting, which correspond to out of plane bending vibrations. These four oscillations are presented in Figure 11.

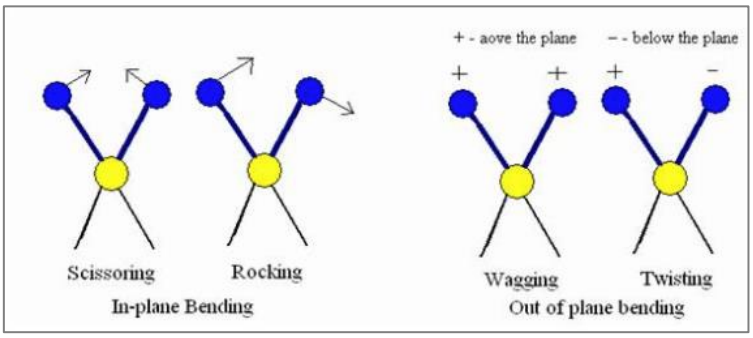

Figure 11: Bending vibrations in Infrared rays. (Source: Lancashire, 2004)

If a molecule presents two or more atoms, all types of vibrations are possible to occur. Not only that but also, some of these vibrations can even interact or couple with each other if these involves bonds with the same central atom. As a result of this coupling, a change in the characteristics of the vibrations is produced (Skoog et al., 2008). Frequently in experimental work fewer peaks are observed than the ones expected, due to some of the following factors presented by Higson (2007):

- If a molecule can have two or more different vibrations with almost identical energy, absorption IR peaks of these vibrations can fusion and appear as just one sinlge peak.
- If a molecular vibration produces an extremely low absorption, sometimes it will be too weak to be detected.
- When the symetry of a molecule is such that there is no dipole moment change due to one or more molecular oscilations.

In this context, in the Near Infrared's spectral range, overtones and combination vibration are excited. In vibrational spectroscopy an overtone band is the spectral band that occurs in a vibrational spectrum of a molecule when the molecule makes a transition from the ground state (v=0) to the second excited state (v=2), where v is the vibrational quantum number got after solving Schrödinger equation for the molecule under consideration.

In contrast, in the case of MIR's range, fundamental vibrations are typically excited. The Far Infrared's range covers the vibrational frequencies of both backbone vibrations of large

molecules, as well as fundamental vibration of molecules that include heavy atoms, as inorganic or organometallic compounds. Pure rotational bands in gases are also seen in the FIR (Bruker, 2011b).

Bearing all of this in mind, it is not surprinsing that techniques and applications of the methods based on each of the three IR spectrum regions (NIR, MIR and FIR) differ considerably. In this way, NIR measurements are performed with similar photometers and spectrophotometers, in terms of its design and components, to the ones employed in UV-vis spectroscopy. Most important applications in this spectral region are found in the quantitative analysis of industrial and agricultural materials and control processes.

On the other hand, intstruments employed in MIR region have experimented an obvious and important evolution. The different instruments employed, which will be presented afterwards, belong to two different groups: Dispersive IR spectrometers and Fourier-Transformed Infrared (FT-IR) spectrometers. The first ones were employed in the 1940's as a common analytical technique for organic compound characterization in laboratories (Thermo Nicolet, 2002). FT-IR spectrometers on the other hand, are the current standard instruments for organic compound identification work in modern analytical laboratories. Next paragraph will explain in a deeper way the differences and principles in which both techniques are based.

Finally, despite FIR region's useful potential, its employment in the past has been limited as a consequence of the experimental difficulties that presents. The few sources of this particular type of radiation that are available are notoriously weak and they are atenuated by the necessity of employing spectral order selection filters to avoid higher orders radiation to reach the detector. In this case, as happened in MIR, FT-IR spectrometers have helped to relieve much of the problem and make the FIR region much more accesible.

3.2. Instrumentation and techniques

As it was presented in the last paragraph, two different kind of spectrometers are found regarding the study of Infrared absorption measurements. These are the **Dispersive** Infrared insturments and the **Fourier-Transformed** Infrared spectrometers. In this paragraph, both techniques will be explained, as well as their differences, advantages and purposes.

3.2.1. Dispersive Infrared Instruments

The dispersive infrared spectrometer emerged in the 1940's. This design helped to spread the use of infrared spectroscopy as a common analytical technique for organic compound characterization in laboratories (Thermo Nicolet, 2002), however nowadays it is a quite obsolete technology overcome by more modern, faster and more accurate instruments. Bearing in mind this, just a general overview of the technique will be presented.

A dispersive IR spectrophotometer has a **source** and mirrors and this kind of instruments are also called grating or scanning spectrometers. In this kind of technology, the source energy is sent through both a **sample** and a **reference** path, through a **chopper** to moderate the energy achieving the **detector**, and directed to a diffraction **grating**, which is like a prism. Grating separates the wavelengths of light in the spectral range and directs each wavelength individually through a **slit** to the detector. Each wavelength is measured one at a time, with the slit monitoring the spectral bandwidth and the grating moving to select the wavelength that is being measured.

The x-axis of a dispersive infrared spectrum is typically expressed in nanometers which can be converted to FT-IR units (wavenumbers) by dividing by 10 and taking the reciprocal. An external source of wavelength calibration is required, as there is no high-precision laser wavelength to reference in the system. Figure 12 shows a representation of the main components of a dispersive IR spectrometer.

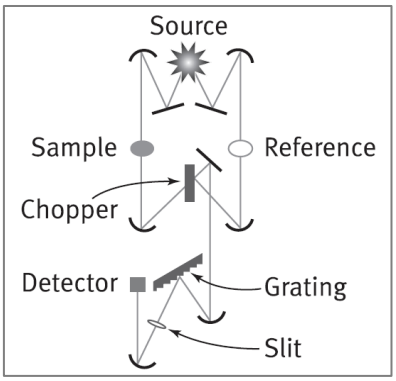

Figure 12: Main components of a Dispersive IR spectrometer. (Source: Thermo Nicolet, 2002)

3.2. Fourier-Transform Infrared Instruments

Fourier transform infrared (FT-IR) spectrometers were developed for commercial use in the 1960's, but at that time it tended to be used for advanced research only. This was due to the cost of the instrument components and the large computers required to run them. Gradually, technology advancements in computers and instruments have reduced the cost and improved the capabilities of an FT-IR spectrophotometer. Today, an FT-IR instrument is the standard for organic compound identification work in modern analytical laboratories (Thermo Nicolet, 2002).

It was not until middle 80's when dispersive spectrometers died out and gave way to FT-IR instruments. At that time, these instruments started to be way more reliable, convenient and powerful than dispersive ones. Results presented a higher signal/noise ratio and a higher resolution, accuracy and reproducibility, allowing the study of more complex spectra.

Most of the infrared spectrometers that employ Fourier Transform are based on the interferometer of Michelson. These devices present among other elements, a stationary mirror, a moving one and a beamsplitter, as well as an infrared source (laser) and a detector (Skoog et al. 2008). Figure 13 shows a representation of this interferometer.

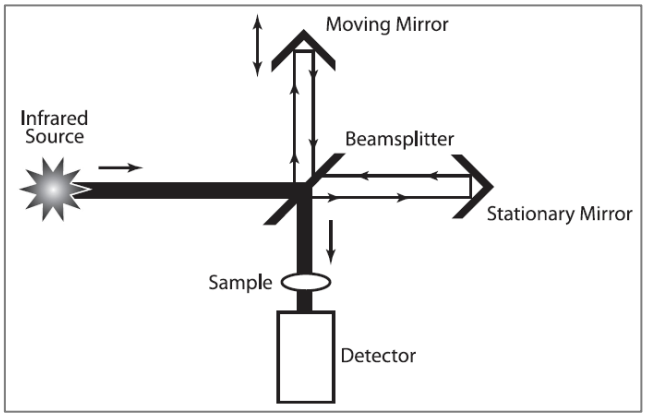

Figure 13: Main components of the Interferometer FT-IR spectrometer. (Source: Thermo Nicolet, 2002)

The energy goes from the source to the beamsplitter which splits the beam into two parts. One part is transmitted to a moving mirror; one part is reflected to a fixed mirror. The moving mirror moves back and forth at a constant speed. This speed is timed according to the very precise laser wavelength in the system which also acts as an internal wavelength calibration. The two beams are reflected from the mirrors and recombined at the beamsplitter. The beam from the moving mirror has traveled a different distance than the beam from the fixed mirror. When the beams are combined an interference pattern is created, since some of the wavelengths recombine constructively and some destructively. This interference pattern is called an interferogram. This interferogram then goes from the beamsplitter to the sample, where some energy is absorbed and

some is transmitted. The transmitted portion reaches the detector. The detector reads information about every wavelength in the infrared range simultaneously.

To obtain the infrared spectrum, the detector signal is sent to the computer, and an algorithm called a **Fourier transform** is performed on the interferogram to convert it into a single beam spectrum (Higson, 2007). A reference or "background" single beam is also collected without a sample and the sample single beam is ratio-ed to the background single beam to produce a transmittance or "%T" spectrum. This transmittance spectrum can be converted to absorbance by taking the negative $\log_{10}$ of the data points. This process of spectrum acquisition is presented in Figure 14.

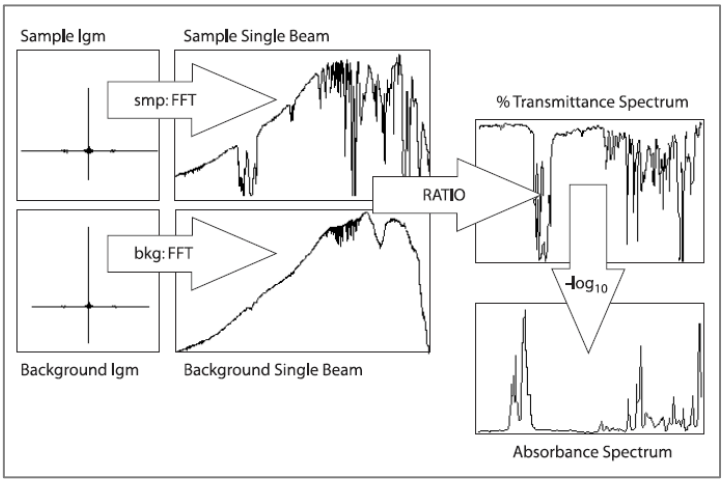

Figure 14: Process of collecting and IR spectrum in an FT-IR spectrometer. (Source: Thermo Nicolet, 2002).

The x-axis of the FT-IR spectrum is typically displayed in "wavenumbers", or cm^{-1}. This unit is a product of the Fourier transform algorithm operating on the interferogram and it is the reciprocal of the actual wavelength of light measured in centimeters at a point in the infrared spectrum.

In this kind of instruments, it is mostly used the **Attenuated Total Reflectance (ATR**) technique. ATR allows to obtain spectra through infrared radiation's reflection when a radiation beam passes from a denser medium (spectrometer mirror) to a less dense one (the sample), in other words, between two mediums with different refractive indexes.

An infrared beam is directed onto an optically dense crystal with a high refractive index at a certain angle. This internal reflectance creates an evanescent wave that extends beyond the surface of the crystal into the sample held in contact with the crystal. This evanescent wave protrudes only a few microns (0.5 µm - 5 µm) beyond the crystal surface and into the sample. Consequently, there must be good contact between the sample and the crystal surface. In regions of the infrared spectrum where the sample absorbs energy, the evanescent wave will be attenuated or altered. The attenuated energy from each evanescent wave passed back to the IR beam, which then exits the opposite end of the crystal and is passed to the detector in the IR spectrometer. The system then generates an infrared spectrum (Perkin Elmer, 2005). Figure 15 shows the representation of and ATR device.

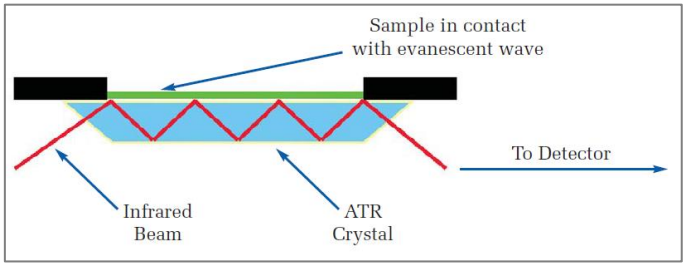

Figure 15: ATR device components. (Source: PerkinElmer, 2005).

Different materials have been employed for the crystal component of ATR devices, which include Zinc Selenide (ZnSe) and Germanium as the most common used for ATR sampling since they present a relatively low cost and a high refractive index, specially Germanium (PerkinElmer, 2005). However, they are not particularly robust with a working pH range of 5-9 and they scratch quite easily and so care must be taken when cleaning this type of crystals. In order to overcome this, the use of diamond is by far the best option as ATR crystal, because of its robustness and durability. The original purchase cost is obviously higher than that of other crystal materials available, but over the instrument's lifetime replacement costs should be minimal.

As with all FT-IR measurements, an infrared background is collected, in this case, from the clean ATR crystal. The crystals are usually cleaned by using a solvent soaked piece of tissue. Typically, water, methanol or isopropanol are used to clean ATR crystals. The ATR crystal must be checked for contamination and carry over before sample presentation, for both liquid and solid samples.

The advantages of ATR devices in comparison to traditional transmission infrared analyses are focused in the two most common forms of sample preparations: solid and liquid sample preparation for IR analysis.

Traditionally, **solid** sample preparation for IR measurements involved both grinding the material to a fine powder and dispersing it in a matrix, such as nujol or Potasium bromide (KBr). The mixture was transferred to a die and pressed to obtain a glassy disk, which would be prepared to be analyzed. **Liquids** were traditionally analyzed as thin films in cells which consist of two IR transparent windows. A Teflon® spacer was generally used to produce a film of the desired thickness.

As it can be observed, preparation could be very messy and time consuming and was further complicated by difficulties in getting sample to matrix ratios correct and homogenous throughout the sample. The materials involved were fragile and hydroscopic and the quality of measurements could be adversely affected if handled or stored incorrectly.

In this way, ATR units overcome these issues as sample preparation is minimum. When analyzing liquids, they are simply poured into the crystal which must be whole covered. In the case of solids, material is placed onto the small crystal area and pressured over the surface with a built-in pressure arm that presents the ATR device.

Advantages of FT-IR spectrometers over Dispersive devices

An interferometer in an FT-IR instrument does not separate energy into individual frequencies for measurement of the infrared spectrum. Each point in the interferogram contains information from each wavelength of light being measured. Every stroke of the moving mirror in the interferometer equals one scan of the entire infrared spectrum, and individual scans can be combined to give better representation of the actual absorbance of the sample. In contrast, every wavelength across the spectrum must be measured individually in a dispersive spectrometer. This is a slow process, and typically only one measurement scan of the sample is made in a dispersive instrument. The FT-IR advantage is that many scans can be completed and combined on an FT-IR in a shorter time than one scan on a dispersive instrument. The multiplex advantage results in **faster data collection** of an FT-IR spectrum.

There are also fewer mirror surfaces in an FT-IR spectrometer than in a dispersive one, so there are less reflection losses than in a dispersive spectrometer, so more energy reaches the sample and the detector in an FT-IR spectrometer than in a dispersive spectrometer. This means that the signal/noise ratio of an infrared spectrum measured on an FT-IR is higher than the signal-to-noise ratio attained on a dispersive instrument. Higher signal/noise means that the **sensitivity** of small

peaks will be **greater**, and details in a sample spectrum will be **clearer** and more **distinguishable** in the FT-IR spectrum.

Finally, **accuracy** and **precision** in infrared spectra are much higher when collected on an FT-IR. This is due to the use of the laser to control speed of the moving mirror and to time collection of data points throughout the mirror stroke length for each scan in an FT-IR spectrometer. The laser wavelength is a constant value, and the x-axis data points of the FT-IR spectrum are automatically referenced to this known value to maintain internal precision and accuracy of the wavelength positions, for easy later comparisons of different spectra collected in different moments or devices. This capability is not available on a dispersive infrared system. External calibration standards are required to control the accuracy of a dispersive instrument, making spectra less comparable due to instrumental unknowns during and between scans.

3.3. Applications and perspectives of MIR spectroscopy in meat quality assessment

Since IR spectroscopy's beginnings, Mid-Infrared region has been of great interest due to its capability of determining molecules structure and reliability and reproducibility of the results. Progress in instrumentation combined with exponential development in computer science and robust multivariate analyses make this technology ideal for the analysis of great volumes of samples through rapid scanning to detect food components and compounds.

According to Lozano (2015), MIR spectroscopy has been employed for several applications regarding food quality assessment since 1990s. One of the ambits is the chemical composition determination of food, with examples as fatty acid composition determination by Ripoche & Guillard (2001), protein content in milk by Etzion et al. (2004), carotenoid content in peaches by Ruiz et al. (2008), minerals in milk by Soyeurt et al. (2009) or sugars and citric acid in tomatoes by Scbisz et al. (2011).

Moreover, MIR spectroscopy was also employed for the detection of bacterial presence in food systems. As Lozano (2015) references, Ellis and Goodcare in 2001 stated that this technique would be faster and less time consuming than current microscopic analyses employed, studying chicken breast though FT-MIR. Also, Sahar (2014) studied MIR spectroscopy use as a technique for monitorization of microbial alteration in broiler breasts stored in aerobiosis.

Also, Lozano (2015) cited diverse studies that had employed MIR spectroscopy to difference geographical origin of wine, cheese, olive oil or honey, in a context of fraud in Protected Designation of Origin products.

Despite its increasing employment, MIR spectroscopy use for meat quality analysis is still very limited, mostly restricted to the determination of microbial-related alterations or to the detection of adulterations in different animals' meat. Few studies have been performed regarding chemical parameters in meat products, so it is still a wide field of research with multiple chances and possibilities for future research. That is why this project was firstly proposed, in order to deepen in the study of chemical characteristics (lipid and protein oxidation) involving the quality of horse meat.

To end up with this chapter, Table 5 presents a revision of the references found involving MIR application in meat products.

Table 5: MIR spectroscopy application references in meat products analysis

Parameter	Processing technique	Wavenumbers range (cm^{-1})	References
Differentiation between pork, chicken and turkey minced meat.	Reflectance	4,000-800	Al-Jowder et al. (1997)
Determination of the content of lamb meat in beef and lamb meat	Reflectance	4,000-640	McElhinney et al. (1999)
Differentiation between pork, chicken, turkey and beef raw minced meat.	Reflectance	4,000-640	Downey et al. (2000)
Bacterial development in chicken meat	Reflectance	4,000-600	Ellis et al. (2002)
Bacterial development in beef meat	Reflectance	4,000-600	Ellis et al. (2004)
Aminoacids composition in animal feed	Reflectance	4,000-400	Qiao & Van Kempen (2004)
Air stored and MAP stored beef meat	Reflectance	4,000-400	Ammor et al. (2009)
Adulterations detection in beef with meat horse, fat or vegetable protein	Reflectance	4,000-650	Meza-Márquez. 2010)
Adulteration detection in beef with turkey meat	Reflectance	4,000-700	Alamprese et al. (2013)
Bacterial development in chicken breast	Reflectance	4,000-700	Sahar. (2014)
Adulteration detection in beef meat with non-meat ingredients (NaCl, phosphates, carrageenan and maltodextrin)	Reflectance	4,000-400	Nunes et al. (2016)
Determination of fatty acid content (SFA, MUFA, PUFA and Palmitic acid) in meat products	Reflectance	4,000-400	Lucarini et al. (2017)
Characterization of microbial deterioration of fallow deer and goat meat	Reflectance	4,000-400	Pinho-Moreira et al. (2018)

Chapter II. Objectives

The main goal that is pretended to achieve throughout this current Master in Agricultural Engineering project is to deepen in the study of lipid and protein oxidation in horse meat employing FT-MIR spectroscopy, in a context of contributing to find better profitability on the meat equine sector. This main objective includes the following specific ones:

1. To obtain and study the typical MIR spectra of TBA and Carbonyls as oxidation markers, regarding their main peaks of absorption.

2. To stablish prediction models (calibration and validation) between the spectral measurements of lipid and protein oxidation markers obtained by FT-MIR and the classical quantification of the compounds. This way, what is intended is to decide if this technology is useful to estimate the values of this kind of marker compounds employing MIR spectroscopy simply from raw meat samples directly, or if it is preferable to perform a previous extraction of these compounds before executing the MIR analysis.

3. To determine the influence of slaughter age and feeding regime of the animals used on the degradation of lipids and proteins of horse meat.

4. To perform an initiation in Mid-Infrared spectroscopy technology applied to food quality analysis.

5. To complement the agronomic, industrial and project-elaboration skills acquired during the MSc in Agricultural Engineering, adding a more scientific researcher profile.

Chapter III. Materials and Methods

In this chapter, materials and methods employed throughout the project will be explained. First of all, it will be described the experimental design employed in this work. Through the second section, animal samples will be described. In third place, instrumentals used to perform the analysis will be presented, explaining the equipment used for this task and its function, as well as the methodology employed in order to analyze the different samples. Finally, it will be detailed the statistical treatment applied to all the obtained data, as well as a detailed theoretical background important for the understanding of the work.

1. Experimental design

Galician Mountain x *Burguete* crossbred foals

A-C GROUP
- **Slaughter age**: 26 months (Adult)
- **Finishing diet**: Conventional concentrate
- **n** = 12

Y-L GROUP
- **Slaughter age**: 13 months (Young)
- **Finishing diet**: Linseed concentrate
- **n** = 11

24h post-mortem

Vacuum packed: 4 days

Vacuum packed: 0,4,8 or 12 days

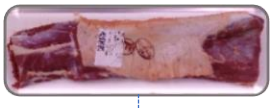

Longissimus dorsi

CLASSICAL OXIDATION ANALYSIS

Lipid: *TBARS* → TBA (mg MDA/kg sample)

Protein: *DNPH* → Carbonyls (nmole/g protein); Protein Content (%)

FT-MIR SPECTROSCOPY ANALYSIS

LO extracts

PO extracts

Frozen storage (-18ºC)

PREDICTION MODELS CONSTRUCTION

FT-MIR SPECTROSCOPY ANALYSIS

COMPARISON OF THE MODELS

SPECTRA CHARACTERIZATION

PREDICTION MODELS CONSTRUCTION

2. Animal material

As shown in last paragraph *1. Experimental design*, oxidation marker compounds employed in this project were extracted from twenty-three out of forty-six *Galician Mountain* x *Burguete* crossbred foals which are part of a wider PhD Thesis elaborated by Ruiz-Darbonnens (2017).

As mentioned during Chapter I, in the North of Spain horsemeat production is based on extensive systems. The 46 foals were kept with their mothers and allowed to suck freely on pasture from the birth to the weaning at the age of 6-7 months (1st period). Then, foals were randomly divided in two groups to be slaughtered at two different ages: 22 foals were slaughtered at 13 months (403 ± 30 days), which correspond to the "Young" (Y) group and 24 foals were slaughtered at 26 months of age (784 ± 37 days) which correspond to the "Adult" (A) group. Both groups of animals were fed on the same pasture following a rotational grazing (2nd period). This period lasted 3 months (± 15 days) and 16 months (± 15 days) for Young and Adult groups, respectively. Finally, foals were supplemented for 104 days (± 10 days) with a finishing diet based on concentrate (3rd period). The vegetation during the three periods was composed by seeded (*Lolium perenne* and *Trifolium repens*) and natural fields (*Agrostis spp.*, *Lotus corniculatus*, *Holcus lanatus*, *Bromus mollis* or *Pseudoarrenatherum longifolium*, among others).

During the 3rd period, 11 foals from Young group and 12 from Adult group were randomly chosen and supplemented with standard/conventional concentrate (C). Then again, the others 11 foals from Young and 12 from Adult group were randomly chosen and supplemented with linseed-rich concentrate (L) (at 5%). Thus, 4 experimental groups were obtained: Y-C, Y-L, A-C and A-L. Foals were supplemented with 2 kg of the mentioned concentrates to carry out an optimal animals' fattening and to improve the meat lipid profile (linseed supplementation). These supplementations were increased from 0.3 kg to 2 kg per foal/day for the first 10 days (adaptation term). It should be noted that for this project the LO and PO marker compounds used were obtained just from the A-C and Y-L groups, with a total of 12 and 11 animals respectively, as shown in the last paragraph *1. Experimental design.* Table 6 shows the number of animals employed for this work and the oxidation quantification performed for each one.

Table 6: Number of animals employed for the LO and PO quantification and further FT-MIR measurement

YOUNG – LINSEED (Y-L)			**ADULT – CONVENTIONAL (A-C)**		
No Animal	**Ageing (days)**	**Analyses**	**No Animal**	**Ageing (days)**	**Analyses**
9026	0,4,8,12	LO	9914	4	LO, PO
9027	0,4,8,12	LO, PO	9915	4	LO, PO
9028	0,4,8,12	LO	9916	4	LO, PO
9459	0,4,8,12	LO	9917	4	LO, PO
9460	0,4,8,12	LO	9918	4	LO, PO
9461	0,4,8,12	LO	9919	4	LO, PO
9462	0,4,8,12	LO	10368	4	LO, PO
9463	0,4,8,12	LO	10369	4	LO, PO
9464	0,4,8,12	LO	10370	4	LO, PO
9465	0,4,8,12	LO, PO	10371	4	LO, PO
9466	0,4,8,12	LO	10372	4	LO, PO
			10373	4	LO, PO
Total animals: 11		**Total samples: 60**	**Total animals: 12**		**Total samples: 36**

Foals were transported 50 km to the abattoir the day before slaughter in compliance with current European regulations (Council Regulation 1/2005EC, 2005), and were stunned with a captive bolt, slaughtered and dressed according to the specifications outlined in the European legislation (Council Directive 93/119/EC, 1993). 24 hours post-mortem, *Longissimus dorsi* muscles of each

of the animal were extracted and vacuum and fridge-stored for 0, 4, 8 or 12 days at 4ºC before executing LO and PO quantification, which will be explained in the next paragraph *3. Samples analysis procedure and Instrumentation*.

3. Samples analysis procedure and Instrumentation

In this paragraph it will be presented the oxidation compounds analyses carried out in this work. Firstly, it will be briefly presented the classical techniques employed for extracting the marker compounds of LO and PO from raw meat samples, cited in paragraphs *2.2 Lipid Oxidation* and *2.3 Protein Oxidation* from Chapter I. After that, it will be explained the technique employed for the acquisition of all the spectra once the marker compounds were isolated. Also, in this paragraph the instruments employed for the analyses performed throughout this project are presented. It should be noted that the equipment employed for the FT-IR analyses will be more explained in detail, as it corresponds to the instrumentation employed through this work, while the extraction of the compounds had been previously performed in a previous project.

3.1 Oxidation quantification and Marker compounds extraction

This paragraph includes the procedures followed during the analytic method for both lipid and protein oxidation quantification of the 23 meat samples employed for this project. Through them, the marker compounds of both oxidation reactions were extracted for their later FT-MIR spectra measurement.

3.1.1. LO quantification procedure (TBARS analysis)

Lipid oxidation was evaluated through the method proposed by Vyncke (1975) with some variations applied. This corresponds to the TBARS analysis, previously presented in paragraph *2.2.1. Thiobarbituric Acid Reactive Substances method*, which was employed for every meat sample studied.

Two grams of meat were minced and 10 mL of 5% TCA was added. Then, it was homogenized with an Ultra-Turrax (IKA T25 digital ULTRA-TURRAX) for 1 min at 11,500 rpm. The homogenized was stored at -10ºC for 10 min and was centrifuged at 5,000 rpm, for 10 min at 4ºC. Supernatant was filtered using a Filter-lab no 1246 filter on ice. 1 mL of the filtered substance was taken and reacted with 1 mL 0.02 M TBA. Immediately, it as incubated in a water bath at 96ºC for 40 minutes. Then, tubes were chilled and centrifugated at 10,000 rpm for 4 minutes at 20ºC.

Absorbance was measured at 530 nm employing an Spectrophotometer UV/vis with diodes detector, model Shimadzu UV-2101PC. TBARS values were calculated from a pattern curve of 1,1-3,3 tetraethoxypropane (TEP) and expressed as mg of MDA/kg of meat sample.

Then, once the quantification of TBA was performed for each of the samples, the resulting compounds were frozen-stored at -18ºC inside Eppendorf tubes® 3810X in a fridge located in Laboratory 14 from *Los Olivos* building at Universidad Pública de Navarra (UPNA). Remaining meat samples were also frozen-stored at -18ºC at UPNA.

3.1.2. PO quantification procedure (DNPH method)

Protein carbonyls, measured as total carbonyl content, were quantified according to the method described by Oliver et al. (1987) and modified by Vuorela et al. (2005), commonly known as DNPH method. Two different measurements were made for protein oxidation in every meat sample: carbonyl quantification ((a) samples) and protein quantification ((p) samples).

Each of the meat samples was homogenized with 20 mL of 0.6 M NaCl for 60 s using an Ultra-Turrax homogenizer (IKA T25 digital ULTRA-TURRAX). Two aliquots of homogenate were taken (0.1 mL) and were transferred into Eppendorf vials. Proteins were precipitated with 10% (1 mL) trichloroacetic acid (TCA) and were centrifugated for 5 minutes at 10.000 g. One of the

pellets was treated with 2N HCl (1 mL) in order to quantify proteins and the other one with 0.2% 2,4-dinitrophenyl hydrazine (DNPH) in HCl 2M (1 mL) to quantify carbonyls.

After 1 hour in darkness incubation of the samples (shaken every 20 minutes) 10% TCA was added (0.8 mL). Then, samples were vortexed shaken (Vortex Mixers ZX3 Velp Scientifica) for 30 s and were left incubating for 15 minutes at 0-4ºC. They were centrifugated for 5 minutes at 10.000 g and supernatant was removed carefully without damaging the pellet with the Pasteur pipet. Pellet was twice washed with ethanol/ethyl acetate (1:1) and was dried with N_2 gas.

Finally, the pellet was dissolved in 1.5 mL of 20 mM sodium phosphate buffer with 6 M guanidine hydrochloride, shaken, and centrifuged for 5 min at 10.000 g in order to precipitate insoluble fragments. Protein concentration samples (p) were measured spectrophotometrically attending to absorbance at 280 nm (Spectrophotometer UV/vis with diode detector, Shimadzu UV-2101PC) using Bovine Serum Albumin (BSA) as standard. Carbonyl content was expressed as nmole of carbonyls per milligram of protein using an extinction coefficient of 21.0 mM^{-1} cm^{-1} at 370 nm.

Then, once the quantification of Protein and Carbonyls was performed for each of the samples, the resulting compounds were frozen-stored at -18ºC inside Eppendorf tubes® 3810X in a fridge located in Laboratory 14 from *Los Olivos* building at Universidad Pública de Navarra, as well as mentioned with TBA. As well as with LO, remaining meat samples employed for PO were frozen-stored at -18ºC in a freezer located in Universidad Pública de Navarra.

Prior to analysis, these compounds and TBA ones were transferred to a different fridge in the same storage conditions, located in Navarra Biomed biomedical research center, where FT-MIR analysis was later performed.

3.2 MIR spectra acquisition

Firstly, it will be explained in detail the procedure followed in order to obtain the total amount of MIR measurements from the TBA and Carbonyls compounds. It should be noted that the experimental procedure carried out was specifically designed for this project via trial and error, as no similar analyses had been done previously regarding MIR spectroscopic measurements of the studied compounds. After that, an introduction to infrared spectra interpretation will be presented.

3.2.1. Experimental procedure and Instrumentation

In the first place, materials employed for the analyses of the samples will be presented as a list:

- Spectrometer FT-IR Vertex 80v – Bruker Germany
- Accessory A225/QPlatinum-ATR – Bruker Germany
- PC with OPUS v7.0 installed
- TBA, Carbonyl (a) and Protein Content (b) frozen-stored Eppendorf samples
- Advanced IR Vortex Mixer – Velp® Scientifica
- Crushed ice
- Plastic Tupperware (2x)
- Adjustable-volume micropipette (10-100 µl)
- Micropipette sharps
- Isopropyl alcohol
- Distilled water
- Nitrile disposable gloves
- Berkshire Durx® 670 optic cleaning wipes
- Biohazard bin
- Disposables bin
- Permanent marker

Before samples preparation, a start up of the working place was performed for every measurement. In this way, firstly the spectrometer device was set on. In order to do that, a compressor should firstly be turned on. Then, the FT-IR Vertex 80v device itself was turned on, and afterwards PC was switched on. After that, evacuation of the interferometer compartment had to be performed as this equipment allows to work under vacuum conditions in the optical system which reduces the possible interferences produced by the water steam or the carbon dioxide in the measurements. During this, preparation of the Tupperware with crushed ice was performed, as well as the checking of distilled water and isopropyl alcohol bottles. Finally, A225 / QPlatinum-ATR accessory, made of a diamond crystal, was attached to the spectrometer. Figures 16 and 17 show the device and components of the spectrometer employed.

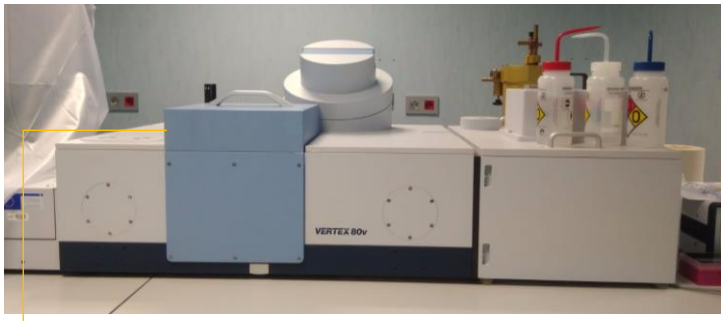

Figure 16: FTIR Vertex 80v device in Navarra Biomed's laboratory

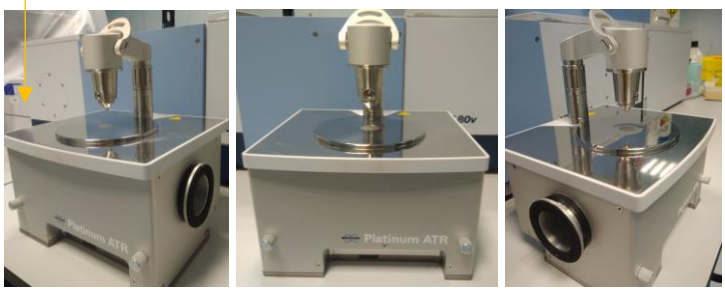

Figure 17: ATRATR A225 / QPlatinum-AT accessory

Once the equipment was prepared, samples were removed from the freezer at -18ºC. Samples were transferred to a Tupperware full of crushed ice, in order to maintain the temperature and perform a gradual "defrosting". It was not an actual defrosting as the freezing point of the compounds was below -18ºC, so the samples were in liquid state even during frozen-storage.

Then, the measurement process began. Firstly, a reference spectrum was taken with the ATR device empty. This reference was taken before each measurement as it was observed that if more than one measure was made with the same reference, the spectra obtained were not clean, and presented high noise signal. In this point it must be noted that previously to the final analyses from this work, it was first carried out a training period in which several measurements were performed in order to detail and develop a consistent protocol for the definitive samples analyses. During this fine-tuning period, different materials and compounds were measured (solids, liquids, mashes, mixtures, pure compounds…) and as aforementioned, it was observed that it was necessary to perform an empty-device measurement before every sample measurement in order not to obtain high noise signals in the final spectra.

Once the reference measurement was finished, the sample measurement was performed. In the first place, during the training period it was observed the necessity of uniformly mixing the samples before measuring them, as some of the compounds were decanted over the bottom of the Eppendorf tubes due to their long-time storage. For that, the Vortex Mixer was employed, applying 2,500 rpm for 15-20 seconds. Then, 15 µl of the Eppendorf tube were extracted using

the adjustable micropipette. This quantity was enough to ensure that all diamond crystal surface was completely covered and that there was a perfect contact between the sample and the crystal. Micropipette's sharp was disposed after every use, leaving them in the biohazard bin. Figure 18 shows the materials employed in this point.

Figure 18: Adjustable Micropipette and micropipette sharps (left) and Advanced IR Vortex Mixer (right)

A total of 6 repetitions were performed per sample analyzed. For each sample, 32 scans in the 4,000–400 cm^{-1} spectral range were recorded with a resolution of 4 cm^{-1}. This total amount of repetitions per sample was also stablished during the fine-tuning period. It was observed that, on average, 1 out of 15 measurements of the same sample usually showed outlier or anomalous spectra results in comparison to the 14 others (this was performed for a total of 105 measurements from 10 different samples). In this way, it was stablished that 6 repetitions of the same sample would be enough to obtain consistent and similar results. A total of 240 measurements were performed during TBA final analyses, while a total of 216 measurements were carried out during PO final analyses (108 from Carbonyls and 108 from Protein content).

Once every sample measurement was performed, it was necessary to clean the crystal surface in order to leave it ready for the next sample's reference measurement. For that, a piece of Berkshire Durx® 670 optic cleaning wipe was employed along with distilled water and isopropyl alcohol. Detritus were introduced into the disposables bin.

Every measurement provided a single and unique spectrum, which was saved in the PC in order to employ them for the chemometric model of the data obtained.

3.2.2. Interpreting resulting spectra

Now, a brief theoretical introduction will be presented in order to understand the basis of how to "read" the resulting spectra obtained.

A functional group within a molecule is considered as a harmonic oscillator which in a first approximation vibrates without being affected by the rest of the molecule. This results in the fact that a particular functional group shows IR absorption bands within characteristic spectral ranges.

This fact serves as the basis for spectral interpretation, whereby the position, intensity and half-width of a band decide whether a band can be assigned to a specific structural group. Many functional groups of organic molecules show characteristic vibrations corresponding to absorption bands within defined ranges of the IR spectrum. This way, the position and intensity of the absorption bands are extremely specific in the case of a pure substance. This enables the IR spectrum to be used as a highly characteristic feature for identification (Nikonenko et al. 2005).

So, once the spectra of both LO and PO marker compounds were acquired, bibliographic references were consulted in order to identify the different bonds that had appeared.

First of all, it is important to explain that MIR spectra of organic compounds are said to have two general areas: The Functional Group Region and the Fingerprint Region. First one is

comprehended between 4,000 cm^{-1} and 1,500 cm^{-1} and peaks in this region are characteristic of specific kinds of bonds, and therefore can be used to identify if a specific functional group is present. The Fingerprint region, on the other hand, is referred to the area between 1,500 and 400 cm^{-1} and peaks in this region arise from complex deformations of the molecule. They may be characteristic of molecular symmetry, or combination bands arising from multiple bonds deforming simultaneously (Gable, 2014).

Most spectra using electromagnetic radiation are presented with wavelength as the X-axis. Originally, IR spectra were presented in units of micrometers. Unfortunately, a linear axis in micrometers compresses the region of the spectrum (10-15 μm) that usually has the largest number of peaks. It can be rectified this by presenting the spectrum on a linear scale vs. frequency (Hz), but the magnitude is unwieldy (10 μm = 3 x 1013 Hz). A different measure, the wavenumber, is given in the unit cm^{-1}, as it was presented in the equation from paragraph *3.1 Fundamentals* of IR from Chapter I.

The spectra obtained may appear to be "backward" (large wavenumber values on the left, running to low values on the right) but this is a consequence of the μm to cm^{-1} conversion. It should be noted that old spectra in microns did read from low wavelength on the left to large wavelength on the right. Figure 14 from paragraph *3.2. Fourier-Transform Infrared Instruments* from Chapter I shows this measuring unit change.

4. Statistical/Chemometric treatment

4.1 Uni-Multi variate calibration introduction

Chemometrics is the science of extracting information from chemical systems by data-driven means. Chemometrics is inherently interdisciplinary, using methods frequently employed in core data-analytic disciplines such as statistics, applied mathematics, and computer science, to address problems in chemistry, biochemistry, medicine, biology and chemical engineering (Massart et al., 1988).

In order to study and obtain conclusions about the MIR spectra analysis performed, chemometrics will be employed, specifically multivariate calibrations for the quantitative analysis of spectra. The purpose of calibration techniques is to correlate measured quantities like, in this work's case, the absorption of infrared radiation with properties of the system, for example, the concentration of one component in a multicomponent system. Usually, two steps are required: the calibration of the method and the analysis to determine a value of an unknown sample.

On the one hand, it will be explained the Univariate calibration analysis, a method well known in analytical laboratory work. For calibrating the system, a set of calibration samples needs to be measured. The concentration of the substance in question contained in the calibration samples has to be known, e.g. it has to be determined by a different analytical technique. Then, the height of a peak characteristic for the substance is determined from the spectra and plotted versus the known concentrations. The resulting graph will be used to evaluate the concentration of an unknown sample by measuring the peak height and reading the corresponding concentration from the graph. In order to analyze multicomponent samples, a signal characteristic for each component must be used for the calibration and analysis. These signals must be well separated to be indicative.

Multivariate calibrations make use of not only a single spectral point but they take into account spectral features over a wide range. Therefore, the analysis of overlapping spectral bands or broad peaks becomes feasible. The information contained in the spectra of the calibration samples is compared to the information of the concentration values using a Partial Least Square (PLS) regression. This method assumes that systematic variations observed in the spectra are a consequence of the concentration change of the components. However, the correlation between the components concentration and the change in the infrared signal does not have to be a linear one.

Multivariate calibrations require a large number of calibration samples and yield a large amount of data (several spectra with hundreds or thousands of relevant data points). In order to conveniently handle the data, the spectral data and the concentration data are written in the form of matrices, where each row in the spectral data matrix represents a sample spectrum. The concentration data matrix contains the corresponding concentration values of the samples. The matrices will be broken down into their Eigenvectors which are called factors or principal components. The advantage of this approach is, that not all of the principal components are necessary to describe the relevant spectral features; for example, some of these vectors simply represent the spectral noise of the measurement.

Only the relevant principal components will then be used instead of the original spectral data, thus leading to a considerable reduction of the amount of data. A PLS regression algorithm will be deployed to find the best correlation function between spectral and concentration data matrix. This will be explained in paragraph *4.3 Theoretical background.*

The determination of the number of principal components is a crucial point for the quality of the calibration model. Using an insufficient number of principal components leads to a poor reproduction of the spectral data and therefore the model will not be able to recognize changes in the spectral features. This is called "underfitting". On the other hand, including too many principal

components just adds spectral noise to the regression and does not increase the amount of valuable information ("overfitting").

Multicomponent systems can be analyzed for each component separately (PLS 1 algorithm) or simultaneously for all components (PLS 2 algorithm). However, the PLS 1 analysis usually yields better results, and therefore is mainly used for multivariate calibrations. PLS method is explained in following paragraph *4.3 Theoretical background.*

4.2 Procedure and software employed for quantitative analysis

In order to perform the quantitative analysis employing all the spectra acquired, it was used a software package: QUANT 2, from Bruker's Opus v.7.0.

The purpose of QUANT is the quantitative analysis of an unknown multicomponent sample. However, in order to perform an analysis, QUANT first had to learn about the system of this work. This means it was necessary to develop a chemometric model, using a number of calibration samples of known composition that were representative for the system studied. The MIR spectra of these samples would be used by QUANT to calculate a calibration function, which essentially is the model used for the analysis of unknown samples later. However, the model must be evaluated to test its reliability of prediction (validation). There are two validation types: "Cross Validation" and "Test Set Validation". While in the latter case two different sets of samples are used, the Cross Validation uses the same set of samples for calibration and validation.

In the present work it has been used Cross Validation. With this method only one set of samples representative for a multicomponent system is used to calibrate and validate a system via cross validation. Before starting the calibration, one sample is excluded from the entity of samples. This sample is used for the validation. The remaining samples are used to calibrate the system. The sample used for validating the system must not be part of the calibration set.

The advantage of cross validation is the smaller number of samples required. Especially, if the number of samples available is limited this method should be preferred upon the test set validation.

Frequency Region

The method employed by QUANT is a "full spectrum method"; what means that the model should improve with an increasing number of data points. However, in some cases spectral noise or additional components in the samples may cause the algorithm to interpret these features, which can degrade the model. In the Figure 19 it is shown an example of what spectral noise is.

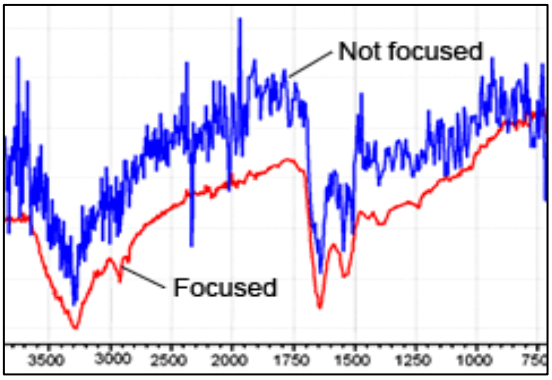

Figure 19: Spectral noise representation from two spectra (Source: Shimadzu, 2018)

In these cases, it is advisable to limit the frequency region used for the PLS regression. Usually this step is taken to improve a regression that did not yield a satisfactory model.

When narrowing down a spectrum to a few absorption bands it is found, that in general bands between 0.7 and 1.0 absorbance units (AU) generate the best results. Values greater than 2.5 should not be used. Also, it is not necessary to identify substance specific peaks, but rather to include the complete frequency region of the functional groups (e.g. alcohols) from a spectrum. Nevertheless, in case of a minor component, it can be helpful to know the absorptions in the spectrum to find relevant frequency regions.

Data Preprocessing

Data preprocessing is an important stage when performing a calibration. To ensure the reproducibility of the calibration samples, several spectra of each sample must be acquired. If the spectra of the same sample are not identical, a data preprocessing procedure must be chosen to bring them into line with each other.

Data preprocessing can eliminate variations in offset or different linear baselines. In quantitative analysis, it is assumed that the layer thickness (i.e. the effective pathlength of the infrared light in the sample) is identical in all measurements. A lack of reproducibility in sample preparation can easily cause variations in sample thickness. If the thicknesses are different or unknown, this effect can be eliminated by a normalization of the spectra. The purpose of data preprocessing is to ensure a good correlation between the spectral data and the concentration values. The following methods can be applied:

- **Linear Offset Subtraction:** shifts the spectra in order to set the y-minimum to zero.
- **Straight Line Subtraction**: fits a straight line to the spectrum and subtracts it. This accounts for a tilt in the recorded spectrum.
- **Vector Normalization (SNV):** normalizes a spectrum by first calculating the average intensity value and subsequent subtraction of this value from the spectrum. Then the sum of the squared intensities is calculated and the spectrum is divided by the square root of this sum. This method is used to account for different samples thickness, for example.
- **Min-max Normalization:** first subtracts a linear offset and then sets the y-maximum to a value of 2 by multiplication with a constant. Used similar to the vector normalization.
- **Multiplicative Scatter Correction:** performs a linear transformation of each spectrum for it to best match the mean spectrum of the whole set. This method is often used for spectra measured in diffuse reflection.
- **First Derivative**: calculates the first derivative of the spectrum. This method emphasizes steep edges of a peak. It is used to emphasize pronounced, but small features over a broad background. Spectral noise is also enhanced.
- **Second Derivative**: similar to the first derivative, but with a more drastic result.

No general recommendation can be stablished whether a given data set should be preprocessed or which method is suited best for it. Therefore, the optimal data preprocessing method can only be found empirically by applying several methods to the spectral data and comparing the results.

Taking all of this in consideration, what was done with the FT-MIR spectra acquired from TBAs, Carbonyls and Proteins along this work was the following:

- All the spectra were acquired, as explained in paragraph *4.2 MIR Spectra acquisition*, 6 times per sample of TBA, Carbonyl and Protein.
- In some cases, an average spectrum from the 6 repetitions was performed using OPUS v.7.0 tool: *Promedio.*
- The set of spectra was introduced in package QUANT 2 as well as the value of the quantitative parameter studied (TBA, Carbonyl or Protein) for each of the spectra.
- A first Cross Validation was performed.

- Preprocessing methods were applied and afterwards, new cross validations were performed.
- Results were checked, outliers were subtracted and validation was once again performed, cyclically until the best parameters (R^2, RMSECV, RPD…) were obtained for each group of spectra.

4.3 Theoretical background

Once it has been explained the method employed in order to perform the quantitative analysis of the samples of study, it is presented the theoretical background of this methodology.

In general, the aim of a quantitative analytical method is to determine the property *Y* of a system from an experimentally observable *X*, whereby *X* and *Y* are correlated by a calibration function *b*.

$$\vec{Y} = X \cdot \vec{b}$$

$$\begin{bmatrix} Y_1 \\ Y_2 \\ .... \\ Y_3 \end{bmatrix} = \begin{bmatrix} \text{Spectrum 1} \\ \text{Spectrum 2} \\ .... \\ \text{Spectrum 3} \end{bmatrix} . \vec{b}$$

The vector *Y* consists of the component values (of a single component) as determined by the reference measurements. The row vectors of the matrix *X* are formed from the calibration spectra. The aim is to determine the vector *b*. When *b* is known, the prediction of unknown values for *Y*n can be done. The solution of the above system of equations is given by:

$$b = (X^T \cdot X)^{-1} \cdot X^T \cdot Y$$

The PLS Method

During PLS regression, the matrices X are reduced to only a few factors. The difficulty is the inversion of the matrix X^TX. The PLS method involves the calculation of a restricted inverse instead of the complete. PLS requires the matrix X is bi diagonalized:

$$X = UBV^T$$

The matrices U and V are orthonormal, and B is of bi-diagonal form. This can also be expressed as:

$$X = TV^T$$

The elements of the matrix T are known as “scores” and the PLS vectors are sometimes called “loadings.” A starting vector v_1 for the PLS analysis is chosen:

$$v_1 = X^T \cdot Y / \|X^T \cdot Y\|$$

The first PLS vector shows the correlations between the component values and the spectral intensities of the calibration spectra. The PLS analysis can be terminated if the component values Y are reproduced in a consistent way with the help of the vector b (regression).

The number of PLS vectors used is defined in the QUANT program by the size of the “rank”. Optimum PLS rank can be calculated only if the number of calibration spectra is sufficiently high (e.g. one component and 20 calibration spectra). The PLS regression has the advantage that the PLS factors are arranged in correct sequence, according to their relevance to predict the component values. The first factor explains the most drastic changes of the spectrum.

The residual (Res) is the difference between the true and the fitted value. Thus, the sum of squared errors (*SSE*) is the quadratic summation of these values.

$$SSE = \sum[Res_i]^2$$

The root mean square error of estimation *RMSEE* is calculated from this sum, with *M* being the number of standards and *R* the rank:

$$RMSEE = \sqrt{\frac{1}{M-R-1} \cdot SSE}$$

The coefficient of determination (R^2) gives the percentage of variance present in the true component values, which is reproduced in the regression. R^2 approaches 100% as the fitted concentration values approach the true values:

$$R^2 = (1- \frac{SSE}{\sum(yi-ym)2}) \; x \; 100$$

R^2 can be negative. This is true (in some cases) for low ranks, when the residuals are larger than the variance in the true values (*yi*): The sum of residuals (*SSE*) decreases with increasing rank, so R^2 approaches a limiting value of 100%.

An important measure is the Leverage value (h_i):

$$h_i = diag(UU^T)$$

The *hi* values are a measure of the influence a spectrum has on the PLS model for a particular component. A large value can arise if a spectrum has been measured under irregular conditions.

The hi values are always smaller than 1 and the total sum of all *hi* is equal to the rank (*R*):

$$\sum h_i = R$$

R/M is the mean leverage value.

The lowest and the highest concentration values have the largest leverage values. The leverage values which are above the limit are not outliers as it might be suspected. The user must be very careful in removing spectra from the calibration list for a one component system.

The measured calibration spectrum after the data preprocessing is represented by *xi* and the spectrum reconstructed from the PLS vectors *vr* as *si*. *ti,r* are the score coefficients:

$$s_i = \sum t_{i,r} v_r$$

The spectral residual ("*SpecRes*") is calculated by a summation of all selected frequency points of the difference spectrum:

$$SpecRes = \sqrt{\sum (x_i - s_i)^2}$$

The better the reproduction of a spectrum is, the smaller is the spectral residual. To recognize outliers, the squared spectral residual is compared with the mean value of all others (by calculating the *FValue* using the following formula):

$$FValue_i = \frac{(M-1)(SpecRes_i)^2}{\sum_{j \neq i}(SpecRes_j)^2}$$

F-values are used for recognizing outliers in the calibration data set. They can generally be derived from the spectral and concentration values of the measured sample. There are two kinds of F-values: those which are calculated directly from the spectral residue, and those which result from the difference of the true and the predicted values (predicted by the chemometrical model). The larger the F-value of the analyzed sample, the more likely it is an outlier.

Spectra poorly represented by the PLS vectors have a high *FValue*. From the *FValue* and the number of degrees of freedom a probability *FProb* can be calculated. *FProb* indicates the probability that a standard is a spectral outlier. The limit for the automatic outlier detection is 99%.

It is important to not be deceived by good results from a calibration, particularly at high ranks. Since the spectra and the component values are present as input, it is not difficult to reproduce the component values (Fit = True) using enough PLS vectors. This fact is completely different than the prediction of a sample which is not contained in the calibration set, as it is done in the validations

In case of a cross validation, the **r**oot **m**ean **s**quare **e**rror of **cross validation** (*RMSECV*) can be taken as a criterion to judge the quality of the method:

$$RMSECV = \sqrt{\frac{1}{M} \cdot \sum_{i=1}^{M} (Differ_i)^2} = \sqrt{\frac{1}{M} \cdot PRESS}$$

In case of a test set validation this value is called the **r**oot **m**ean **s**quare **e**rror of **p**rediction (*RMSEP*).

$$PRESS = \sum_{i=1}^{M} (Differ_i)^2$$

A recommendation for the optimal PLS rank is given, using these values, to prevent overfitting.

1) The rank with the smallest *PRESS* value is searched. (This presumes that enough PLS ranks are calculated.)
2) For all lower ranks, the quotient of their *PRESS* values and the minimum is calculated (= *FValue*).
3) From this *FValue* a probability is calculated: *FProb* (*FValue*, *M*, *M*).
4) The rank, having a probability smaller than 0.75 for the first time, is marked as the optimum rank.

The *PRESS* calculation is meaningful only if there is a large number of calibration standards, because the set should not change significantly when reduced by one or more standards.

The size of the prediction error is another important number. This value can be judged only if the distribution of the component values is known. This is taken into consideration in the calculation of R^2 and therefore is a direct measure for the quality of the prediction.

$$R^2 = \left(1 - \frac{\sum (Differ_i)^2}{\sum (y_i - y_m)^2}\right) \times 100$$

"Bad" calibration standards can be recognized by their true values not being predicted using the remaining spectra. Using the difference values, an automatic outlier detection is performed to mark the samples whose deviation from the true concentration value is particularly large and statistically significant. In these cases, an *FValue* is calculated.

$$FValue_i = \frac{(M-1)(Differ_i)^2}{\sum_{j \neq i} (Differ_i)^2}$$

If the standards are divided up into a set of calibration spectra and a set of test (or validation) spectra an external validation (test set validation) can be performed. The calibration is done with the original set of calibration spectra and the test spectra are predicted. The mean prediction error is called **r**oot **me**an **s**quare **e**rror of **p**rediction *RMSEP*:

$$RMSEP = \sqrt{\frac{1}{M} \sum (Differ_i)^2}$$

Another useful term is the **RPD value**. It is the quotient of the standard deviation of the reference values (*SD*) and the bias-corrected mean error of prediction of the validation (*SEPbias*). To evaluate the quality of a validation, calculating the *RPD* is more meaningful than only looking at the error of prediction.

For example, validating a calibration with a relatively small range will most likely lead to a small error of prediction. For historical reasons, the *RPD* value is often used in the agro market, for example in the NIR spectroscopic analysis of wheat. The following rule of thumb is valid for assessing the quality of a calibration:

- RPD between 2.5 -3: method OK for rough screening
- RPD > 3: method OK for screening
- RPD > 5: method OK for quality control
- RPD > 8: method excellent for all analytical tasks.

These values are very dependent on the kind of sample and the calibration range. The rule of thumb above should be valid for most applications in the food industry (for natural, heterogeneous and solid samples). For chemical analysis (synthetic, homogeneous liquid samples), the calibrations should show higher *RPD* values.

Bias: Generally, the bias is the systematic averaged deviation between the data set of the true and the predicted values. It is calculated by averaging all particular deviations of the samples inside the data sets.

To summarize, the setup of a reliable PLS model is an iterative process:

1) Look at the validation report to select a suitable rank.
2) For this rank remove possible outliers.
3) A new determination of the optimum rank is then necessary.
4) Several data preprocessing options should be tested and the selected frequency regions should be changed.

Chapter IV. Results and Discussion

The first part of this chapter consists of the results from oxidation marker compounds quantification. Firstly, lipid oxidation results will be presented in form of TBA, and then protein oxidation quantification will be presented both for protein content and total carbonyls. For both LO and PO some tables will be presented which show the results of the quantification for the different animal samples and for the different finishing diets, as well as some graphs to help their visualization.

The second part includes the spectral characteristics of the different LO and PO samples analyzed through FT-MIR. Major absorption bands will be presented according to bibliography and compared with the typical spectra acquired with every group of samples (TBA, Carbonyls and Protein Content).

Finally, the quantitative analysis results from chemometric model will be presented in form of graphs and tables with statistical results for both LO and PO. At the end, a summary table will be included which presents the comparison of these results with the ones obtained through FT-MIR analysis of raw meat, that were obtained in a previous work.

1. Oxidation quantification results

As above mentioned, this first part includes the results from oxidation marker compounds obtained through classical quantification methods. Firstly, lipid oxidation will be presented and then protein oxidation results will follow.

1.1. Lipid oxidation quantification results

Now the results from the TBARS analysis explained in paragraph *4.1.1. LO quantification procedure (TBARS)* performed with the samples introduced in paragraph *2. Animal material* from Chapter III will be presented.

Quantification results from both animal groups will be presented. On the one hand, results from Young (slaughter age) – Linseed (finishing diet) animals will be presented. These results are shown in Table 7.

Table 7: LO quantification results for Young-Linseed meat samples in mg of MDA/kg of meat sample. (Source: Own elaboration)

No Sample	No Animal	Ageing post-mortem			
		0 days	4 days	8 days	12 days
13-16	9462	0.6	0.48	0.57	0.59
17-20	9461	0.57	0.58	0.56	0.59
21-24	9028	0.28	0.32	0.39	0.43
25-28	9460	0.32	0.43	0.44	0.36
29-32	9026	0.46	0.44	0.44	0.53
33-36	9459	0.47	0.43	0.62	0.66
37-40	9465	0.32	0.35	0.45	0.48

In order to visualize better the results shown in Table 7, data is also presented in Figure 20 as a graph.

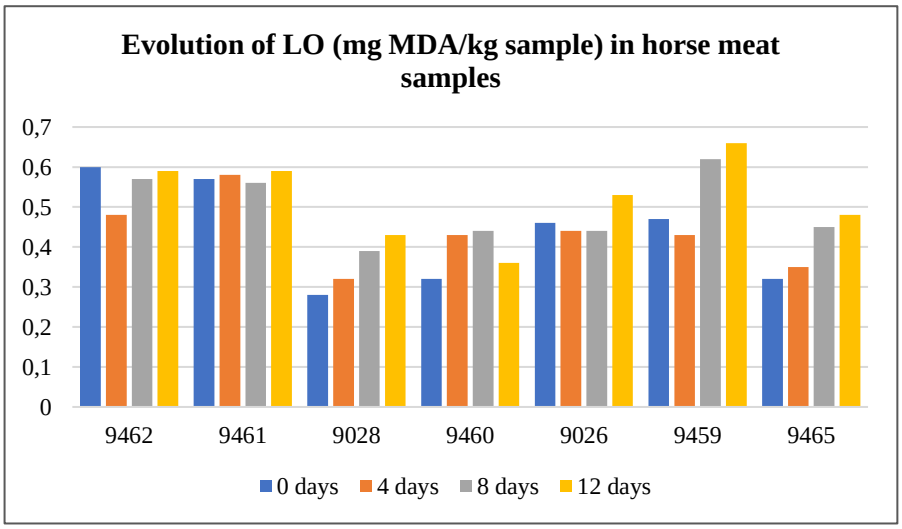

Figure 20: Graph of the evolution of LO in horse meat samples along ageing, in mg of MDA/kg of meat sample. (Source: Own elaboration).

As it is shown in both Table 7 and Figure 20, there is not a clear behavioral pattern followed by the samples.

On the one hand, animals 9028 and 9465 follow a clear crescent pattern of lipid oxidation linked to the ageing of the samples. In other words, as ageing of the sample increases (0-12 days), total content of MDA rises, as it was expected according to other researches references (Lorenzo & Gómez, 2012).

On the other hand, the rest of the samples do not show that clear crescent pattern. For example, animals 9462 and 9459 follow this pattern except for the TBA result from day number 0, which shows a higher value than subsequent days of ageing. Besides, animal 9461 presents MDA contents very close to each other in terms of ageing days, not showing clear differences between them. Finally, animal 9460 shows lower TBA result for day 12 than for previous ageing days, what does not match with the expected pattern.

Once Young-Linseed animals' results have been presented, results for Adult-Conventional animals are introduced. This time, the only ageing time of study was 4 days. Results are shown in Table 8.

Table 8: LO quantification results for Adult-Conventional meat samples for 4 days ageing, in mg of MDA/kg of meat sample.

No Sample	No Animal	mg MDA/kg meat sample
1	9917	3.26
2	9914	2.04
3	10370	1.88
4	9918	2.19
5	10373	1.45
6	9919	3.58
7	9915	2.37
8	10369	1.47
9	10372	1.67
10	10368	1.1
11	9916	2.14
12	10371	2.1

As it is shown in Table 8, variety of results were obtained regarding to Adult-Conventional animal group in TBA analysis at day 4 of ageing. The range went from 1.1 to 3.58 mg MDA/kg of meat, in comparison to the 0.32-0.48 mg MDA/kg of meat obtained with the Young-Linseed group for and ageing time of 4 days post-mortem. These results suggest that the content of MDA in meat (lipid oxidation marker compound) increases as the slaughter age increases, and it may also be influenced by the finishing diet.

1.2. Protein oxidation quantification results

In this paragraph, results from the Total Carbonyl and Protein Content obtained through DNPH method explained in paragraph *4.1.2. PO quantification procedure (DNPH)* from Chapter III are presented.

As well as with LO, firstly it will be presented the results obtained from Young-Linseed animals group and then Adult-Conventional results will be presented. It should be noted that this time just two animal samples came from Y-L, whereas 12 different animals were employed for the A-C study.

The samples from Young-Linseed animals group are now presented in Table 9.

Table 9: PO quantification results for Young-Linseed meat samples in nmole of Carbonyl/mg of protein for Total Carbonyl and % for Protein Content.

No Sample	No Animal	Compound	Ageing post-mortem			
			0 days	4 days	8 days	12 days
13-16	9027	Carbonyl	0.103	0.114	0.114	0.095
		Protein	25.8	26.1	26.4	25
17-20	9465	Carbonyl	0.100	0.102	0.106	0.105
		Protein	26	25.7	24.5	25.4

In order to facilitate the visualization of the data, Figures 21 and 22 show Total Carbonyls and Protein Content evolutions, respectively.

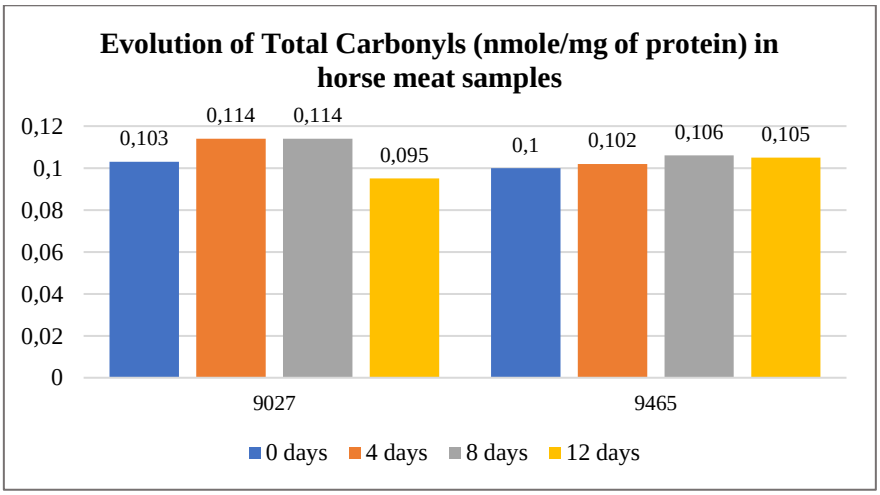

Figure 21: Graph of the evolution of Total Carbonyl in horse meat samples along ageing, in nmole/mg of protein. (Source: Own elaboration).

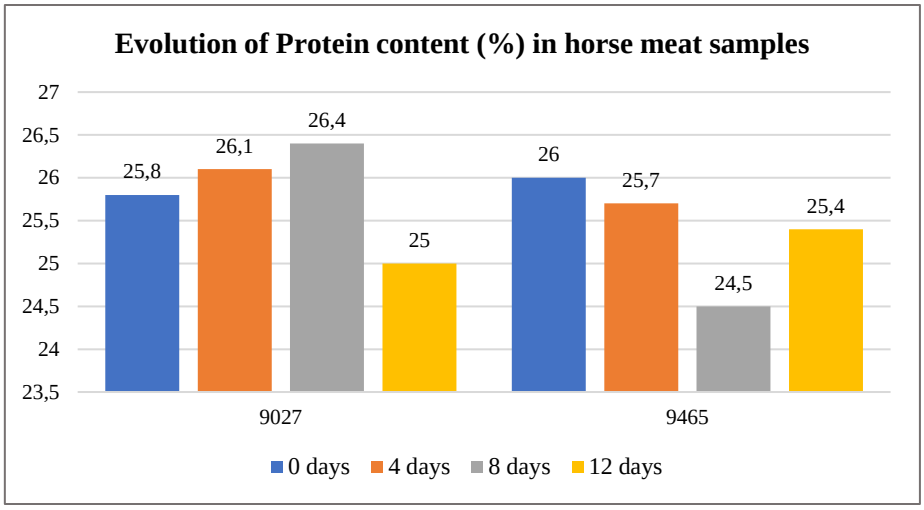

Figure 22: Graph of the evolution of Protein Content in horse meat samples along ageing, in %. (Source: Own elaboration).

According to Zakrys-Waliwander et al. (2010) and Zakrys et al. (2008) protein oxidation in beef meat samples increased with oxygen and conservation ageing time. That is why it is expected to observe that if ageing time increases, protein oxidation does it as well.

However, as it is shown in both Table 9 and Figures 21 and 22, there is not an apparent increase or decrease clear pattern followed by the samples, neither for total carbonyls evolution or protein content.

On the one hand, animal 9027 shows an apparent increase in Total Carbonyls during first 8 ageing days. Nevertheless, result from day 12 shows a decrease, what does not match with what was expected regarding bibliography. Protein content of animal 9027 showed a decreasing difference between day 0 and day 7 as it could be expected, however, it also appears an increase during days 4 and 8 which offers confusion with the results.

On the other hand, animal 9465 shows a better increasing Total Carbonyls pattern than last one, However, results are quite similar among them and it appears a decrease on day 12, what again does not match with what was expected. According to protein content, animal 9465 shows very variable results which do not give apparent useful information about its PO.

Once Young-Linseed animals' results have been presented, results for Adult-Conventional animals are shown. The only ageing time of study was 4 days, as happened with Lipid Oxidation, as animals employed this time are the same that with LO. Results are shown in Table 10.

Table 10: PO quantification results for Adult-Conventional meat samples for 4 days ageing, in nmole/mg of protein in Total Carbonyls and % in Protein Content.

No Sample	No Animal	Total Carbonyl	Protein Content
1	10372	0.117	23.3
2	9915	0.127	28.9
3	10371	0.094	28.7
4	10368	0.107	25.4
5	9919	0.119	20.3
6	9917	0.134	26.4
7	10370	0.105	20.3
8	9918	0.101	25.8
9	9916	0.1	26
10	10369	0.101	22.8
11	10373	0.088	24.8
12	9914	0.101	24.4

As it appears in Table 10, a variety of results were obtained regarding Adult-Conventional animal group in PO analysis at day 4 of ageing.

Regarding Total Carbonyls, the range went from 0.1 to 1.134 nmole/mg of protein, in comparison to the 0.095-.114 nmole/mg of protein obtained with the Young-Linseed group.

According to Protein Content results, Y-L group showed values of 26.1% and 25.7% (mean=25.9%) at day 4 of ageing while A-C showed values from 20.3% to 28.9% (mean=24.8%).

2. Spectral characteristics of the samples

In this paragraph it will be presented the results obtained regarding the 356 different spectra acquired through the FT-MIR analyses performed to the marker compounds of LO (TBA) and PO (Carbonyls). Firstly, the total amount of spectra obtained through MIR analysis will be presented, as a first visualization of the results obtained. This is shown in Figures 23, 24 and 25.

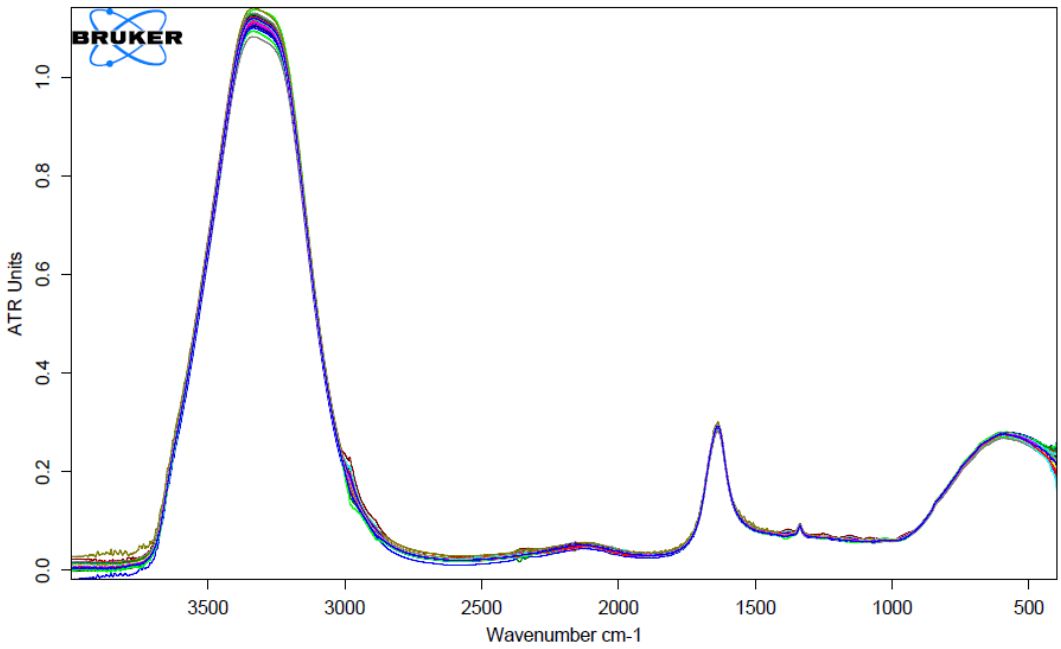

Figure 23: Results of FT-MIR spectral measurements of TBA samples (240 analyses)

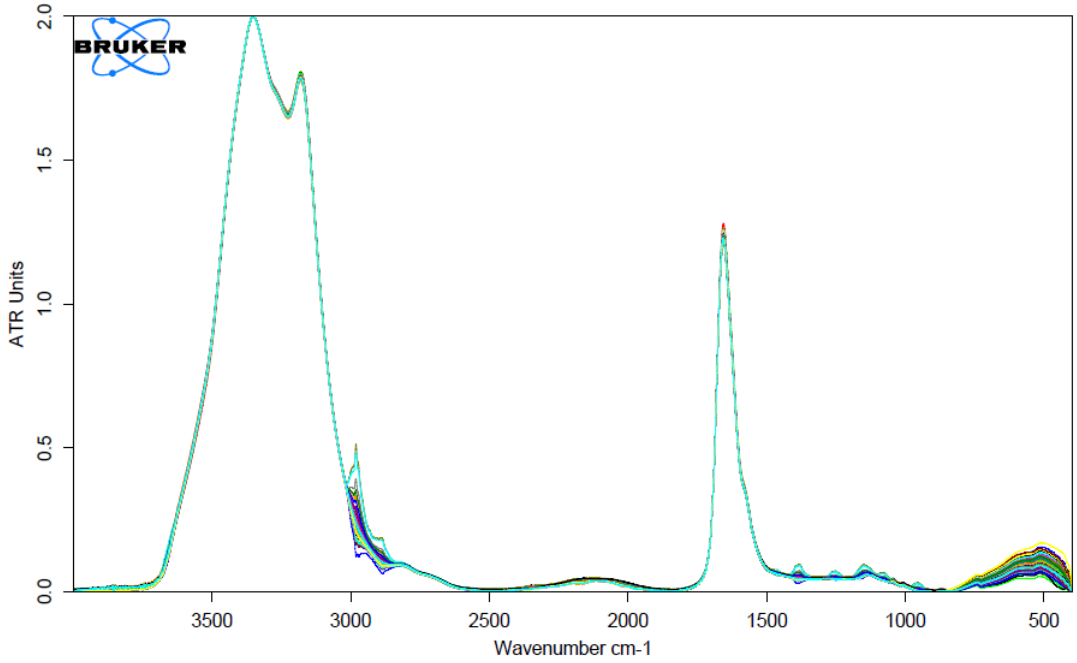

Figure 24: Results of FT-MIR spectral measurements of Carbonyl samples (108 analyses)

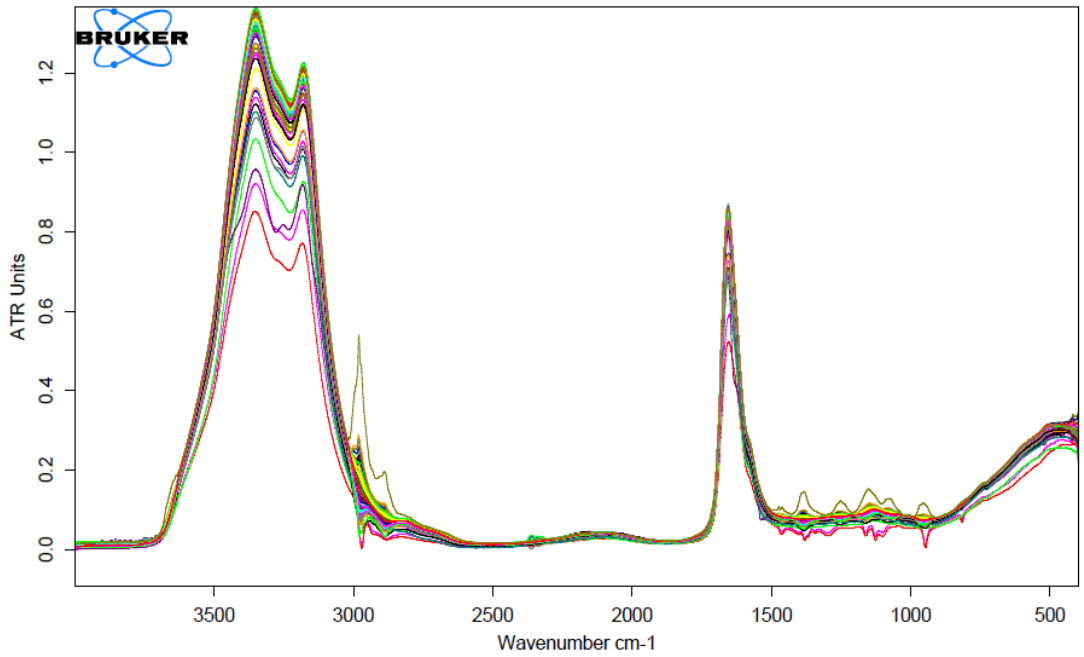

Figure 25: Results of FT-MIR spectral measurements of Protein content samples (108 analyses)

As it can be observed in the last figures, quite variability is shown in both Carbonyl and Protein content samples' spectra, while less variability is found regarding TBA samples' measurements. Once the spectra were acquired, a bibliographic revision of main peaks obtained was performed.

Table 11 contains a first compilation of the major wavenumbers associated to their functional groups according to bibliography consulted, regarding the compounds of study.

Table 11: Compilation of principal wavenumbers associated to functional groups.

Wavenumber (cm^{-1})	Assignement	Reference
3,700-3,200	Stretching vibration of bonded and non bonded -O-H groups (water vibration)	Pretsch et al. (2000)
3,500-3,300	Amines	Jabs (n.d.)
~3,400	Amide A (N-H stretching vibrations)	Jabs (n.d.)
~3,100	Amide B (N-H stretching vibrations)	Tamm & Tatulian (1997)
3,000-2,850	Simmetrycal and asymmetrical stretching vibrations of C-H groups (Alkanes); fatty acids backbone	Silverstein (1981)
1,659-1,653	=C-H stretching vibrations / Amide I (C=O stretching vibration)/ O-H bending vibrations in water	Kanou et al. (2005), Jabs (n.d.).
1,680-1,620	Stretching vibration of C=H groups(Alkenes)	Rohman (2011)
~1,640	Hydrogen covalent bonds bending of water	Eisenberg & Kauzmann (1969)
1,580-1,540	C-O vibrations / Amide II (N-H bending vibration mixed with C-N stretching vibration) /Aromatic -C=C stretching vibrations	Nikonenko et al. (2005)
1,400-1,200	Amide III (N-H, C-C and C-N vibrations)	Tamm & Tatulian (1997)
970-920	*trans*= C-H out-of-plane bending	Sun (2009)
610-711	Amide V (C-N and N-H vibrations)	Tamm & Tatulian (1997)
900-400	Stretching of O-H (water vibraiton)	Pretsch et al. (2000)

Now, spectral characteristics regarding peaks of both PO and LO marker compounds will be presented.

2.1 Spectral characteristics of PO marker compounds

In order to explain the results obtained, Figures 26 and 27 are presented, which show a typical spectrum obtained through the FT-MIR analysis performed in both Carbonyl and Protein content random samples. At these figures, bonds which provoke the most remarkable peaks are highlighted.

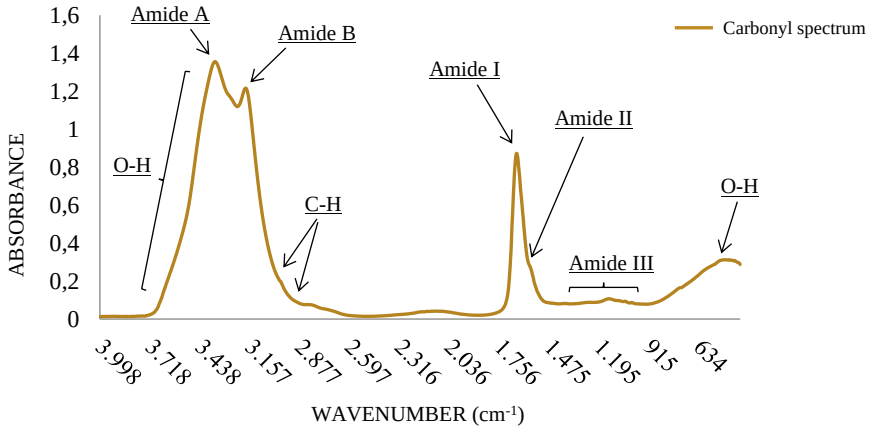

Figure 26: MIR spectrum of Sample 31 from Carbonyls compounds

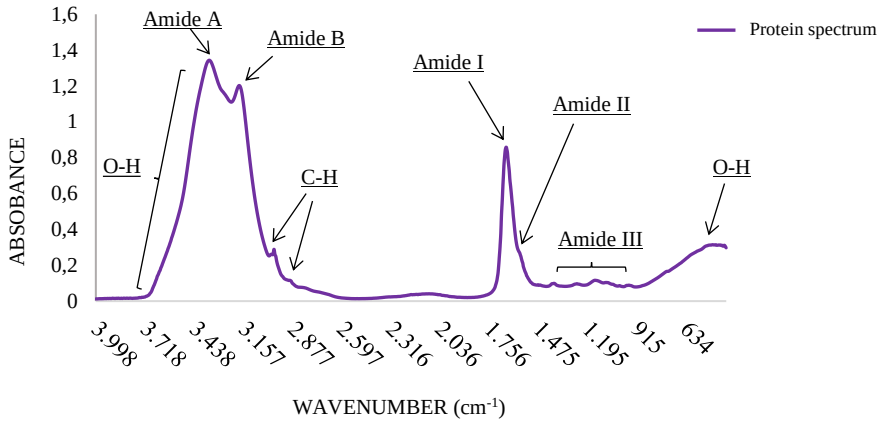

Figure 27: MIR spectrum of Sample 29 from Protein content compounds

Same explanation will be presented for both Carbonyl and Protein spectrum characteristics since both typical spectra present the same peaks of absorption, greater or lesser sharp.

As it was mentioned in paragraph *3.2.2 Interpreting resulting spectra* from Chapter III, samples spectra can be separated in two different zones. First one, the Functional Group Region, between 4,000 cm^{-1} and 1,500 cm^{-1}, corresponds to the vibration oscillations of the bonds that contain hydrogen atoms such as C-H, O-H and N-H. Second area is extended from approximately 1,500 cm^{-1} until 400 cm-1 (end of MIR region) and is attributed to the different bending vibrations of bonds, which is called the Fingerprint Region (Karoui et al., 2010).

Among all the absorption peaks that the spectra present, the most remarkable ones are the peaks located between 3,700 cm^{-1} and 3,100 cm^{-1}. In this area it appears the wide band of high absorption associated to the hydroxyl groups O-H of water. Usually, these peaks tend to hide the presence of N-H associated peaks (Carbonaro, 2010), however, it can be observed in both Figures 26 and 27 that two different peaks are clearly differentiated from the O-H groups. These peaks correspond to Amide A at 3,350 cm^{-1} (~3,400 cm^{-1} according to bibliography) and Amide B at 3,175 cm^{-1} (~3,100 cm^{-1} according to bibliography) which originate from a Fermi resonance between the first overtone of amide II and the N-H stretching vibration (Jabs, n.d.).

Another peak that stands out over the rest is found at 1,650 cm-1 and it corresponds to the Amide I band. Amide I is the most intense absorption band in proteins. It is primary due to the stretching vibrations of the C=O (70-85%) and C-N groups (10-20%) and according to bibliography its frequency is found in the range between 1,600 and 1,700 cm^{-1}. Next to Amide I it appears another less pronounced peak, between 1,588 and 1,565 cm^{-1} in both Carbonyls and Protein, known as Amide II. It is found in the 1,510 and 1,580 cm^{-1} region and it is a more complex band than Amide I. Amide II derives mainly from in-plane N-H bending (40-60% of the potential energy). The rest of the potential energy arises from the C-N (18-40%) and the C-C stretching vibrations (about 10%) (Venyaminov & Kalnin 1990). To end up with this area, Amide III band appears along the region 1,400-1,200 cm^{-1} and they correspond to very complex bands dependent on the details of the force field, the nature of side chains and hydrogen bonding (Tamm & Tatulian 1997).

Moreover, some weaker but important peaks appear around the wavenumber 3,000 cm^{-1}, associated to the different vibrational oscillations of C-H bonds. As it can be compared in Figures 26 and 27, these bands present higher absorption in Protein spectra than in Carbonyl ones. Highest peak among these is the one located at 2,980 cm^{-1} and corresponds to the symmetrical and asymmetrical stretching vibrations of Alkanes, which according to bibliography could represent the fatty acids backbone (Carbon atom basis of fatty acids), for both methyl ($-CH_3$) and methylene ($-CH_2$) groups. Finally, from 900 to 400 cm^{-1} it can be observed a wide band with great absorption,

which corresponds again to the same hydroxyl groups O-H of water that hog the region between 3,700 cm^{-1} and 3,100 cm^{-1}, so it does not give much structural information (Pretsch et al. 2000).

2.2 Spectral characteristics of LO marker compounds

As proceeded with PO spectra, in order to explain the results obtained in LO spectra, Figure 28 is presented, which shows the typical spectrum obtained through the FT-MIR analysis of a TBA sample. At this figure, bonds which provoke the most remarkable peaks are highlighted.

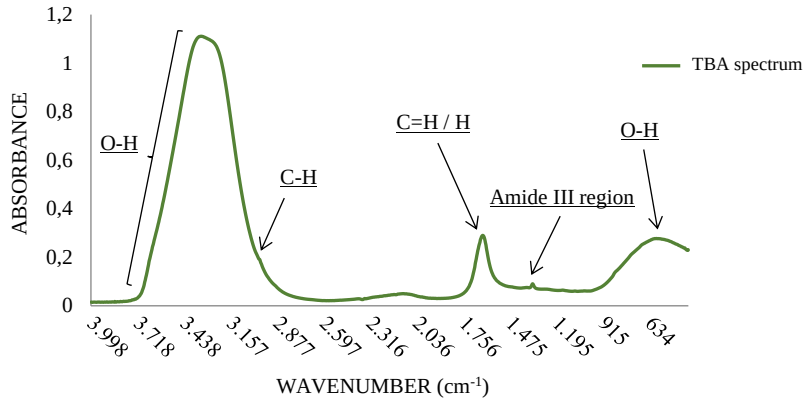

Figure 28: MIR spectrum of Sample 49 from TBA compounds

In this case, as observed in Figure 28 TBA sample shows a different spectrum in comparison to the ones presented in last paragraph *2.3. Spectral characteristics of PO marker compounds.*

Now among all the absorption peaks that the spectra present, the most remarkable one is the band located between 3,700 cm^{-1} and 3,100 cm^{-1}. As cited before, this area corresponds to the wide band of high absorption associated to the hydroxyl groups O-H of water. In this case, it hides the possible presence of other peaks. In the same way as before, vibrational oscillations of these O-H groups provoke the apparition of another wide band between 900 to 400 cm^{-1}.

After these two bands, the band with highest absorption appears in the region between 1,680 and 1,590 cm^{-1}, with the highest peak at 1,636 cm^{-1}. This area, according to Rohmann (2011) corresponds to the stretching vibrations of C=H groups (Alkenes). However, it is known too that peak 1,640 cm^{-1} corresponds to the hydrogen covalent bonds bending of water. This way, results are not clear enough to determine the type of bond that provokes that absorbance.

Moreover, a slight peak can be also observed at 2,981 cm^{-1}, again associated to the different vibrational oscillations of C-H bonds. This one in particular was assigned to the stretch of C-H when IR-studying Tertiary Amine-Triethylamine (Bacher, 2002).

Finally, it can be clearly observed an isolated peak in the Fingerprint Region present in every of the 240 samples measured. The peak is located at 1,336 cm^{-1} and has a low but repeated absorption from 0.086 to 0.095 (mean = 0.088). It has not been found any reference regarding this particular peak in any of the articles consulted, however it is located in the region correspondent to Amide III band (1,400-1,200 cm^{-1}), so it is supposed to belong to this kind of peptide complex band.

As a curiosity, the only reference found regarding the apparition of a peak at this particular frequency was the study of Socaciu et al. (2012) in which they found that the band 1,336 cm^{-1} may be considered a sensitive marker for the identification of *Lactobacillus casei* to evaluate lactic fermentation in the production of fermented foods.

3. Quantitative Analysis Results

In this paragraph are presented the main results for which this project was elaborated in order to: deepen in the study of protein and lipid oxidation markers (Protein Carbonyls and TBA respectively) employing MIR spectroscopy, in order to compare the results of these spectra with the ones from raw horse meat, employing chemometric analysis.

In this way, all the spectra acquired that have been presented in paragraph *2. Spectral characteristics of the samples* from this chapter IV were employed for building the prediction models employing reference values obtained through TBARS analysis and PO analysis presented in paragraph *1. Oxidation marker compound results.* At the end of this section, it will be presented a comparative table between the results obtained through these calibrations and the ones obtained with raw meat in previous works.

3.1 Lipid oxidation results

As it was presented in last paragraph, for the construction of the model a total of 240 spectral analysis from 40 TBA samples were employed, extracted from a total of 19 different animals from two different groups (n=7 from YL and n=12 AC). First, it will be presented the results for the whole set of spectra. Then, the results after performing the mean of each TBA sample will be presented.

3.1.1 Entire set of TBA spectra results

Following the procedure previously described in paragraph *5.5 Procedure and software used for quantitative analysis* from chapter III, the whole group of spectra were introduced in QUANT software, as well as the quantitative analysis values of each of the samples of TBA analyzed. With these data, a first calibration was performed. Figure 29 presents the graph of this first calibration performed with the set of 240 spectra.

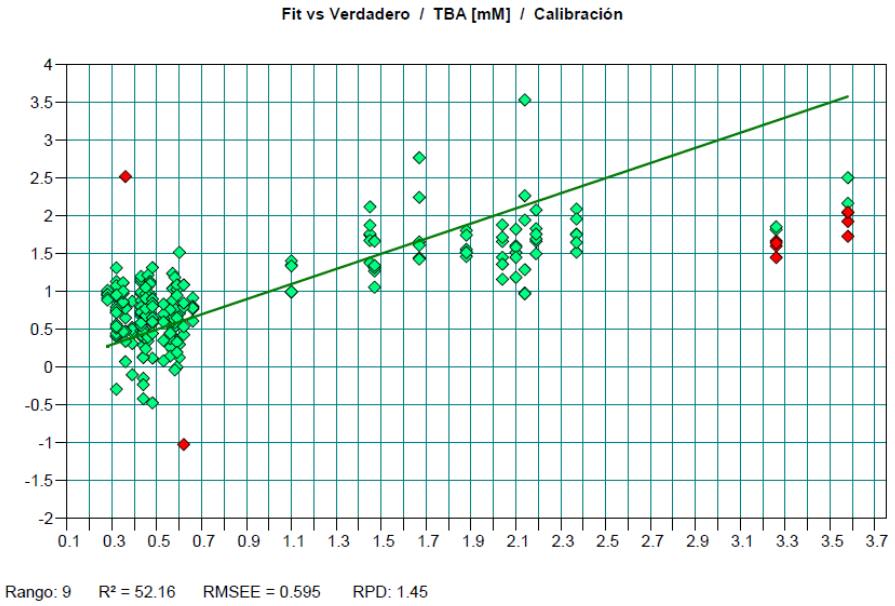

Figure 29: Graph of first calibration equation for the TBA Entire set without preprocessing

After the calibration, a first Cross validation was performed in order to evaluate and test the reliability of prediction. Figure 30 presents the graph of this first Cross Validation.

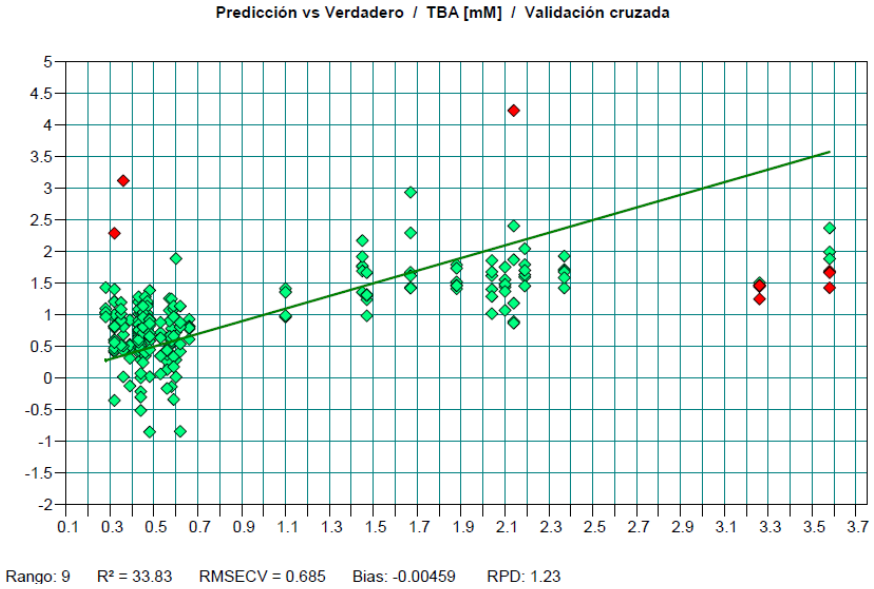

Figure 30: Graph of first validation equation for the TBA Entire set without preprocessing

As it can be observed, results of first Validation are not very consistent, as they present a poor R^2, and a high RMSECV. Because of that, some preprocessing methods were applied to the spectral data. Not only that, but also, the most remarkable outlier points were subtracted from the cross validation in order to obtain a stronger and more reliable result. From all the possibilities, it was selected the one with minimum RMSECV and higher rank and RPD.

Figures 31 and 32 present the graphs of the calibration and validation equation once the preprocessing was performed and once the outliers were subtracted.

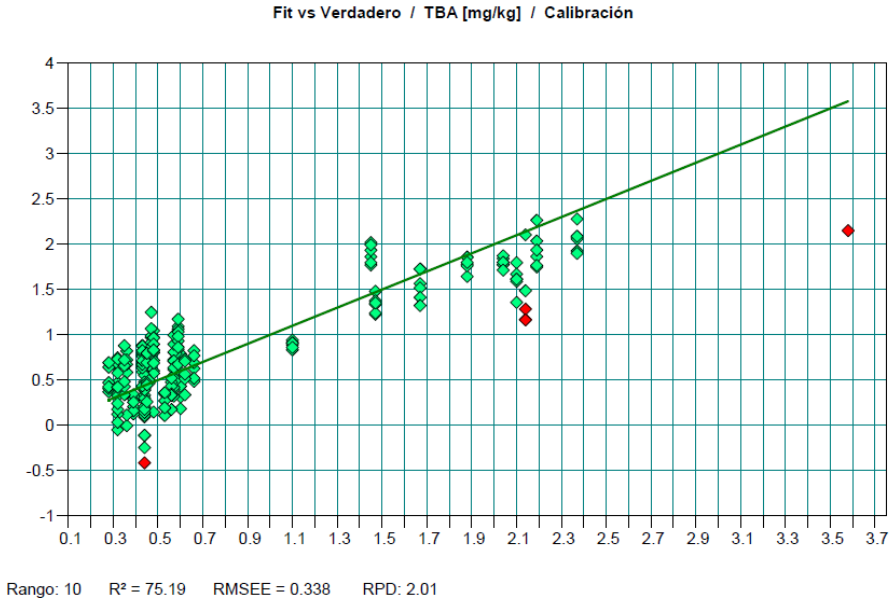

Figure 31: Graph of calibration equation for the TBA Entire set with preprocessing

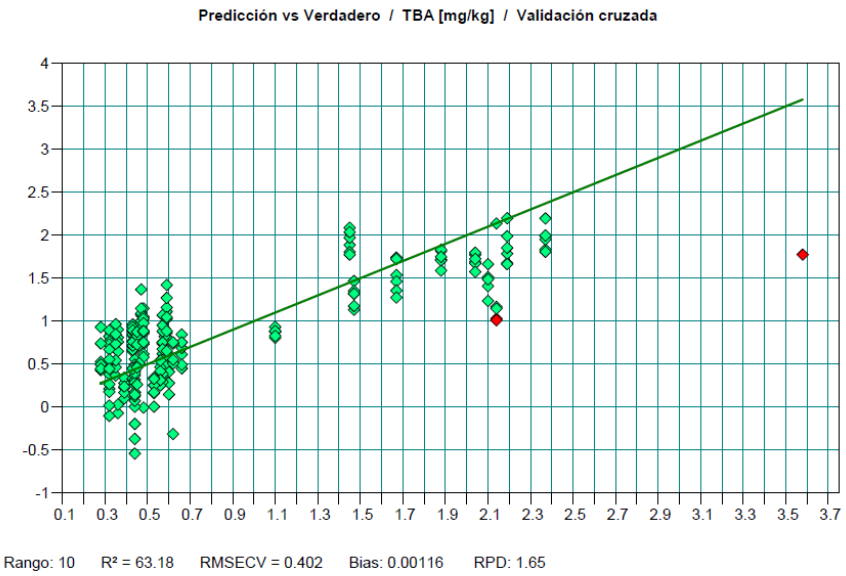

Figure 32: Graph of validation equation for the TBA Entire set with preprocessing

The resulting validation model after the preprocessing procedures (Standard Normal Variate Vectorial Normalization) shows a **Coefficient of Determination** of **63.14%,** a **Root Mean Square Error of CV** of **0.402** and a **RPD** of **1.65**, unlike the first results of validation which showed a poorer R^2 of 33.83%, a quite higher RMSCV of 0.685 and a lower RPD of 1.23.

Type of validation employed was Cross Validation with 1 sample exclusion. In this case, 13 outlier spectra were subtracted, so the total spectra for calibration/validation employed were 227. Spectral range was focused in two areas: Between 3,278-2,918 cm^{-1} and more remarkably between 1.839-759 cm^{-1}. Concentration range for TBA was 0.28-3.58 mg/kg.

3.1.2 Mean TBA set Spectra Results

In order to homogenize the spectral results, it was also elaborated a calibration/validation model for the mean of each group of 6 spectral measurements performed for each TBA sample. This way, the set of spectra was reduced from n=240 to n=40. Following the same procedure as previously explained, a first calibration equation was given. It is shown in Figure 33.

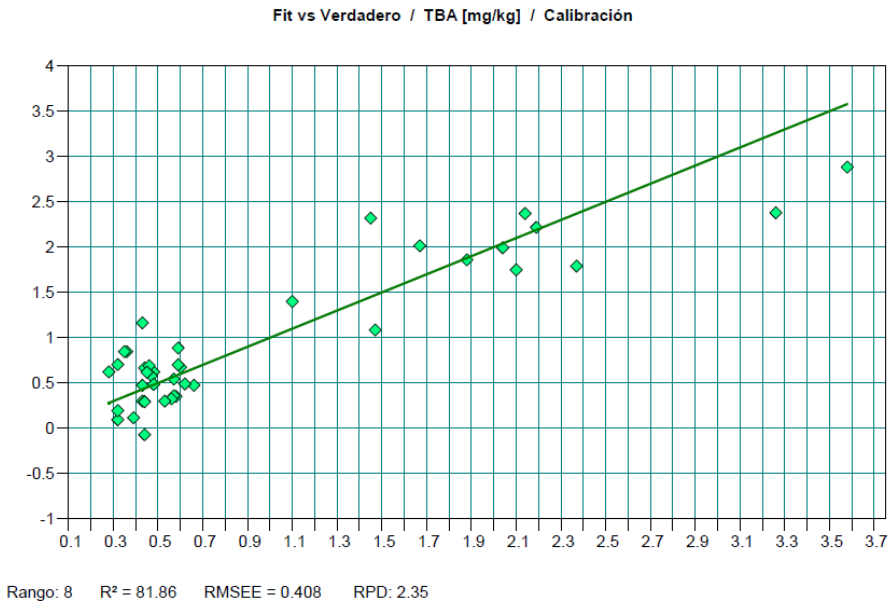

Figure 33: Graph of first calibration equation for the TBA Mean set without preprocessing

After the calibration, a first Cross validation was performed in order to evaluate and test the reliability of prediction. Figure 34 presents the graph of this first validation model.

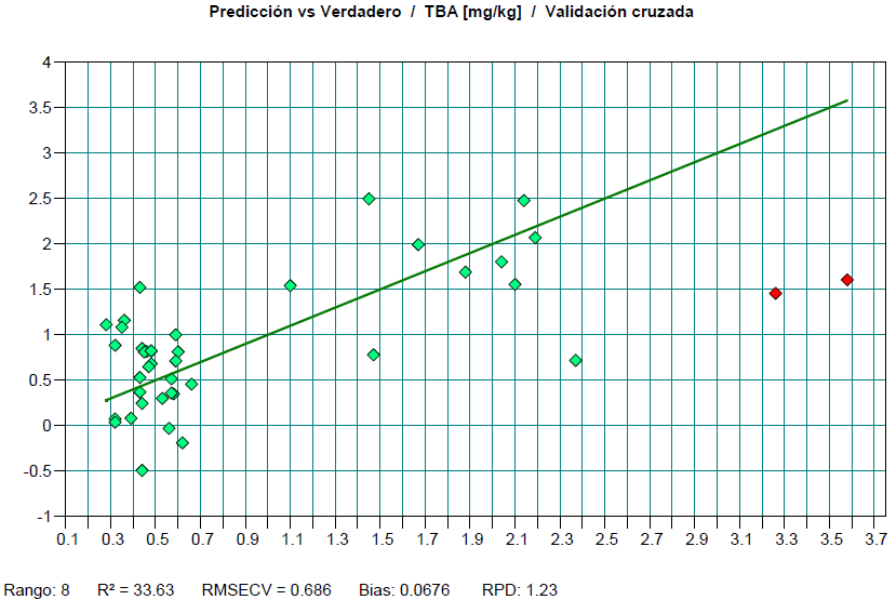

Figure 34: Graph of first validation equation for the TBA Mean set without preprocessing

Exactly as it happened with the entire set of TBA spectra, results of first Validation are not very consistent, as it presents a poor R^2, and a high RMSECV. One more time, preprocessing treatment for the spectral data is needed. In this case, between all the options given by QUANT, Linear Offset Subtraction was performed as it offered the minimum RMSECV with the highest rank.

Figures 35 and 36 present the graphs of the calibration and validation equation once the preprocessing was performed.

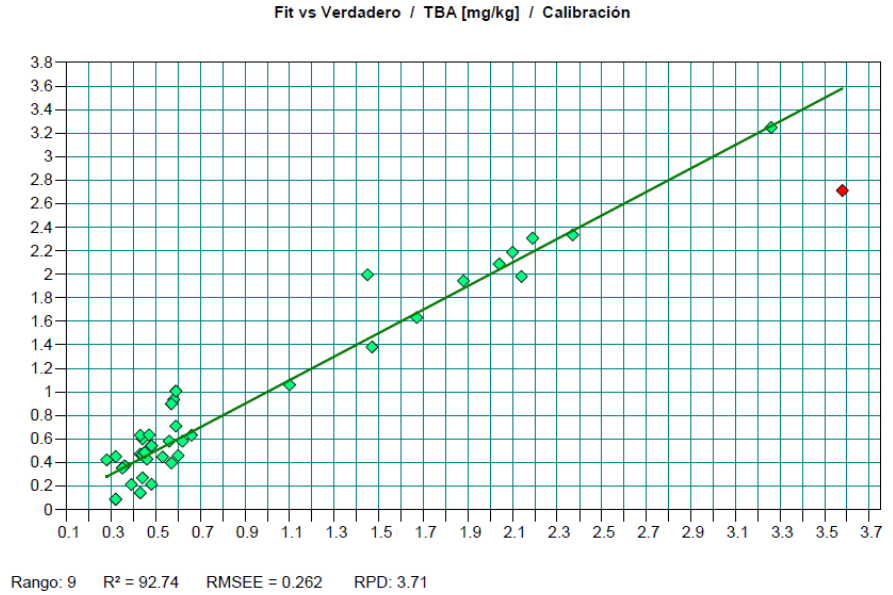

Figure 35: Graph of calibration equation for the TBA Mean set with preprocessing

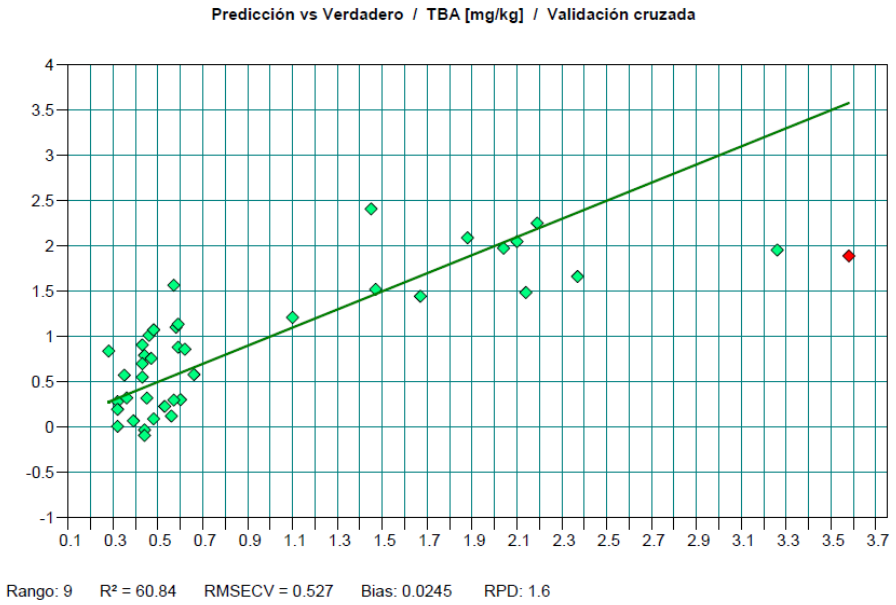

Figure 36: Graph of validation equation for the TBA Mean set with preprocessing

The validation model after the preprocessing procedure (Linear Offset Subtraction) shows a **Coefficient of Determination** of **60.84%,** a **RMSECV** of **0.527** and a **RPD** of **1.6**, unlike the first results of validation which showed a poorer R^2 of 33.63%, a quite higher RMSCV of 0.686 and a lower RPD of 1.23.

Type of validation employed was Cross Validation with 1 sample exclusion. In this case, no outlier spectra were subtracted, so the total spectra for calibration/validation employed were 40. Spectral range was focused in two areas: Between 3,998-3,637 cm^{-1} and more remarkably between 1,479-759 cm^{-1}. Concentration range for TBA was 0.28-3.58 mg/kg

Now, calibration and validation results from the entire set of spectra are presented in comparison to results from mean sets. They are shown in Table 12.

Table 12: Calibration and Cross Validation results for Entire and Mean sets in TBA spectra.

	Parameter	Entire Set (n=240)	Mean Set (n=40)
Calibration	R^2	75.19	92.74
	RMSEE	0.338	0.262
	RPD	2.01	3.71
	Rank	10	9
Validation	R^2_{cv}	63.18	60.84
	RMSECV	0.402	0.527
	RPD_{cv}	1.65	1.6
	$Rank_{cv}$	10	9

On the one hand, as it can be observed, most remarkable improvements appear at the calibration model when performing the mean of the group of spectra. R^2 ascends to 92.74% from 75.9%. RMSEE descends from 0.338 to 0.262 and RPD goes from 2.01 to 3.71.

On the other hand, validation model shows worse results when performing means than employing the whole set of spectra. This is directly related to the employment of a noticeably smaller set of spectra (40 in comparison to 240), so, differences between samples have stronger repercussions over the results.

3.2 Protein Oxidation Results

After presenting the results obtained for the Lipid oxidation chemometric analysis, it will be presented the ones for the Protein oxidation quantitative analysis through multivariate calibration. Both groups of spectra (108 spectral measurements for Carbonyls and the same for Protein) came from 18 Carbonyl and 18 Protein samples extracted from the same 14 animals (n=2 from YL and n=12 from AC).

As well as with TBA analysis, first, it will be presented the results for the whole set of spectra for Carbonyl and for Protein. Then, the results after performing the mean of each group of samples will be presented.

3.2.1 Entire set of Carbonyl and Protein Samples Results

In the same way as previously explained, the procedure consisted of introducing the spectral measurements into QUANT software, versus their Carbonyls and Protein quantitative values. A first calibration equation was given for both Carbonyl and Protein and their graphs are presented in Figures 37 and 38.

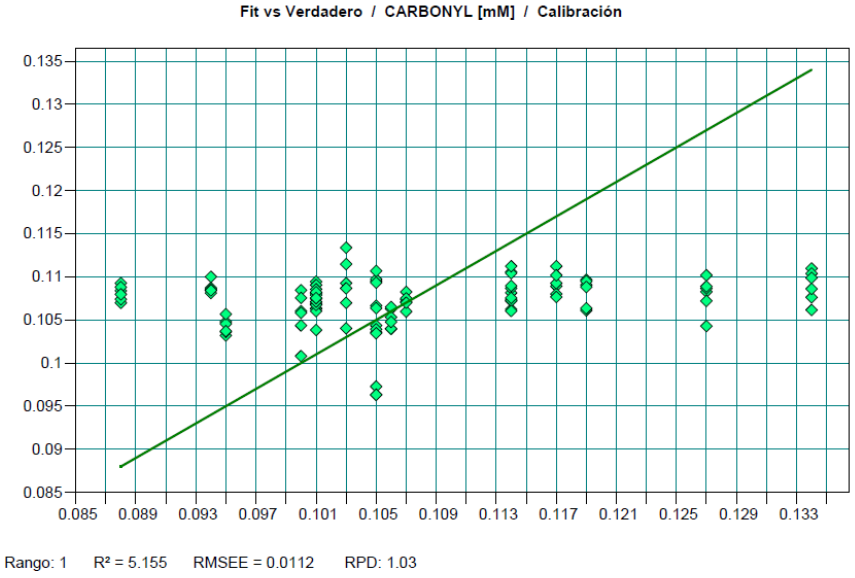

Figure 37: Graph of first calibration equation for the Carbonyl Entire set without preprocessing

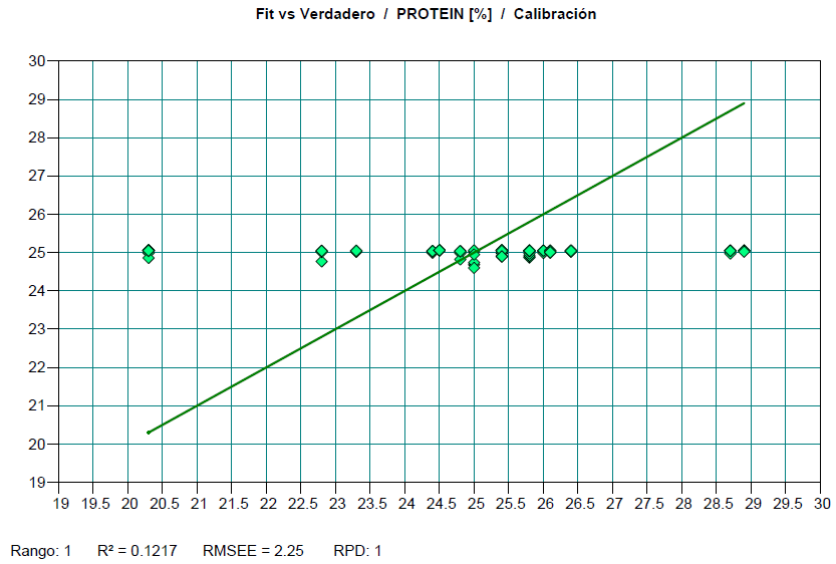

Figure 38: Graph of first calibration equation for the Protein Content Entire set without preprocessing

Despite the poor results of first calibration, a first Cross validation was performed in order to evaluate and test the reliability of prediction, both for Carbonyl and Protein spectra. Figures 39 and 40 present the graphs of these first validation models.

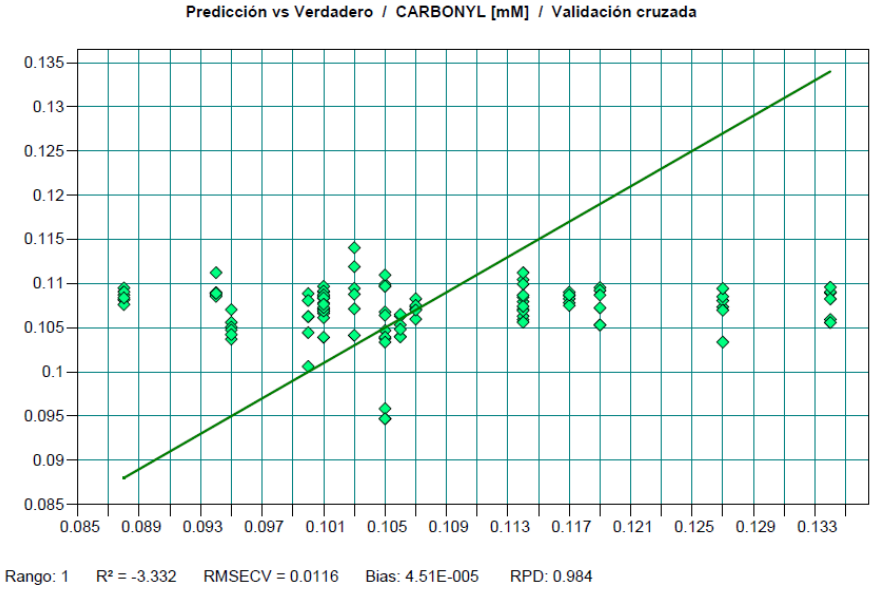

Figure 39: Graph of first validation equation for the Carbonyl Entire set without preprocessing

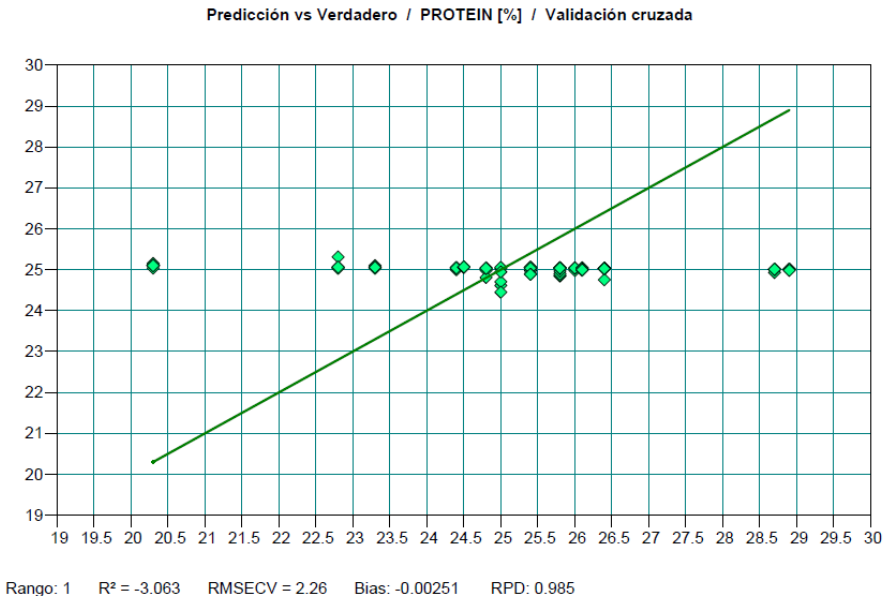

Figure 40: Graph of first validation equation for the Protein Content Entire set without preprocessing

In this case, results of first Validation are not consistent at all, as they present really poor R^2, and high RMSECV. The negative values of R^2_{cv} are due to their low value of rank (1), as the residuals are larger than the variance in true values.

One more time, as it happened with LO sets of spectra, preprocessing treatment for the spectral data was needed.

Carnbonyls results post-optimization

In the case of **Carbonyls**, between all the options given by QUANT, First Derivative + Multiplicative Scatter Correction (MSC) was performed as it offered almost the minimum

RMSECV with the highest rank (5). After that, outlier points were subtracted and repeated the validation. In Figures 41 and 42, graphs for calibration and validation after preprocessing are presented.

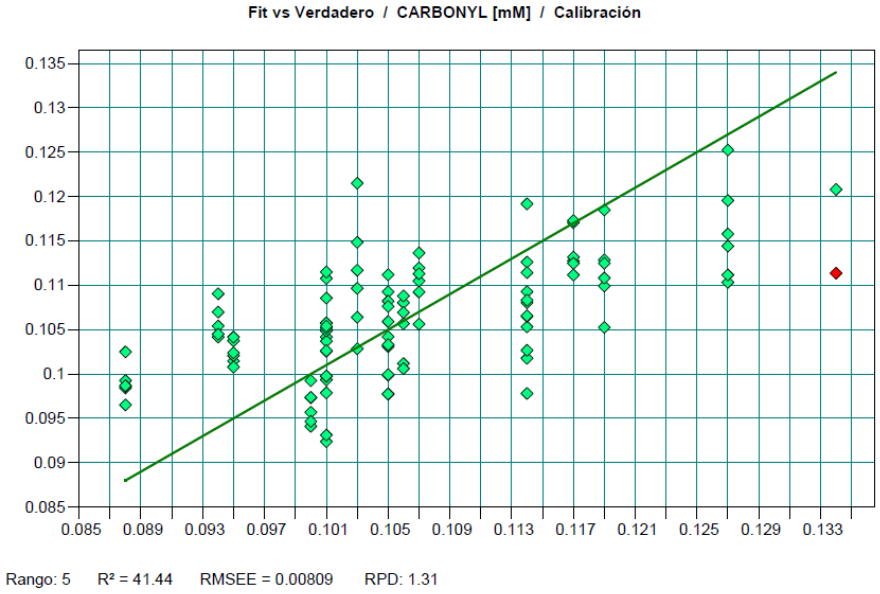

Figure 41: Graph of calibration equation for the Carbonyl Entire set with preprocessing

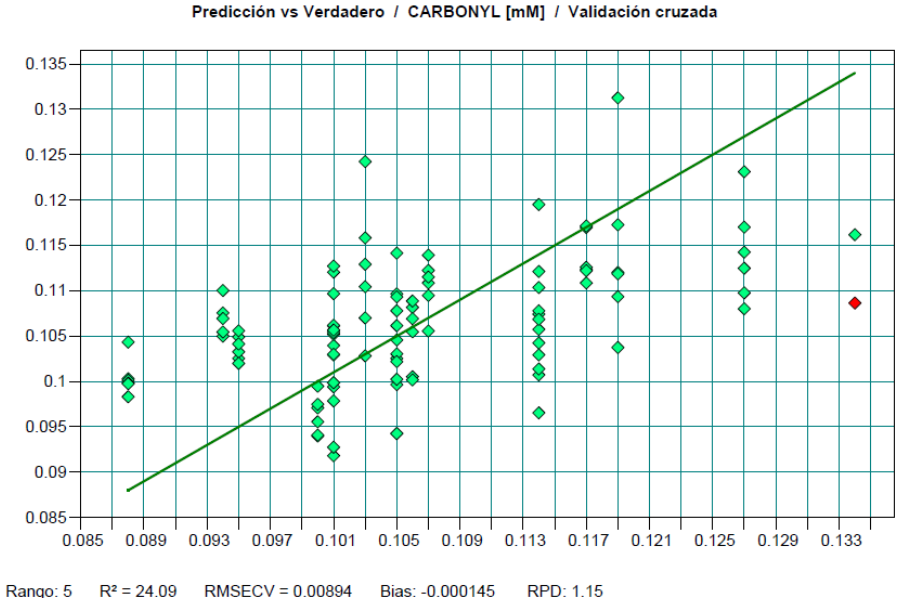

Figure 42 Graph of validation equation for the Carbonyl Entire set with preprocessing

The validation model after the preprocessing procedure (MSC) shows a **Coefficient of Determination** of **24.09%,** a **RMSECV** of **0.00894** and a **RPD** of **1.15**, unlike the first results of validation which showed a poorer R^2 of- 3.33%, a quite higher RMSCV of 0.0116 and a lower RPD of 0.984.

This time type of validation employed was Cross Validation with 1 sample exclusion. In this case, 5 outlier spectra were subtracted, so the total spectra for calibration/validation employed were 103. Spectral range was focused in one particular area: Between 1,839-1,478 cm^{-1}. Concentration range for Carbonyls was 0.088-0.134 mM.

Proteins results post-optimization

In the case of **Protein** content, between the different options given by software, Straight Line Subtraction was performed as it offered the minimum RMSECV with almost the highest rank (7). In Figures 43 and 44, graphs for calibration and validation after preprocessing are presented.

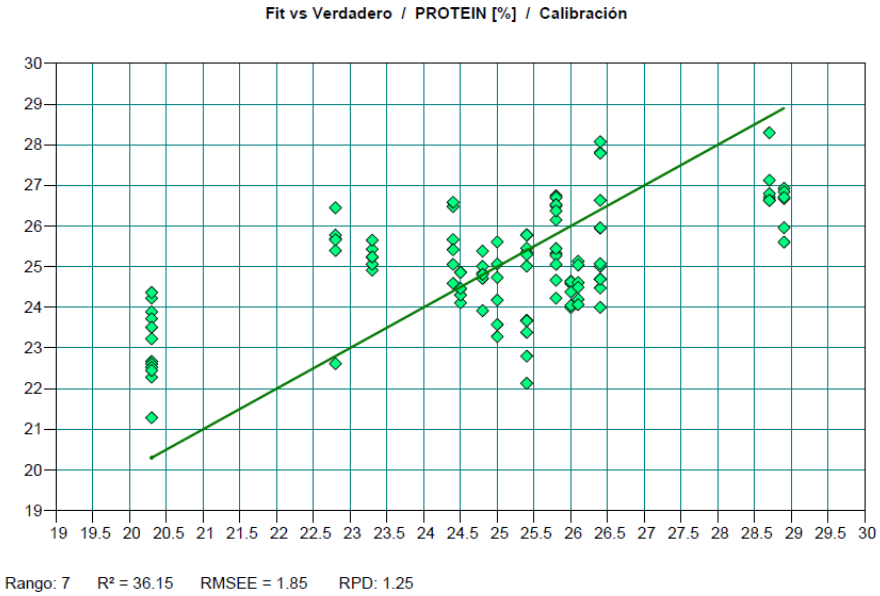

Figure 43: Graph of calibration equation for the Protein Content Entire set with preprocessing

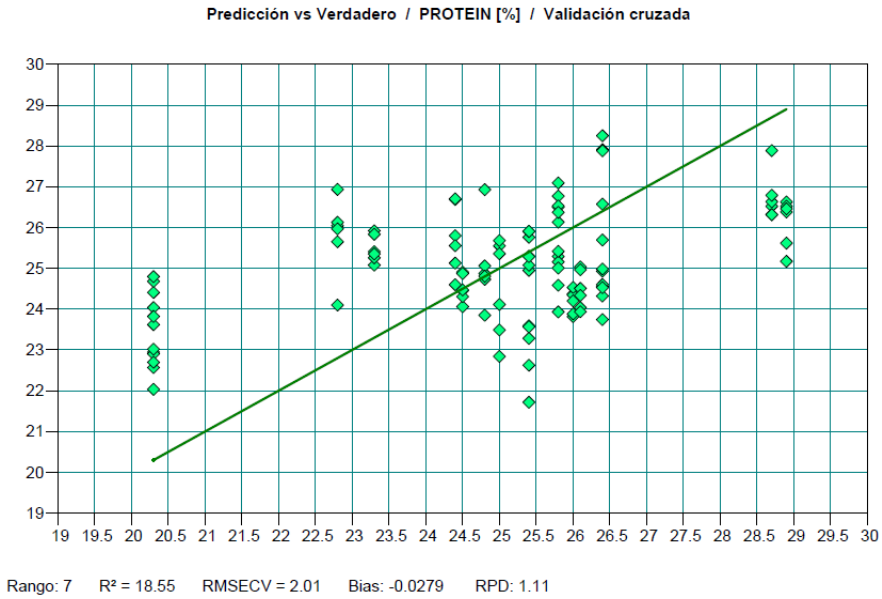

Figure 44: Graph of validation equation for the Protein Content Entire set with preprocessing

The validation model after the preprocessing procedure shows a **Coefficient of Determination** of **18.55%,** a **RMSECV** of **2.01** and a **RPD** of **1.11**, unlike the first results of validation which showed a poorer R^2 of -3.063%, a higher RMSCV of 2.26 and a lower RPD of 0.985.

The type of validation employed was Cross Validation with 1 sample exclusion. In this case, no outlier spectra were subtracted, so the total spectra for calibration/validation employed were 108. Spectral range was focused in three areas: Between 3,278-2,918 cm^{-1}, between 2,198-1,118 and between 760-399 cm^{-1}. Concentration range for Proteins content was 20.3-28.9 %.

3.2.2 Mean Carbonyl and Protein Spectra Results

Following the same procedure as the one followed with TBA analysis, calibration/validation models were set for the mean of the spectral measurements of Carbonyl and Protein. Sample Sets in this case were reduced from n=108 to n=18.

This way, better results were looked for in comparison to the ones obtained through the analysis of the whole set of spectra from PO. Following the same procedure as previously explained, a first calibration equation was given for both Carbonyl and Protein. They are shown in Figures 45 and 46.

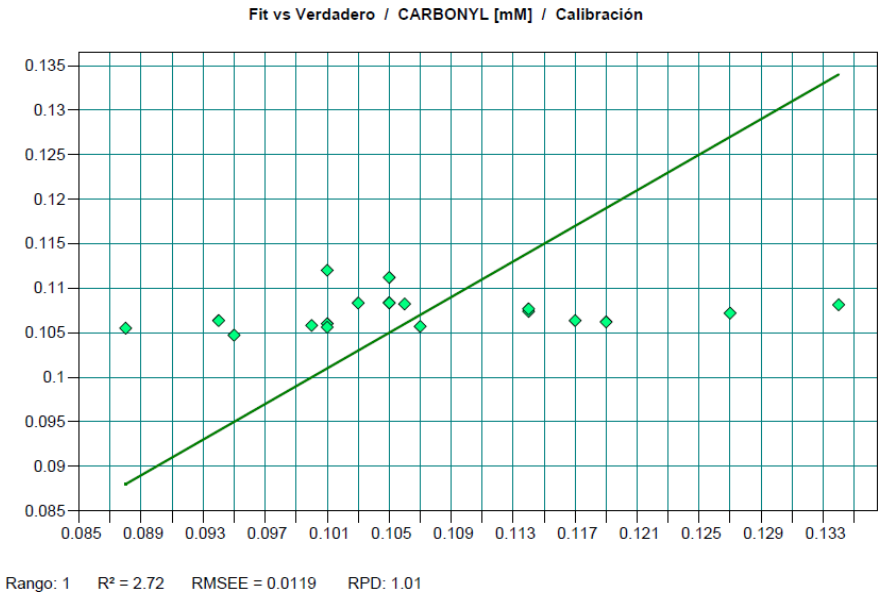

Figure 45: Graph of first calibration equation for the Carbonyl Mean set without preprocessing

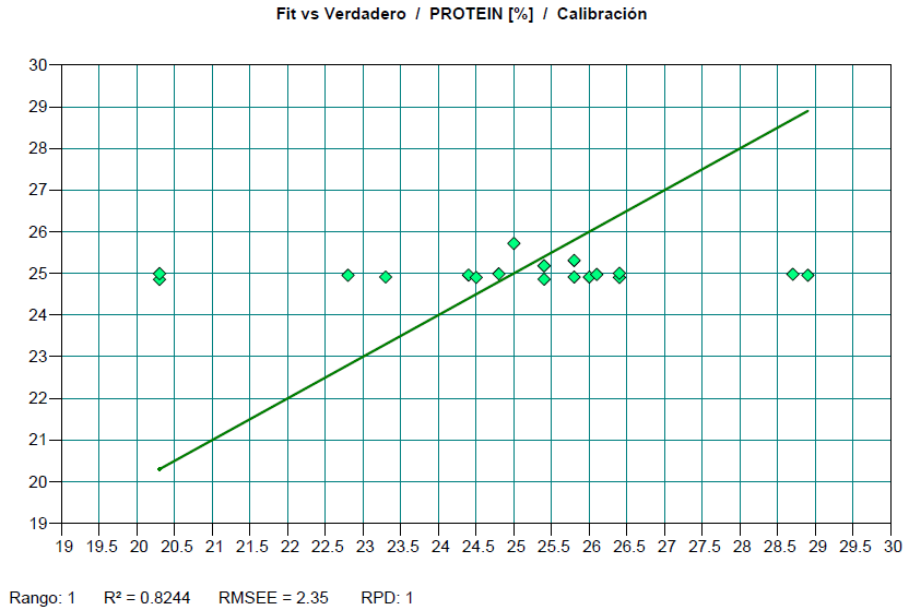

Figure 46: Graph of first calibration equation for the Protein Content Mean set without preprocessing

Even attending to the poor results of first calibration, a first Cross validation was performed in order to evaluate and test the reliability of prediction, both for mean Carbonyl and Protein spectra. Graphs are presented in Figures 47 and 48.

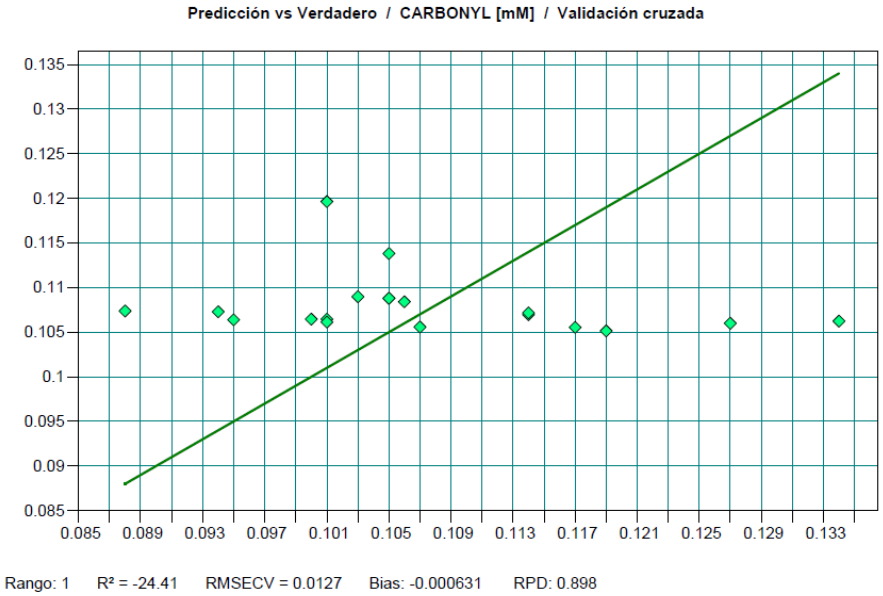

Figure 47: Graph of first validation equation for the Carbonyl Mean set without preprocessing

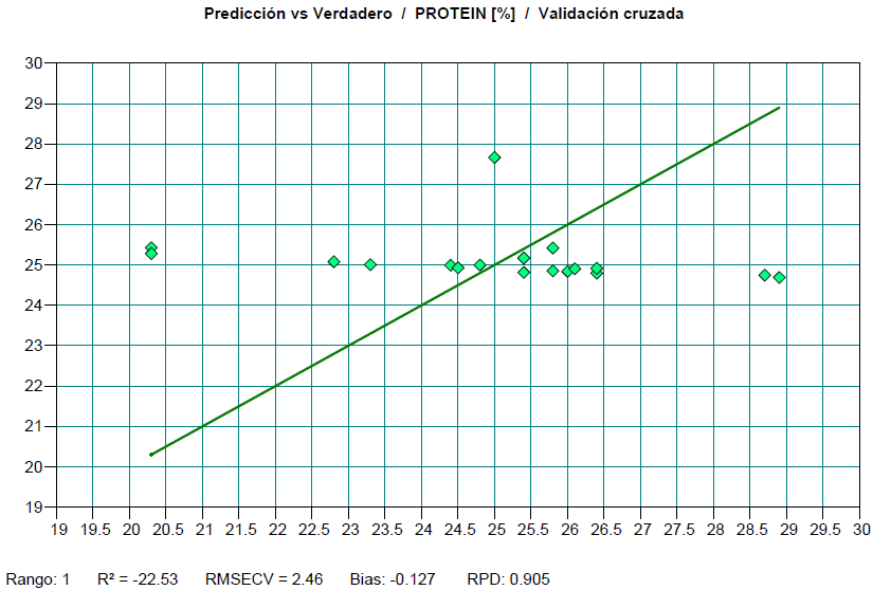

Figure 48: Graph of first validation equation for the Protein Content Mean set without preprocessing

As it was expected attending to the calibration results, results of first Validation were not consistent at all, as they presented the worst R^2 values of all the study (-24.41% for Carbonyls and -22.53% for Protein), and quite high RMSECV values. As happened in all the previous analysis, preprocessing treatment for the spectral data was performed.

Carbonyls mean results post-optimization

Min-Max Normalization was performed as it offered the minimum RMSECV with an acceptable rank (8). In Figures 49 and 50, graphs for calibration and validation after preprocessing are presented.

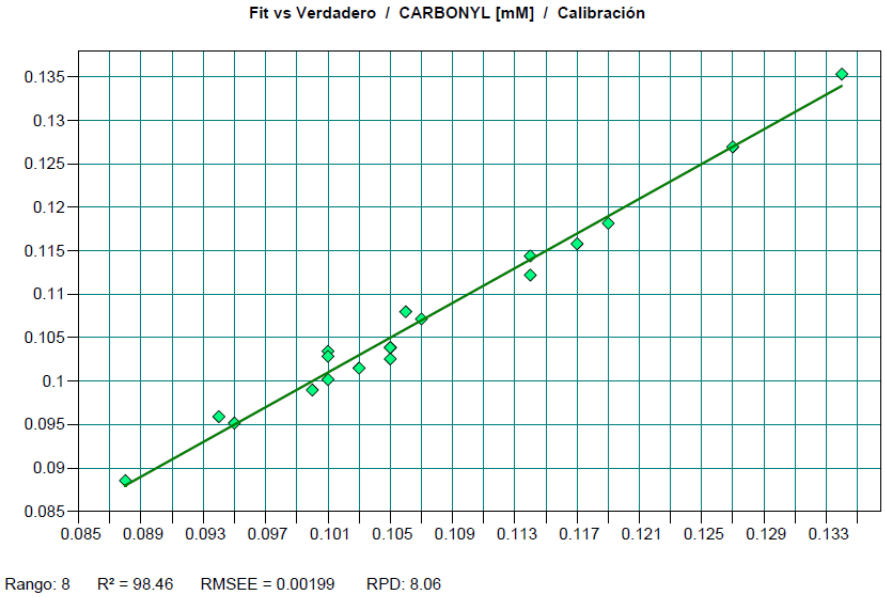

Figure 49: Graph of calibration equation for the Carbonyl Mean set with preprocessing

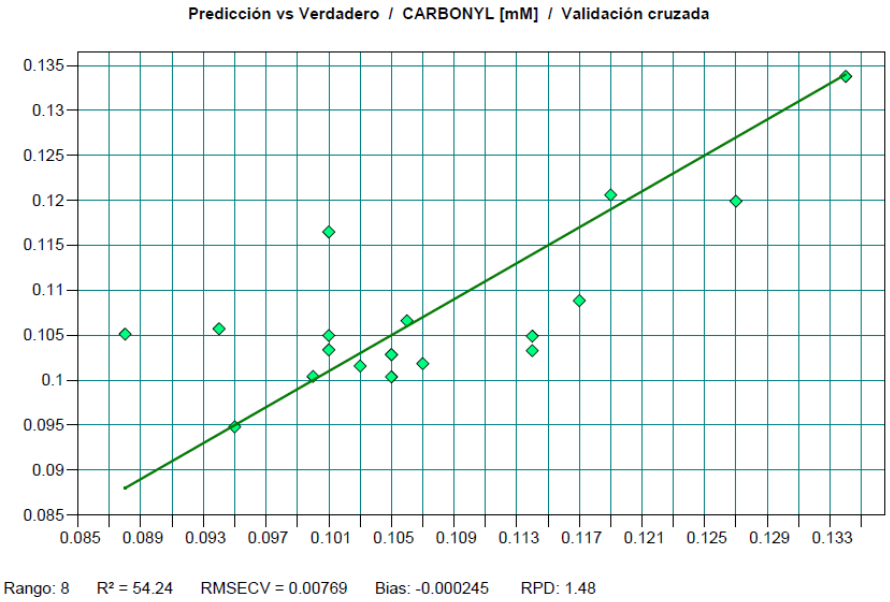

Figure 50: Graph of validation equation for the Carbonyl Mean set with preprocessing

In this case, validation model after the preprocessing procedure of Carbonyl mean spectra shows a **Coefficient of Determination** of **54.24%,** a **RMSECV** of **0.00769** and a **RPD** of **1.48**.

Type of validation employed was Cross Validation with 1 sample exclusion. In this case, no outlier spectra were subtracted, so the total spectra for calibration/validation employed were 18. Spectral range was focused between 3,638-3,277 cm^{-1}. Concentration range for Carbonyls was 0.088-0.134 mM.

Protein mean results post-optimization

In this case First Derivative + Straight Line Subtraction was performed as it offered the minimum RMSECV with most acceptable rank (6). In Figures 51 and 52, graphs for calibration and validation after preprocessing are presented.

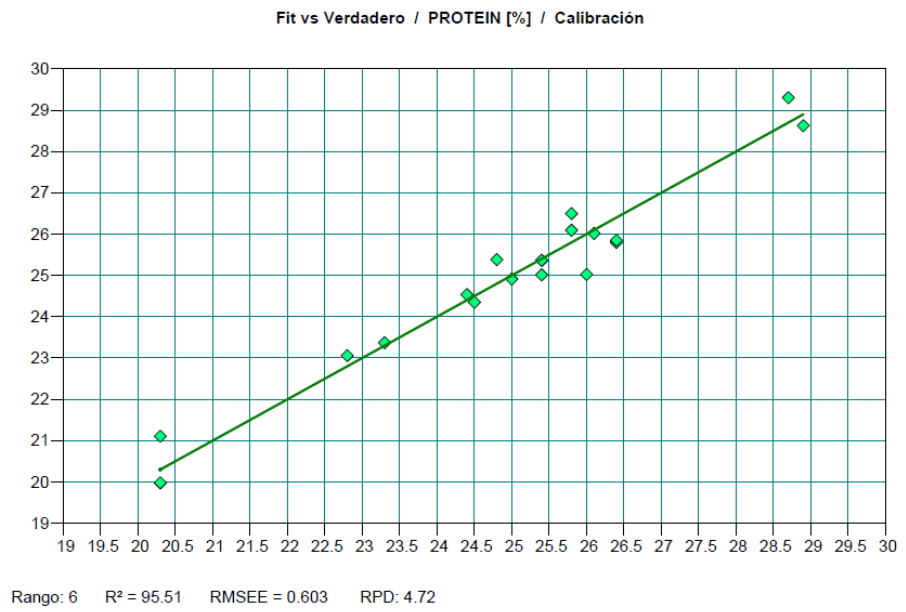

Figure 51: Graph of calibration equation for the Protein Content Mean set with preprocessing

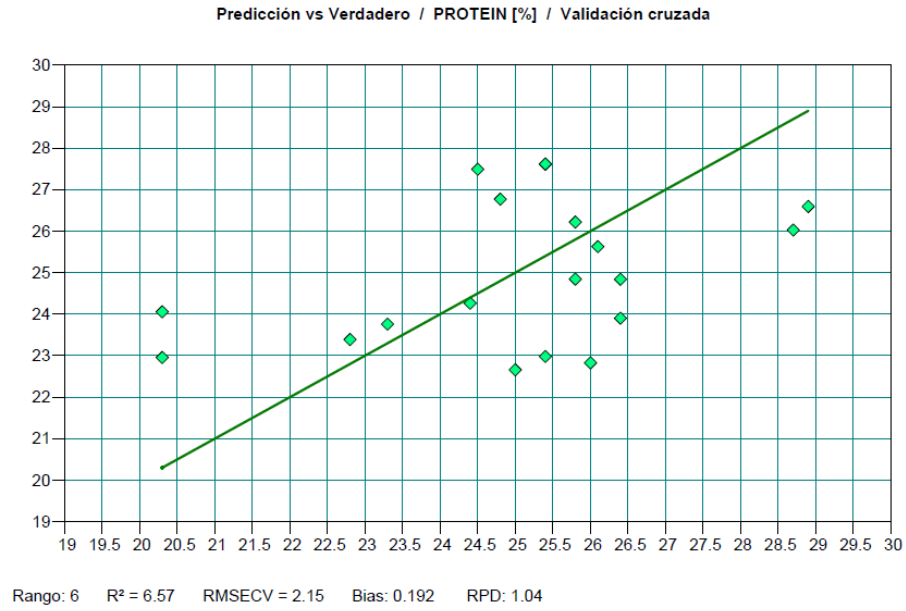

Figure 52: Graph of validaiton equation for the Protein Content Mean set with preprocessing

Despite the hopeful results obtained in calibration, protein mean spectral values validation model after the preprocessing procedure shows a poor **Coefficient of Determination** of **6.57%,** a **RMSECV** of **2.15** and a **RPD** of **1.04**.

Type of validation employed was Cross Validation with 1 sample exclusion. In this case too, no outlier spectra were subtracted, so the total spectra for calibration/validation employed were 18. Spectral range was focused between 760-399 cm^{-1}. Concentration range for Protein content was 20.3-28.9 %.

Now, calibration and validation results from the entire set of spectra are presented in comparison to results from mean sets, both for Carbonyls and Protein. They are presented in Table 13.

Table 13: Calibration and Cross Validation results for Entire and Mean sets in Carbonyl and Protein spectra.

	Parameter	Carbonyl Entire Set (n=103)	Carbonyl Mean Set (n=18)	Protein Entire Set (n=108)	Protein Mean Set (n=18)
Calibration	R^2	41.44	98.46	36.15	95.51
	RMSEE	0.00809	0.00199	1.85	0.603
	RPD	1.31	8.06	1.25	4.72
	Rank	5	8	7	6
Validation	R^2_{cv}	24.09	54.24	18.55	6.57
	RMSECV	0.00894	0.00769	2.01	2.15
	RPD_{cv}	1.15	1.48	1.11	1.04
	$Rank_{cv}$	5	8	7	6

Exactly as happened with TBA results showed in Table 12 from paragraph *3.1.2 Mean TBA Spectra Results*, here in Table 13 most remarkable improvements appear at the calibration model when performing the mean of each group of spectra and comparing the results with their entire sets. R^2 ascends to 98.46% from 41.44% in Carbonyls and from 36.15% to 95.51% in Protein. According to RMSEE, it is shown how it descends signally from 0.00809 to 0.00199 in Carbonyl and from 1.85 to 0.603 in Protein. Not only that but also, RPD shows a great ascent in Carbonyl from 1.31 up to 8.06. In the case of Protein, it also ascends from 1.25 to 4.72.

In the case of Validation models, two different results can be noticed. On the one hand, in Protein spectra, validation model shows worse results when performing means than employing the whole set of spectra, just as happened in TBA results. This is directly related to the employment of a noticeably smaller set of spectra (18 in comparison to 108), so, differences between samples have stronger repercussions over the results.

On the other hand, Carbonyl results show an improvement when performing means than employing the whole set of spectra, just on the contrary. R^2_{cv} value ascends from 24.09 in the entire set to 54.24 when employing the mean spectra set. Here, the most important factor is the rank chosen. When performing preprocessing methods in the entire set of Carbonyls, it was chosen a very low rank what may had affect to these results. However, in the Carbonyl mean set a higher rank was obtained what could have helped to obtain more consistent results of R^2_{cv}, RPD_{cv} and RMSECV.

3.3 Comparison between Raw Meat and Marker Compounds quantitative analysis results

Finally, in this last part of this chapter it is presented a comparison of the results obtained in the quantitative analysis of the spectra from the oxidation marker compounds (TBA and Carbonyls) and the ones obtained in the quantitative analysis of the spectra analyzed directly from raw meat in previous work.

The absorbance spectra of raw meat from these animals are part of a wider thesis which involves the study of crosses between different foal species, the public perception of horse meat and a deeper research of horse meat characteristics such as tenderness, texture or L*a*b colorimetric values among many other characteristics. So, what it is meant is that the quantitative analysis results of raw meat were not performed during this work but results were consulted from this other wider thesis from Ruiz-Darbonnens (2017).

Even if raw meat analyses were not executed during this project, animals employed for this work are included within the MIR analyses performed in the thesis aforementioned. That is why it is

considered acceptable to compare the results of this project's quantitative analysis with the ones from the research thesis, at least to achieve the objective of this project: to stablish whether it is enough to perform MIR analysis in raw meat or if it is necessary to extract marker compounds before MIR to give consistent results for the study of lipid and protein oxidation in horse meat.

As an approach to this comparison, some spectra are presented in Figure 53, which contain the spectra of a random TBA, Carbonyl and Protein Content sample with its correspondent raw meat MIR spectrum.

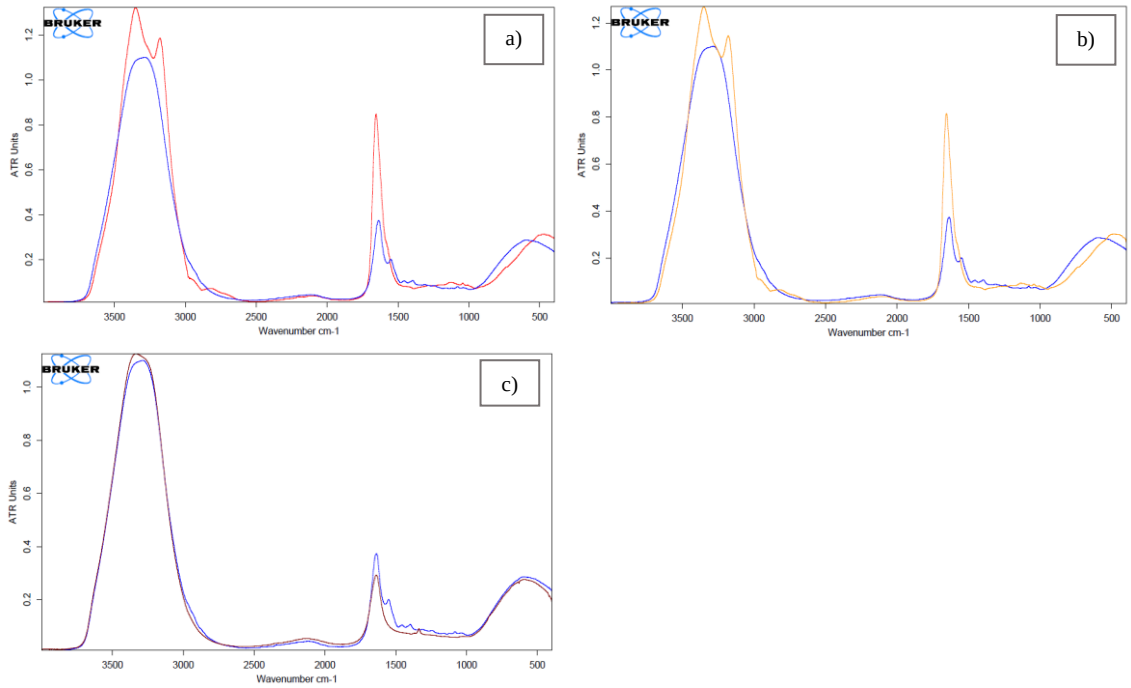

Figure 53: Comparison of marker compounds spectra vs its raw meat samples: a) Carbonyl 27 in red vs Raw meat animal 9627 in blue b) Protein 27 in orange vs Raw meat animal 9627 in blue c) TBA 59 in burgundy vs Raw meat animal 96226 in blue

It can be observed that some differences appear when regarding to PO spectra. Main difference is the apparition of a double peak in the band 3,500-3,000 cm^{-1}. As presented in paragraph *2.1 Spectral characteristics of PO compounds*, these two peaks correspond to Amide A and Amide B area, which correspond to N-H bond stretching vibrations. A higher absorption peak appears at around 1,650 cm^{-1} which, as cited, corresponds to Amide I. This one is the most intense absorption band in proteins and is due to the stretching vibrations of the C=O (70-85%) and C-N groups (10-20%). It makes sense that these peaks present higher absorption values in the Carbonyl and Protein spectra than in raw meat ones, as these peaks are associated to peptidic bonds which may be much more concentrated in the PO marker compounds than in raw meat samples which present a much more complex tissue matrix which may interfere with the IR measurements.

Regarding to TBA spectra, fewer differences can be appreciated between LO markers and raw meat samples with a naked eye. Spectra are quite similar; however, raw meat spectra present several peaks at 1.650-1,400 cm^{-1} region that TBA samples do not show. As mentioned in 2.1, a characteristic peak appears at 1,336 cm when attending to TBA samples, which does not appear in raw meat samples.

Once spectra differences have been presented, quantitative analyses comparison of both groups of spectra is presented. For that, Table 14 is introduced. Here, results obtained in paragraph *3.1 Lipid Oxidation Results* and *3.2 Protein Oxidation Results* are presented along with the ones from the raw meat samples MIR analysis obtained by Ruiz-Darbonnens (2017).

Table 14: Results of the predictive models (calibration and validation), of the TBA, Carbonyls and Protein content studied in Raw Meat and LO and PO Marker Compounds

	Parameter	TBA Raw Meat Samples	Carbonyl Raw Meat Samples	TBA Entire Set	TBA Mean Set	Carbonyl Entire set	Carbonyl Mean Set	Protein Entire Set	Protein Mean Set
Calibration	R^2	9.96	94.99	75.19	92.74	41.44	98.46	36.15	95.51
	RMSEE	0.143	0.136	0.338	0.262	0.00809	0.00199	1.85	0.603
	RPD	1.05	4.47	2.01	3.71	1.31	8.06	1.25	4.72
	Rank	1	8	10	9	5	8	7	6
Validation	R^2_{cv}	2.43	24.6	63.18	60.84	24.09	54.24	18.55	6.57
	RMSECV	0.146	0.492	0.402	0.527	0.00894	0.00769	2.01	2.15
	RPD_{cv}	1.01	1.15	1.65	1.6	1.15	1.48	1.11	1.04
	$Rank_{cv}$	1	8	10	9	5	8	7	6
	Preprocessing Treatment	First Deriv. + Vectorial Normalization (SNV) (2,559-2,199 cm^{-1})	Second Deriv. (3,998-3,637; 3,278-2,918; 2,559-478cm^{-1})	SNV Normalization 3,278-2,918 cm^{-1}	Linear Offset Subtraction Between 3,998-3,637 cm^{-1}	MSC 1,839-1,478 cm^{-1}	Min-Max Normalization 3,638-3,277 cm^{-1}	Straight Line Subtraction 3,278-2,918; 2,198-1,118; 760-399 cm^{-1}	First Deriv. + Straight Line Subtraction 760-399 cm^{-1}
	Outliers (spectra)	6	3	13	0	5	0	0	0

As it is shown in Table 14, several differences can be found among the results obtained. First of all, regarding TBA results, it can be observed a very significant difference between Raw meat samples results and the ones obtained from the compounds themselves, from an R^2 of calibration of 9.96% in Raw meat to an R^2 of 75.19% in TBA Entire set calibration (dif.=+65.23). In validation models, same level of differences can be observed, from an R^2_{cv} of 2.43% in Raw samples to a value of 63.18% in the entire set of TBA samples. All the other parameters of the study present less consistent results in Raw meat than the ones obtained through TBA compounds MIR analysis. It should be noted that through the TBA entire set analysis it was obtained the highest RPD value (1.65) of the whole group of predictive models.

On the other hand, regarding Protein oxidation, different results are obtained when comparing both groups. It can be observed how different results are between the Entire set and the Mean set of Carbonyls. In validation models, R^2_{cv} from Raw meat shows a very similar result to the one obtained through the predictive model of the Entire set of Carbonyls, 24.6% for Raw meat versus 24.09% for Carbonyl compounds. However, when comparing it to the result obtained through the predictive model of the Mean set it can be observed a significant improvement in the latter one, which presents a R^2_{cv} of 54.24% (diff.=+29.69). This may suggest that when studying Carbonyl content through MIR spectroscopy, it is preferable to perform a mean of the spectra obtained before constructing the predictive model.

Finally, it must be noted that there is not data available to compare the Protein content results from this work as they were not measured in previous projects. Even though, the totality of the results obtained through this work regarding Protein content's MIR analysis do not offer any encouraging predictive parameters, especially after validation was performed. This was the case of the results obtained through the analysis of Protein content mean set, which R^2_{cv} offered very weak result (6.57%) once Cross Validation was performed. This suggests that the deceiver result of R_2 of calibration (95.51%) cannot be used as a reliable parameter.

Chapter V. Conclusions

Bearing in mind the material and methods employed and according to the results obtained, the following conclusions have been achieved through this work:

1. According to the results of classical quantification of lipid and protein oxidation, MDA content in Young foals (13m) with a linseed-rich finishing diet was observed between 0.32 and 0.46 g mg MDA/kg meat sample, while the range went from 1.1 to 3.58 mg MDA/kg meat sample in Adult foals (26m) with a conventional concentrate finishing diet. On the other hand, regarding Carbonyls content it was observed that the minimum levels were found in the Young Linseed group (0.1 nmole/mg) while the maximum ones were present in the Adult Conventional group (0.114 nmole/mg). This way it is demonstrated that lipid and protein oxidation of horse meat samples increases as slaughtering age does. Further research must be performed to study the influence of the finishing diet.

2. A Fourier-Transform Mid-infrared spectroscopy experimental protocol has been designed and stablished in order to perform consistent spectral measurements of the marker compounds of lipid and protein oxidation in food systems, which may be useful for future investigation regarding other research fields.

3. Spectral results of the lipid and protein oxidation marker compounds show clear differences between them (TBA vs Carbonyls) and slighter naked-eye differences between samples of each groups. On the one hand, Carbonyls and Protein Content samples show some particular bands (Amide A and B) which are hidden in raw meat spectra, and are easily identified according to bibliography. On the other hand, TBA spectra do not show naked-eyed significant differences between different samples, and absorption peaks are very similar to the ones present in raw meat samples. A particular peak appears at 1,336 cm^{-1} which is present in every TBA sample.

4. Predictive models employing FT-MIR spectroscopy in LO and PO marker compounds show coefficients of determination of cross validation (R^2_{cv}) of 63.18% and 54.24% for TBA and Carbonyls content respectively, versus the coefficients of 2.43% and 24.6% for TBA and Carbonyls performed in previous projects with the raw meat samples from which the compounds were extracted. Weak predictive models were obtained through the analyses of Protein Content samples, so further research with vaster data must be developed regarding this parameter. This way, it has been proved that performing a previous extraction of the marker compounds notably helps to achieve more consistent results for lipid and protein oxidation assessment in horse meat products.

5. It is interesting to continue investigating and supporting research in FT-MIR technology applied to food quality analyses, in particular to meat products quality assessment, as it appears to be a promising tool for this end.

Chapter VI. References

Akagawa, M., Sasaki, D., Ishii, Y., Kurota, Y., Yotsu-Yamashita, M., Uchida K., Suyama, K. (2006). New method for the quantitative determination of major protein carbonyls, α-aminoadipic and γ -glutamic semialdehydes: investigation of the formation mechanism and chemical nature in vitro and in vivo. *Chemical Research in Toxicology*, 19, 1059–65.

Al-Jowder, O., Defernez, M., Kemsley, E. K., & Wilson, R. H. (1999). Mid-infrared spectroscopy and chemometrics for the authentication of meat products. *Journal of Agricultural and Food Chemistry*, 47(8), 3210-3218.

Anastasaki, E., Kanakis, C., Pappas, C., Maggi, L., del Campo, C. P., Carmona, M., et al. (2010). Differentiation of saffron from four countries by mid-infrared spectroscopy and multivariate analysis. *European Food Research and Technology*, 230, 571–577.

Armenteros, M. (2010). *Reducción de sodio en lomo y jamón curados. Efecto sobre la proteolisis y las características sensoriales*. Tesis Doctoral. Universidad Politécnica de Valencia.

Armenteros, S., Ventanas, D., Morcuende D., Estévez, M., Ventanas, J. (2012). *Empleo de Antioxidantes Naturales en productos cárnicos.* University of Extremadura, Veterinary School, Cáceres.

Bacher, A. (2002). *Infrared Spectroscopy: Theory and Examples.* University of California, Department of Chemistry & Biochemistry, Los Angeles, CA 90095-1596.

Barriuso, B., Astiasarán, I., Ansorena, D. (2013). A review of analytical methods measuring lipid oxidation status in foods: a challenging task. *European Food Research and Technology*, 236, 1-15.

Belaunzaran, X., Bessa, R. J. B., Lavín, P., Mantecón, A. R., Kramer, J. K. G., & Aldai, N. (2015). Horse-meat for human consumption - Current research and future opportunities. *Meat Science*, (108), 74–81.

Bou, R., Pignoli, G., Rodriguez-Estrada, M.T., Decker, E.A. (2009). Suitability of saturated aldehydes as lipid oxidation markers in washed turkey meat. *Meat Science*, 83, 412-416.

Brewer, S. (2004). *Irradiation effects on meat color – a review.* Meat Science, 68, 1-17.

Bruker Optik. (2011a). *QUANT User manual*. Rudolf-Plank-Str. 27, D-76275 Ettlingen.

Bruker Optik. (2011b). *Bruker optics IR Tutorial.* Rudolf-Plank-Str. 27, D-76275 Ettlingen.

Caballero, J. (12th July 2017). *Carne de potro, la nueva favorita de la alta gastronomía por su alto valor proteico y su poca grasa.* Expansión. Recovered in January 2018 from: http://www.expansion.com/fueradeserie/gastro/2017/07/11/595f50cee2704ef94d8b45f2.html

Carbonaro, M. (2010). Secondary structure of food proteins by Fourier transform spectroscopy in the mid - infrared region. *Amino Acids*, 38 (3), 679 - 690.

Climent, I., Tsai, L., & Levine, R. L. (1989). Derivatization of gamma-glutamyl semialdehyde residues in oxidized proteins by fluoresceinamine. *Analytical Biochemistry*, 182, 226–232.

Coates, J. (2000). Interpretation of infrared spectra, a practical approach. In R. A. Meyers (Ed.), *Encyclopedia of analytical chemistry*. (pp. 10815–10837). John Wiley & Sons Ltd.

Eisenberg, D. & Kauzmann, W. (1969). *The structure and properties of water*. Oxford University Press, London.

Estévez, M. (2011). Protein Carbonyls in meat systems: A review. *Meat Science*, 89, 259-279.

Estévez, M., Ventanas, S., & Cava, R. (2007). Oxidation of lipids and proteins in frankfurters with different fatty acid compositions and tocopherol and phenolic contents. *Food Chemistry*, 100, 55–63.

Estévez, M., Morcuende, D., Ventanas, S., & Ventanas, J. (2012). Oxidación de proteínas cárnicas: importancia científica y tecnológica. *Eurocarne, 208*.

FAO. (2015). *FAOSTAT. Livestock Primary: Horse meat production*. Recovered on December 2017 from: http://www.fao.org/faostat/en/#data/QL/

Fernández de Labastida, I. (2011). *Caballos de monte y carne de potro. Análisis antropológico de un proceso contemporáneo de construcción identitaria, cultural y económica en la montaña Alavesa*. Departmento de Filosofía de los Valores y Antropología Social. Universida del País Vasco.

Gable, K.P. (2014). *Infrared Spectroscopy: Identifying Functional Groups*. Oregon State University, Corvallis, OR, 9733.

Halliwell, B., (1995) *Antioxidant characterization: Methodology and mechanism.* Neurodegenerative Disease Research Centre, Pharmacology Group, King's College, London SW3 6LX, U.K.

Higson, S. P. J. (2004). *Analytical Chemistry*. Oxford University Press. ISBN: 9780198502890.

Ichinose, T., Miller, M., Shibamoto, T. (1989). Gas-Chromatographic analysis of free and bound malonaldehyde in rat-liver homogenates. *Lipids*, 24 (10): 895-898.

Jabs, A. (n.d). *Determination of Secondary Structure in Proteins by Fourier Transform Infrared Spectroscopy (FTIR).* Jena Library of biological macromolecules. Recovered on May 2018 from: http://jenalib.leibniz-fli.de/ImgLibDoc/ftir/IMAGE_FTIR.html

Kanou, M., Nakanishi, K., Hashimoto, A., & Kameoka, T. (2005). Influences of monosaccharides and its glycosidic linkage on infrared spectral characteristics of disaccharides in aqueous solutions. *Applied Spectroscopy*, 59, 885–892.

Karoui, R., Downey, G., & Blecker, C. (2010). Mid-Infrared Spectroscopy Coupled with Chemometrics: A Tool for the Analysis of Intact Food Systems and the Exploration of Their Molecular Structure-Quality Relationships - A Review. *Chemical Reviews,* 110(10), 6144-6168.

Lagarda M.J., Manez J.G., Manglano P., Farre R. (2003). Lipid hydroperoxides determination in milk-based infant formulae by gas chromatography. *European Journal of Lipid Science Technology,* 105 (7), 339–345.

Lancashire, R.J. (2004). *Infrared spectroscopy and modes of vibrations.* Department of Chemistry, University of the West Indies, Mona Campus, Kingston, Jamaica.

López, F., Martínez, G., and Segovia, F. (2014). *Evaluación de la oxidación lipídica mediante el test del TBA: Método de destilación*. Univ. Politècnica València.

Lorenzo, J.M., Gómez, M. (2012). Effect of packaging conditions on shelf-life of fresh foal meat. *Meat Science*, 91, 513-520.

Lorenzo, J. M. & Pateiro, M. (2013). Influence of type of muscles on nutritional value of foal meat. *Meat Science*, 93(3): 630-8.

Lorenzo J. M., Sarriés, M.V., Tateo, A., Polidori, P., Franco, D. & Lanza, M. (2014). Carcass characteristics, meat quality and nutritional value of horsemeat: A review. *Meat Science*, 96, 1478-1488.

Lorenzo, J. M., Fuciños, C., Purriños, L., & Franco, D. (2010). Intramuscular fatty acid composition of "Galician Mountain" foals breed. Effect of sex, slaughter age and livestock production system. *Meat Science*, 86, 825–831.

Lozano, M. (2015). *Aplicación de la espectroscopia de infrarrojo medio para la determinación de la textura en muestras de carne pertenecientes a la indicación geográfica protegida (IGP) ternera de navarra*. Master Final Project. Universidad Pública de Navarra.

Lucarini, M., Durazzo, A., Sánchez del Pulgar, J., Gabrielli, P., Lombardi-Boccia, G. (2017). Determination of fatty acid content in meat and meat products: The FTIR-ATR approach. *Elsevier*, in-press.

Lund, M., Heinonen, M., Baron, C. P., & Estevez, M. (2011). Protein oxidation in muscle foods: A review. *Molecular Nutrition & Food Research*, 55 (1): 83–95.

MAPAMA. (2017a). *Composición de la carne de caballo.* Recovered on November 2017 from: http://www.mapama.gob.es/es/ministerio/servicios/informacion/caballo_tcm7-315385.pdf

MAPAMA. (2017b). *Composición de la carne de ternera.* Recovered on November 2017 from: http://www.mapama.gob.es/es/ministerio/servicios/informacion/ternera_tcm7-315435.pdf

Martuzzi, F., Catalano, A., & Sussi, C. (2001). *Characteristics of horse meat consumption and production in Italy*. Annals of Veterinary Medicine Faculty from Parma University, 21: 213–223.

Massart, D. L.; Vandeginste, B. G. M.; Deming, S. M.; Michotte, Y.; Kaufman, L. (1988). *Chemometrics: a textbook.* Amsterdam: Elsevier.

Mendes, R., Cardoso, C., Pestana, C. (2009). Measurement of malondialdehyde in fish: A comparison study between HPLC methods and the traditional spectrophotometric test. *Food Chemistry*, 112(4):1038-1045.

Nikonenko, N. A., Buslov, D. K., Sushko, N. I., & Zhbankov, R. G. (2005). Spectroscopic manifestation of stretching vibrations of glycosidic linkage in polysaccharides. *Journal of Molecular Structure*, 752: 20–24.

Nunes, K. M., Andrade, M.V., Santos Filho, A., Lasmar, M., Sena, M. (2016). Detection and characterization of frauds in bovine meat in natura by non-meat ingredient additions using data fusion of chemical parameters and ATR-FTIR spectroscopy. *Food Chemistry*, 205: 14-22.

Oliver, C.N., Ahn, B.W., Moerman, E. J., Goldstein, S., & Stadtman, E. R. (1987). Aged-related changes in oxidized proteins. *Journal of Biological Chemistry*, 262: 5488–5491.

Oliver, C.N., Levine, R.L., Garland, D., Amici, A., Climent, I., Lenz, A.G., Ahn, B-W., Shaltiel, S., Stadtman, E.R. (1990). Determination of carbonyl content in oxidatively modified proteins. *Methods in Enzymology*, 186: 464-478.

PerkinElmer. (2005). *Technical Note: FT-IR Spectroscopy, Attenuated Total Reflectance (ATR*). PerkinElmer Inc. 710 Bridgeport Avenue Shelton, CT 06484-4794 U.S.A. Recovered in April 2018 from: http://www.utsc.utoronto.ca/~traceslab/ATR_FTIR.pdf.

Pinho-Moreira, M.J., Silva, A.C., Almeida, J.M.M.M., Saraiva, M. (2018). Characterization of deterioration of fallow deer and goat meat using microbial and mid infrared spectroscopy in tandem with chemometrics. *Food Packaging and shelf life*, 15: 169-180.

Premanandh, J. (2013). Horse meat scandal–A wake-up call for regulatory authorities. *Food Control*, 34(2), 568–569.

Requena, J. R., Chao, C. -C., Levine, R. L., & Stadtman, E. R. (2001). Glutamic and aminoadipic semialdehydes are the main carbonyl products of metal-catalyzed oxidation of proteins. *Proceedings of the National Academy of Sciences USA*, 98: 69–74.

Requena, J. R., Levine, R. L., & Stadtman, E. R. (2003). Recent advances in the analysis of oxidized *proteins. Amino Acids*, 25: 221–226.

Rojano, B., Gaviria, C., and Sáez, J. (2008). Determinación de la actividad antioxidante en un modelo de peroxidación lipídica de mantequilla inhibida por el isoespintanol. *Vitae*: 212–218.

Roming, M. & Preindl, B. (2012), *Understanding FT-IR*. Bruker Optik International Training Courses. Rudolf-Plank-Str. 27, D-76275 Ettlingen.

Rossier, E. (1998). *Horse meat. Review, Endocrinology*. Encyclopaedia of Food Science.

Ruiz-Darbonnens, M. (2017). *PhD Thesis*. Environmental Sciences Department. Universidad Pública de Navarra.

Salih A, Smith D, Price J, Dawson L (1987*)* Modified extraction 2-thiobarbituric acid method for measuring lipid oxidation in poultry. *Poultry Science*, 66:1483-1488.

Sarriés, M. V. (2005). *Carcass morphological characteristics and meat quality of the Burguete foal*. Departamento de Ciencias del Medio Natural, Universidad Pública de Navarra.

Shacter E. (2000). Quantification and significance of protein oxidation in biological samples. *Drug Metabolism Reviews*, 32: 307–26.

Shimadzu analytics. (2018). *Shimadzu analytics corporation.* Recovered in March 2018 from: https://www.shimadzu.com/products/index.html

Silverstein, R.M.; Bassler, G.C.; and Morrill, T.C. *Spectrometric Identification of Organic Compounds*. 4th ed. New York: John Wiley and Sons, 1981. QD272.S6 S55

Skoog, D. A., Crouch, S. R., Holler, F. J., & Anzures, M. B. (2008). *Principles of Instrumental Analysis*. Cengage Learning Latin America.

Socaciu, C., Vodnar, D., Pop, O. (2012). Monitoring Lactic Acid Fermentation in Media Containing Dandelion (Taraxacum officinale) by FTIR Spectroscopy. *Notulae Botanicae Horti Agrobotanici*, 40(1): 65-68.

Soladoye, O.P., Juárez, M.L., Aalhus, J.L, Shand, P., Estévez, M. (2015). Protein Oxidation in Processed Meat: Mechanisms and Potential Implications on Human Health. *Institute of Food Technologists, Comprehensive Reviews in Food Science and Food Safety*, Vol. 14.

Stalikas C., Konidari C. (2001). Analysis of malondialdehyde in biological matrices by capillary gas chromatography with electron-capture detection and mass spectrometry. *Anal Biochem*, 290(1):108-115.

Stanciu, S. (2014). *Horse Meat Consumption - Between Scandal and Reality*. The Bucharest University of Economic Studies. 2nd Global Conference on Business, Economics, Management and Tourism, 30-31 October 2014, Prague, Czech Republic.

Stadtman, E. R., & Levine, R. L. (2000). Protein oxidation. *Annals New York Academy of Sciences*, 899(1): 191–208.

Stadtman, E. R., & Levine, R. L. (2003). Free radical-mediated oxidation of free amino acids and amino acid residues in proteins. *Amino Acids*, 25: 207–218.

Sun, D.-W. (2009). Infrared spectroscopy for food quality analysis and control (1st ed.). *New York: Elsevier* (chap. 4).

Tamm, L. & Tatulian, S. (1997). *Infrared spectroscopy of proteins and peptides in lipid bilayers.* Department of Molecular Physiology and Biological Physics, University of Virginia Health Sciences Center, Charlottesville, Virginia.

Thermo Nicolet. (2002) *FT-IR vs. Dispersive Infrared: Theory of Infrared Spectroscopy Instrumentation*. Thermo Nicolet Corp. Madison, WI, 53711-4495, U.S.A. Recovered in April 2018 from: http://www.thermo.com.cn/resources/200802/productpdf_21615.pdf

Venyaminov & Kalnin (1990). Quantitative IR spectrophotometry of peptide compounds in water (H2O) solutions. I. Spectral parameters of amino acid residue absorption bands. *Biopolymers*. (30), 13-14):1243-57).

Voges, K.L., Mason, C.L., Brooks, J.C., Delmore, R.J., Griffin, D.B., Hal, D.S…Savell, J.W. (2007). National beef tenderness survey – 2006: Assessment of Warner–Bratzler shear and sensory panel ratings for beef from US retail and foodservice establishments. *Meat Science*, 77: 357-364.

Vuorela, S., Salminen, H., Mäkaela, M., Kivikari, R., Karonen, M., Heinonen, M. (2005). Effect of Plant Phenolics on Protein and Lipid Oxidation in Cooked Pork Meat Patties. *Journal of Agricultural and Food Chemistry*, 53: 8492-8497.

Vyncke, W. (1975). Evaluation of the Direct Thiobarbituric Acid Extraction Method for Determining Oxidative Rancidity in Mackerel (Scomber scombrus L.). *European Journal of Lipid Science and Technology*, 77 (6): 239-240.

Zakrys, P.I., Hogan, S.A., O'Sullivan, M.G., Allen, P., Kery, J.P. (2008). Effects of oxygen concentration on the sensory evaluation and quality indicators of beef muscle packed under modified atmosphere. *Meat Science,* 79: 648-655.

Zakrys-Waliwander P.I., O'Sullivan, M.G., Allen, O'Neill, E.E. and J.P., Kery, J.P. (2010). Investigation of the effects of commercial carcass suspension (24 and 48 h) on meat quality in high oxygen modified atmosphere packed beef steaks during chill storage. *Food Research International*, 43: 277-284.